Second Series *November 1, 1932* *Vol. 42, No. 3*

THE

PHYSICAL REVIEW

Cosmic-Ray Ionization as a Function of Pressure, Temperature, and Dimensions of the Ionization Chamber

By JAMES W. BROXON
University of Colorado

(Received August 15, 1932)

Experiments have been performed to test the adequacy of the writer's explanation of the dependence upon pressure of the cosmic-ray ionization in gases at high pressures in terms of subsidiary radiations emitted solely from the walls of the ionization chamber. The ionization in a 436 cc sphere of 33.32 g mass located at the center of the 660 lb. bomb of 13.8 liters capacity used in previous experiments, was found not to differ greatly from the average ionization in the large chamber at corresponding pressures up to 175 atmospheres. At the higher pressures gamma-ray ionization and cosmic-ray ionization were found to vary with the pressure in the same manner. These facts are considered to be incompatible with the explanation mentioned above. The temperature effect was found to amount to 0.19 percent increase in ionization per centigrade degree increase in temperature at a mean pressure of 23.3 atmospheres, and 0.27 percent per degree at 162.1 atmospheres, in qualitative but not entirely in quantitative agreement with the theory and observations of Compton, Bennett and Stearns. The cosmic-ray ionization at 205 atmospheres in the shielded bomb was found to agree within about one percent with the upper limit previously observed in the same chamber with similar shielding at pressures between 130 and 170 atmospheres. Certain transient effects associated with changes in pressure and temperature were observed.

CONTINUING the investigation of the residual ionization in gases at high pressures, the writer found that the ionization produced by the penetrating radiation in air[1] approached an upper limit at about 130 atmospheres in a spherical chamber of 11.72 inches internal diameter. No change in the ionization was observed as the pressure was increased to 170 atmospheres. A similar situation was observed in the case of nitrogen,[2] but in this gas the ionization was greater than that in air at corresponding pressures, and constant values were obtained only at a somewhat higher pressure. Earlier work[3] had shown oxygen to resemble air, and carbon dioxide to resemble nitrogen, at pressures up to about 70 atmospheres.

Amplifying the hypothesis suggested by McLennan[4] and later by Wilson[5]

[1] J. W. Broxon, Phys. Rev. **37**, 1320 (1931).
[2] J. W. Broxon, Phys. Rev. **38**, 1704 (1931).
[3] J. W. Broxon, Phys. Rev. **27**, 542 (1926).
[4] J. C. McLennan, Phil. Mag. **14**, 760 (1907).
[5] W. Wilson, Phil. Mag. **17**, 216 (1909).

and Downey,[6] the writer showed that the relation between ionization and pressure could be explained by assuming that the penetrating radiation produced no appreciable primary ionization, the immediate ionizing agent being secondary radiations excited only in the thick walls of the container. For two reasons the explanation appeared rather unsatisfactory. In order to explain the constant value of the ionization at sufficiently high pressures, it was necessary to assume that all the subsidiary radiations were emitted in directions normal to the inner surface of the chamber. Further, it appeared unlikely that secondary radiations should not be excited in the gas at the high pressures as well as in the vessel walls, inasmuch as altitude measurements indicate that the penetrating radiation is absorbed in air as in other materials.

Compton, Bennett and Stearns,[7] and Millikan and Bowen[8] have emphasized an alternative explanation. According to them the attainment of constant ionization values at the high pressures is due to a lack of saturation. This lack of saturation is due to a selective recombination, the recombination of the ion with the parent from which the electron was ejected, rather than to random recombination. On this account, the ordinary tests for saturation are found to be inadequate.

With this point of view, Compton, Bennett and Stearns were able to deduce an equation giving the proper variation of the ionization with pressure. They were further able to deduce a dependence upon temperature, insignificant in the neighborhood of atmospheric pressure, but considerable in the neighborhood of 100 atmospheres. The temperature effect was checked experimentally by measurements of the ionization produced in air and nitrogen by gamma-rays, greater ionization currents being observed at higher temperatures.

Bowen[9] has also provided experimental evidence for the selective recombination hypothesis by showing that at pressures up to 93 atmospheres the ionization produced by gamma-rays increases with the potential gradient up to 1000 volts/cm, and that the dependence upon the gradient is nearly independent of the intensity of the ionization. This observation conflicts with the detailed theory of Compton, Bennett and Stearns, according to which a very much higher gradient would be required to increase the ionization current above the apparent saturation value.

The dependence of the ionization by gamma-rays in air and carbon dioxide upon pressure, temperature and potential gradient was carefully investigated by Professor Erikson[10] in 1908. He found that as the pressure was varied from 1 to 400 atmospheres the ionization in air actually passed through a maximum, thereafter decreasing linearly with increase of pressure. The magnitude of this maximum and the pressure at which it occurred increased

[6] K. M. Downey, Phys. Rev. **16**, 420 (1920); **20**, 186 (1922).
[7] A. H. Compton, R. D. Bennett and J. C. Stearns, Phys. Rev. **39**, 873 (1932).
[8] R. A. Millikan and I. S. Bowen, Nature **128**, 582 (1931).
[9] I. S. Bowen, Phys. Rev. **41**, 24 (1932).
[10] H. A. Erikson, Phys. Rev. **27**, 473 (1908).

with the potential gradient, the maximum gradients being provided by 2500 volts between gauze cylinders differing by 0.8 cm in radius. He found at a constant pressure that after an initial rapid increase the ionization continued to increase slightly with the potential gradient to the highest values used. At constant gas density, he found the ionization increased with temperature when high potential gradients were applied, whereas the ionization decreased with increasing temperature at low field intensities. The effects were explained by Professor Erikson in terms of the selective recombination with the parent atoms.

In addition to explaining the variation with pressure, an interesting feature of the secondary radiation hypothesis was that it led to correct values of the absorption coefficient of the primary penetrating radiation, upon assuming that the ranges of these radiations were represented by the diameter of the vessel at the lowest pressure at which the maximum ionization was attained, and the further assumption that they consisted of electrons scattered in such a manner that the Compton equation was applicable. That the application of this equation was quite unjustified was recognized, but the assumption that the secondary radiations consisted of protons ejected from the nucleus upon absorption of an incident quantum led to a similar conclusion. In this connection it is of interest that Millikan and Anderson[11] have found from expansion chamber observations in a magnetic field, that the secondary radiations are chiefly positive. Compton, Bennett and Stearns[7] provide evidence in contradiction of this phase of the explanation. They have found the ratio of the ionization by a given intensity of gamma-radiation to that produced by the cosmic penetrating radiation in the same vessel at the same pressure, to be quite independent of the pressure within the range of their measurements. If the ionization in both cases were due almost entirely to secondary radiation from the walls, then a maximum ionization should be attained at a considerably lower pressure in the case of the gamma-radiation, in view of the much lower energy of the incident quanta in this case.

Sievert[12] and Tarrant[13] have also observed a pressure effect in gamma-ray ionization corresponding to that observed by the writer with cosmic-ray ionization, and the former has obtained pressure-ionization curves with x-radiation which somewhat resemble Professor Erikson's high-pressure γ-ray ionization curves. They also consider the secondary radiation hypothesis unsatisfactory.

In an attempt to test further the adequacy of the suggested explanations of the characteristics of the ionization due to the penetrating radiation in gases at high pressures, the present investigation was undertaken.

Ionization in Thin Central Sphere

The assumption that the ionization in a gas by the cosmic penetrating radiation is due entirely to secondary radiations emitted normally from the

[11] R. A. Millikan and C. D. Anderson, Phys. Rev. **40,** 325 (1932). Also, see the conclusions of E. G. Steinke and H. Schindler, Zeits. f. Physik **75,** 115 (1932).

[12] R. M. Sievert, Nature **129,** 792 (1932).

[13] G. T. P. Tarrant, Proc. Roy. Soc. **A135,** 223 (1932).

walls, would lead to the conclusion that the ionization in the central region of a spherical chamber should vary considerably from the average. At the lower pressures the ionization should be greater at the center whereas at high pressures it should be less, becoming negligible at sufficiently high pressures.

The difficulty with ascertaining the ionization in a given region is that solid material must be introduced in order to perform the measurement, and this material modifies the conditions. To approximate the desired conditions, an exceedingly thin vessel should be introduced into the central region.

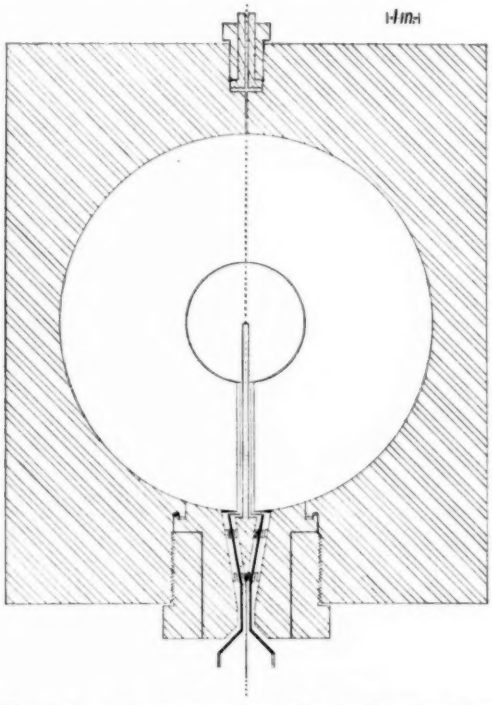

Fig. 1. Longitudinal section of ionization chamber.

Because it was highly desirable to know very definitely the region from which ions were drawn in the present instance, it was decided to construct a chamber with thin but continuous walls. Consequently, two thin steel hemispheres were spun, ground down to a still smaller thickness, and soldered together. This sphere was mounted at the center of the 11.72 in. bomb used in recent work,[1] as shown in Fig. 1.

The mass of the central sphere was 33.32 g. Its volume, as determined by filling and weighing with benzene whose density was carefully determined at the temperature of the experiment, was 436.7 cc, giving a mean internal diameter of 3.706 in. Division of the mass of the sphere by its area and the probable density of the steel gave an average wall thickness of about 0.006 in. Micrometer measurements showed the external diameter to vary between 3.712 and 3.746 in.

The large tube supporting the thin sphere had an outside diameter of 0.532 in., a wall thickness of 0.008 in., and weighed 7.40 g. The central tube, forming a continuation of the guard system, had an O.D. of 0.342 in., a wall thickness of 0.007 in., and weighed 4.09 g. The innermost tube, forming the collector, had an O.D. of 0.168 in., a wall thickness of 0.011 in., and weighed 3.90 g. The end of this tube was spun to an approximate hemisphere. The hole in the sphere through which this tube was admitted was 9/32 in. in diameter. The volume of the tube inside the sphere was 0.67 cc, leaving a free volume of 436 cc inside the sphere.

The tubes and sphere were mounted on the plug[14] of the large bomb, and when the latter was screwed into place the eccentricity of the central sphere relative to the interior of the bomb did not amount to more than 1/32 in. The tubes were beneath the sphere. Twenty small holes were drilled in the outer tube to allow an equalization of pressure inside and outside the thin sphere. None were drilled within $\frac{1}{2}$ in. of the ends of the tube, however.

Because of the very much smaller volume, the ionization currents were correspondingly smaller than in the large sphere. However, for purposes of comparison, it was considered desirable to use precisely the same measuring equipment which had been used in the preceding high-pressure work. This equipment, the location, the method of measurement, etc., have been described fully.[1] The insertion of the small sphere constituted the only alteration; the same constant, modified by the volume ratio, yielding the number of pairs of ions per cc per sec. when multiplied by the number of volts/sec. applied to the compensating condenser. Because of the smaller currents, however, six or eight 15-minute readings or three or four 30-minute readings were made at each pressure, instead of the usual three 8-minute readings. Also, positive and negative ions were usually collected during alternate readings to insure that the smaller readings would not be affected by possible contact potentials or zero drift. That no appreciable deformation of the sphere occurred during the observations was shown by the fact that its induction coefficient relative to the central system varied linearly with the pressure, a situation which had been found to hold in the case of the rigid bomb.[15]

As in all previous work, the gas used throughout the present investigation was aged at least four weeks, often much longer, and was dried and freed from dust. With the bomb surrounded by the water shield only, observations of the ionization in the central sphere were made at various pressures between about 7 and 175 atmospheres. These are shown in Fig. 2, pressures again being reduced to 18°C. The dotted curve represents the average ionization measured in the large bomb under the same conditions; it is curve III of Fig. 5 of the paper of reference 1. The small square represents an observation of the

[14] In order to eliminate a small leak, the main plug was redesigned to conform with the small one at the top of the bomb, so that the portion of the plug in contact with the gasket was not allowed to rotate as the plug was tightened. This design proved to be thoroughly satisfactory.

[15] J. W. Broxon, Phys. Rev. **37,** 1338 (1931).

ionization in the small sphere with the lead shield only, and the cross represents the ionization measured with both the lead and water shields. The barometric pressures during the two series of observations with only the water shield did not differ by more than 0.05 in. It appears that the two observations designated by the square and the cross should be reduced by about 0.6 percent to conform to this barometric pressure.

The striking thing about the curve is its proximity to the dotted curve. The ionization in the central sphere seems to be definitely higher than the average in the large bomb at the lower pressures and a little lower at the highest pressures. However, constant values at high pressures are again attained,

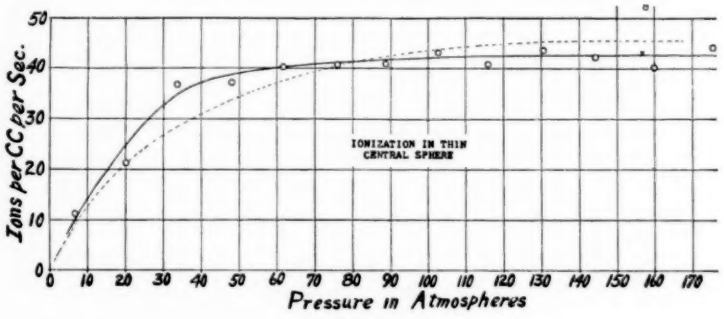

Fig. 2.

in this case at a lower pressure than in the large chamber. There are apparent differences between the curves, but not at all of the magnitude to be expected on the hypothesis of ionization due entirely to radiation from the walls. It is a striking observation that at the highest pressures the ionization in this small central sphere, weighing little more than an ounce, containing air weighing nearly three times as much, and surrounded by a blanket of air equivalent to a layer more than 50 ft. thick at atmospheric pressure, should be so nearly the same as the average ionization in the 660 pound bomb containing more than thirty times as much air.

Ionization by Gamma-Rays

In order to compare the effects of cosmic rays and gamma-rays, about 2.85 mg of radium sulphate equivalent to 2 mg of Ra in Aug., 1923, sealed and enclosed in a container (apparently with 7.5 mm lead and 1.5 mm steel walls) was placed in a cabinet about two ft. outside the water tank surrounding the bomb. The radium was thus displaced horizontally about 9 ft. from the axis of the bomb, and about 21 in. below its center. The lead and water shields were removed from about the bomb, but the gamma-rays still had to penetrate the 9 mm lead-steel container, 2.5 in. of wood, 8.5 ft. of air, and the 1.7 to 6 in. steel walls of the bomb. With this arrangement, the gamma-ray ionization produced in the 13.8 liter chamber at the high pressures was about five times as great as that produced by the cosmic radiation with lead and water shields. Although the same potential, about 875 volts, which has been impressed across the ionization chamber throughout these investigations was

still used, it was perhaps not sufficient to produce saturation. At the highest pressure employed a decrease of 29 percent in the impressed voltage produced a decrease of about 1 percent in the ionization current.

The gamma-ray ionization is shown plotted against the pressure in Fig. 3. The values shown are not those actually observed. From the observed values were subtracted the residual ionization observed at corresponding pressures with no shields, curve I, Fig. 5, of the paper of reference 1. The differences,

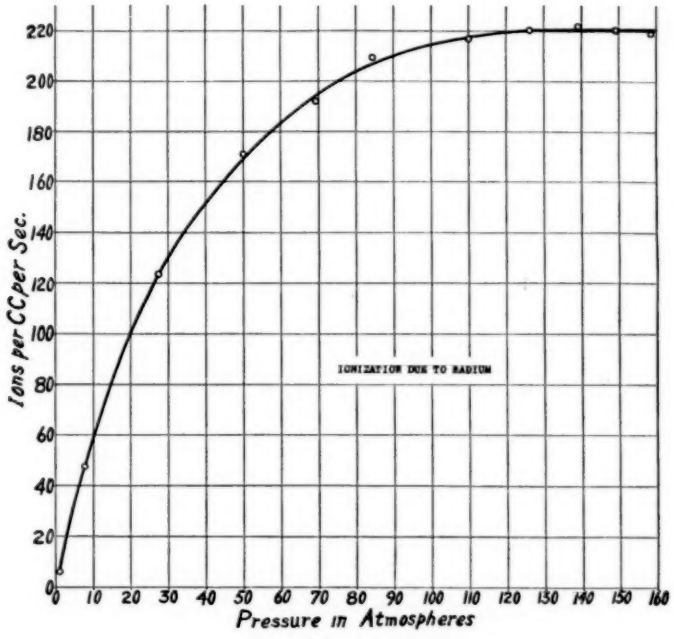

Fig. 3.

considered to represent the ionization actually produced by the gamma-radiation, are shown in Fig. 3.

The ratios of the gamma-ray ionization I_R to the cosmic-ray ionization I_C at corresponding pressures are shown in Table I. The cosmic-ray ionization values considered in this table are those obtained with both lead and water shields, represented by curve IV, Fig. 5, of the paper of reference 1. It is seen that the ratio is not quite constant, although it is nearly so at pressures above 60 atmospheres. This is not in full agreement with the observations of Comp-

TABLE I.

Atm. press.	0.82	10	20	30	40	50	60	70	80	90
I_R/I_C	4.21	4.90	4.97	5.07	5.07	5.13	5.17	5.20	5.20	5.17
Atm. press.	100	110	120	130	140	150	160			
I_R/I_C	5.16	5.16	5.17	5.17	5.18	5.18	5.18			

[16] J. C. Stearns and W. Overback, Phys. Rev. **40**, 636 (1932).

ton, Bennett and Stearns.[7] Stearns and Overback[16] have recently found the ratio to be constant for pressures between 5 and 70 atmospheres. The smaller ratios at low pressures in the present instance might possibly be explained in terms of a very minute contamination of the vessel with decreasing effectiveness at higher pressures, of the type described by Millikan.[17] That such a contamination must necessarily be very small has been shown by the experiments with different shields at high and low pressures.[1] In any case, however, it is seen that the agreement between the gamma- and cosmic-ray ionization-pressure curves is entirely too good to permit of the explanation solely in terms of secondary radiations from the walls, in view of the conclusion that the ranges of these radiations should increase with the penetrability of the incident radiation.

Temperature Effect

To vary the temperature of the bomb, steam was passed from the University heating plant into the water surrounding the bomb and circulation was provided by a centrifugal pump which withdrew water from the bottom of the tank and returned it at the top. The lead shield was not used during

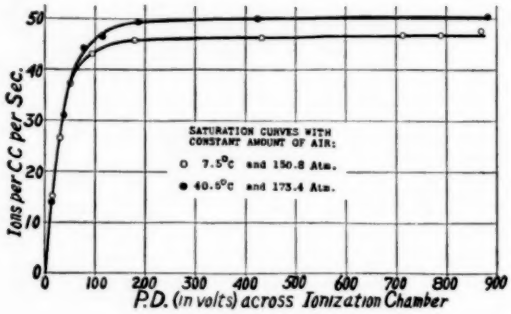

Fig. 4.

the temperature measurements. The water level was maintained constant during the temperature changes, this level being about $\frac{5}{8}$ in. lower than the top of the tank whereas previous experiments with the water shield were all made with the tank full. The steam was available only at a low pressure. In view of this fact it is apparent that changes in the temperature of the 660 lb. steel bomb, surrounded by an air space about 3 to 4.5 in. thick and then by more than 15,000 gallons of water, could be produced only very slowly.

Cold water was first passed rapidly into the tank through fire hoses. About 24 hours later ionization measurements were begun. In order to demonstrate the degree of saturation, observations were made with different applied potentials. The relation between the ionization and the potential drop across the ionization chamber, itself, is shown by the lower curve of Fig. 4. During these observations the average temperature of the bomb was 7.5°C, the average pressure of the gas was 150.8 atmospheres, and the barometric pressure, 24.55 in. The value of the ionization was considered to be

[17] R. A. Millikan, Phys. Rev. **39**, 397 (1932).

46.8 ions per cc per sec. The high potential observations were made first, and during the 10.5-hour period of the observations the temperature was decreasing at the rate of about 0.05°C per hour.

Steam was next passed into the water for several days. The steam was then shut off and another series of observations similar to those at the low temperature were made. During this period the average temperature was 40.5°C, the average pressure 173.4 atmospheres, and the barometric pressure, 24.87 in. The ionization under these conditions was considered to be 50.1 ions/cc sec. The temperature was again decreasing at the rate of about 0.05°C per hour. The ionization-potential relation under these conditions is shown by the upper curve of Fig. 4.

The air used during these observations was retained in the chamber at constant density for about a month, during which period a 15-day series of observations relative to the diurnal variation[18] were made, the same air being used later for the γ-ray measurements described earlier in this paper. During this time no leak was observed. During the 15-day series of observations, the average ionization was 47.25 ions/cc sec., the average temperature, 17.42°C, and the average barometric pressure, 24.73 in.

After measurements at 205 atmospheres to be described later, the air was released to about 22.2 atmospheres. The ionization at this pressure is designated by the lower curve of Fig. 6. After apparent equilibrium had been attained the ionization was found to be 23.43 ions/cc sec. at a pressure of 22.2 atmospheres and a temperature of 14.45°C, the barometric pressure being 24.87 in. During these observations the temperature of the bomb was increasing at the rate of 0.12°C per hour.

Later the same air was heated in the manner described above. At an average temperature of 47.25°C and a pressure of 24.3 atmospheres, with the temperature decreasing at the rate of 0.13°C per hour, the average of 12 ionization readings was 25.48 ions/cc sec., the barometric pressure being 24.43 in. The dependence of the ionization upon impressed P.D. was not investigated at the lower pressures, the maximum P.D. employed at the high pressures being used as usual. It should be mentioned that all pressures given are pressures read directly from the gauge, plus the atmospheric pressure.

It is seen that at a mean pressure of 162.1 atmospheres, changing the temperature from 7.5°C to 40.5°C resulted in an increase of the ionization amounting to about 7 percent of the lower value. At a mean pressure of 23.3 atmospheres, changing the temperature from 14.45°C to 47.25°C resulted in an increase of 8.7 percent. These are the values given in a recent note.[19] As stated there, these values had not been corrected for effects of variations in the density of the water shield with temperature, or for the effects of variations in barometric pressure. It appears that the alteration of the ionization due to change in the shielding provided by the water would amount to considerably less than 1 percent and may be neglected. A correction for barometric pressure appears to be necessary, however. When the 15-day series of

[18] The results of this investigation will be presented in an early publication.

[19] J. W. Broxon, Phys. Rev. **40**, 1022 (1932).

observations was considered, it was found that an increase of about 0.187 in. in the barometric pressure appeared to result in a decrease of 1 percent in the ionization.

The variation of the ionization with barometric pressure as designated above was somewhat larger than had been expected. Moreover, it was found that an error had been made in recording the barometric pressure during the high pressure observations. When the readings are reduced to the average barometric pressure during the 15-day series, it is found that the variation with temperature at the high pressures is greater than that at the low pressures. Thus when the barometric correction is made, the temperature effect at 23.3 atmospheres amounts to 6.2 percent for 32.8°C change in temperature, or 0.19 percent per degree. At 162.1 atm. the increase is 8.9 percent for an increase of 33.0°C, or 0.27 percent per degree. When the three ionization values, measured at constant density but different temperatures at the high pressures, are plotted against the temperature, the ionization appears to increase slightly more rapidly with increase of temperature at the higher temperatures. With such a limited number of observations, however, this observation is probably of little consequence.

The temperature effect measured at the higher pressures is seen to agree rather well with that predicted by Compton, Bennett and Stearns.[7] That observed at 23.3 atmospheres, however is considerably larger than that predicted by them, although the variation with pressure is in the right sense. The disagreement with their experimental observation with γ-ray ionization in nitrogen at 20 atmospheres is decided. The effect at 23.3 atmospheres is in good agreement with the 0.14 percent per centigrade degree observed by Wolff[20] for the γ-ray ionization in nitrogen at 21.5 atmospheres, however.

Transient Effects

As mentioned in a former paper,[1] "If measurements were made immediately after filling, larger values were obtained than after the establishment of equilibrium conditions. Therefore, from two to six hours were allowed to elapse after filling the chamber before measurements of the ionization were begun." In view of the observed temperature effect, it was thought that the high values immediately after filling the ionization chamber might be explained by the very considerable increase of the temperature of the air upon compression. The effect is shown clearly by Fig. 5, representing the first complete set of observations made with the present apparatus March 29 and 30, 1930, with no shields. In Fig. 5 as in Fig. 6, the circles represent individual observations instead of the usual average of three or four observations. The curve shown in Fig. 5 is not drawn with reference to the observations therein designated. It is curve I of Fig. 5 of the paper of reference 1, obtained under the same conditions but with a new supply of air on April 26 and 27, 1930, time for equilibrium conditions being allowed in the latter case.

The values observed very soon after filling are seen to be nearly twice as great as the equilibrium value. Increase of temperature of the bomb showed

[20] K. Wolff, Zeits. f. Physik **75**, 570 (1932).

the gas might have been heated some fifty degrees above the final temperature when compressed into the bomb. However, the temperature chart showed that the bomb had acquired a practically constant temperature before measurements were begun. Any change of temperature of the gas during the observations must have been rather small, although its temperature was probably still decreasing slightly.

In order to determine more carefully the relation between the ionization values and the time after filling, the bomb was filled with air to a pressure a

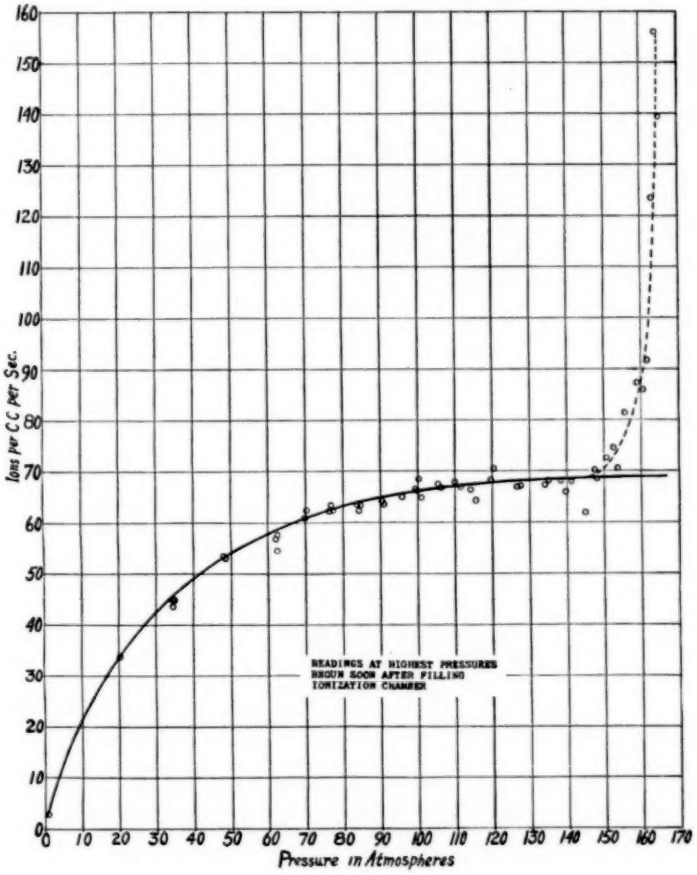

Fig. 5.

little above 205 atmospheres. The water shield with its surface $\frac{5}{8}$ in. below the top of the tank was used in this instance. The limit of the calibrated gauge used heretofore being 2500 lbs. per sq. in., the higher pressures were read on a second gauge which agreed with the first at pressures near its upper limit. After filling, the high potential was applied for a 15-minute interval before observations were begun. This has been the usual procedure. Single observations plotted against the time after filling the chamber are shown in the upper curve of Fig. 6.

The values obtained were again high at first, although as in the earlier

case the bomb appeared to have acquired an equilibrium temperature before readings were begun. That the effect was not an ordinary electrical one is indicated by the fact that when the air is allowed to remain in the bomb for several hours or even days, no initial high values are observed when readings are begun, the preliminary 15-minute application of the potential always being made, of course.

The lower curve of Fig. 6 represents the ionization as a function of the time after releasing the air rapidly from about 169 to about 22 atmospheres. The potential was applied almost constantly while the air was being released, so that observations could be begun very soon after closing the valve. A slight increase was again observed, but much smaller than that following compression. A brief reference to disturbances accompanying variations in pressure has been made by Steinke and Schindler.[21]

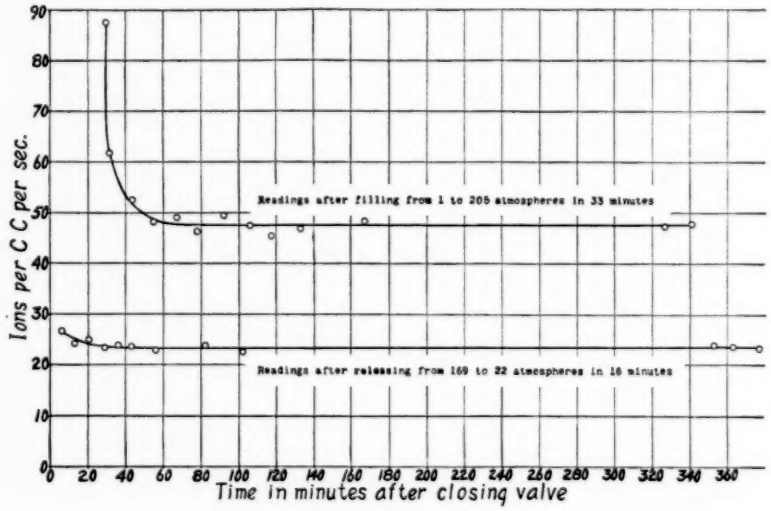
Ions per C C per sec.
Readings after filling from 1 to 205 atmospheres in 33 minutes
Readings after releasing from 169 to 22 atmospheres in 16 minutes
Time in minutes after closing valve

Fig. 6.

Another transient effect of some interest was observed during the temperature variations. Although changes in temperature were necessarily quite slow, the ionization at a particular density and temperature appeared to depend somewhat upon the rate of change of temperature. When the temperature was falling lower values were observed than when it was rising, so that during the investigation of the temperature effect the final steady values at a given temperature were anticipated somewhat.

The natural supposition is that these transient effects may at least to some extent be explained in terms of the characteristics of the measuring equipment. In view of the elaborate guard system and the null method employed, however, the explanation does not appear obvious to the writer.

Occasional sudden increases in the ionization current during a reading have been observed. These are quite infrequent and appear always to be well defined. Such readings have been discarded. It has been suggested that these

[21] E. G. Steinke and H. Schindler, Naturwiss. **20,** 15 (1932).

sudden increases might be due to nuclear disintegration in the gas by the cosmic rays. This possibility will receive attention in future work.

Constancy of Ionization at High Pressures

After making the observations at 205 atmospheres, the air was released to 172 atmospheres. When corrected for barometric pressure, the ionization values at these two pressures were found to be nearly identical. When further corrected for the slight difference in shielding, these observations at 205 and 172 atmospheres, made in May, 1932, are only about one percent greater than the values measured with the water shield in July, 1930, at pressures between 130 and 165 atmospheres. If one may assume that there is no variation with time, the variation of cosmic-ray ionization with pressure between 130 and 205 atmospheres may be considered to be only about one percent.

Saturation

The degree of saturation attained is shown quite well in the curves of Fig. 4. Made with constant gas quantity, they represent the dependence of the current upon the applied P.D. at the pressures and temperatures shown.

Very nearly constant values appear to have been obtained in both cases. However, there is a possible increase in the ionization of one percent at the high potential end of the curves, due to doubling the applied P.D. Saturation appears much more nearly complete than in the curves of Professor Erikson's[10] experiments with γ-rays at corresponding pressures, although he used much more intense fields. Of course, the ionization he employed was vastly more intense, but if all free ions were drawn out before recombination and the lack of saturation at the high gradients was entirely attributable to (initial) recombination with the parent atoms, one should expect the degree of saturation to be independent of ion density, as Bowen[9] points out.

Bowen found that reducing the γ-ray ionization by a factor of about five at a pressure of 93 atmospheres produced very little change in the variation of the ionization current with potential gradient except at the lower gradients. It is rather surprising that the residual ionization, further reduced by a factor of about four, more nearly resembles the intense than it does the weaker γ-ray ionization in its dependence upon the gradient at that pressure, even at the lower gradients. It is these residual ionization currents which are more nearly comparable to those discussed in this paper. Throughout the range of gradients he investigated, Bowen found that at 93 atmospheres an increase of the gradient by a factor of about four produced an increase in the residual ionization current of from nearly 6 to a little more than 12 percent. This is possibly in conflict with the fact that in the present investigation the ionization in the small sphere was slightly less than that in the large one at 93 atmospheres (see Fig. 2). Since the central rods were of nearly the same size in the two cases, reduction of the radius of the surrounding vessel by a factor of more than three with the same applied P.D. of about 875 volts, should have increased the average gradient in the region of weak fields, in the neighborhood of the outer wall, by a factor probably greater than the radius ratio,

although the increase of the volume average may have been small. According to Bowen's observations, then, one might expect that an appreciably greater ionization should have been measured in the small sphere than in the large one at 93 atmospheres.

Conclusions

The experiments herein described constitute further evidence in favor of the contention that the explanation of the characteristics of cosmic-ray ionization at high pressures, entirely in terms of secondary radiations from the vessel walls, is quite inadequate. The experiments with the thin central sphere and with gamma-rays can not be reconciled with that explanation.

As has been mentioned, Bowen's[9] observations of the dependence of the ionization upon potential gradient are in conflict with the details of the initial or selective recombination theory of Compton, Bennett and Stearns.[7] The curves of Fig. 4 and the observations with the small sphere appear to agree rather better with their conclusions than with those of Bowen, although a small final slope persists in the "saturation" curves. The considerable temperature effect at 23.3 atmospheres is not in quantitative agreement with their conclusions, however.

In spite of the remarkable agreement between the ionization curves of Fig. 2, the excess of ionization in the small thin central sphere over that in the large bomb in the region from 30 to 50 atmospheres appears too great to be due to experimental error. This difference might be explained in terms of secondary radiations[22] from the walls.

If, in view of the observed similarities in the characteristics of cosmic- and gamma-ray ionization at high pressures we may consider Professor Erikson's[10] observations comparable with these, the ionization should have passed through a maximum within the pressure range of the present experiments. The constant values in the present instance appear to extend over a region of at least 75 atmospheres. No maxima of such breadth were observed by Professor Erikson. Also, the equation deduced by Compton, Bennett and Stearns to approximate the writer's experimental observations indicates that an increase of 2.8 percent should accompany an increase in pressure from 130 to 205 atmospheres, whereas no increase amounting to half this much was observed. The difference is too small to be conclusive, however.

One common characteristic of both the explanations of the pressure effect is their emphasis of the importance of ionization by secondary radiations. A primary electron or proton ejected by incident cosmic radiation could scarcely be expected to recombine with its parent atom. In view of the fact that the ionization is supposed to occur chiefly through the agency of subsidiary radiations, it seems to the writer that there is another possibility deserving of some consideration. Studies of the ionization produced by alpha-rays in different gases and of the ionization potentials of these gases have shown[23] that "for the diatomic gases examined, *viz.*, H_2, N_2, O_2, the difference

[22] H. Geiger, Nature **127,** 785 (1931); H. Schindler, Zeits. f. Physik **72,** 625 (1931).

[23] Rutherford, Chadwick and Ellis, *Radiations from Radioactive Substances*, p. 81. R. W. Gurney, Proc. Roy. Soc. **A107,** 332 (1925).

between the energy spent and the minimum energy required to ionise the atom . . . is very marked. In fact only about half the energy spent is required to ionise the atom. This would indicate that a considerable part of the energy of the α-particle is used up in processes which do not involve ionisation, i.e., in excitation or dissociation of the molecules." The differences are found to be much smaller in the case of the monatomic gases, particularly helium.

If this explanation is correct, it seems that a considerable portion of the gamma- and cosmic-ray energies, through the agency of subsidiary radiations, might eventually be used otherwise than in the formation of ions. Should a portion of the energy finally be dissipated in some manner such as that suggested above, such molecular processes and consequently the efficiency of ionization might be expected to depend to a considerable extent upon temperature and pressure. If such a point of view is tenable, one might expect the effects to be less in the monatomic gases.

If, as Compton, Bennett and Stearns[7] maintain, the differences between the values of the ionization measured in nitrogen and in air may be explained in terms of the selective or initial recombination hypothesis, then it should follow that complete saturation is very difficult to obtain even at atmospheric pressure. The writer has shown that the greater ionization in nitrogen persists even to atmospheric pressure.[2] In view of this and the considerable temperature effect in the neighborhood of 20 atmospheres, it seems that a careful scrutiny of ionization processes in different gases with especial regard to molecular structure should be of value. Further work of this nature is being carried on.

The writer is again indebted to Professor G. B. Williston, Mr. L. Strait and Mr. G. T. Merideth for assistance in recording observations, and to Professor S. L. Simmering and Mr. C. A. Wagner for compressing the air used in these experiments. The splendid work of Mr. M. M. Eaton, departmental mechanician, in constructing the ionization chamber and accessories is very much appreciated.

X-Ray Diffraction in Ethyl Ether near the Critical Point

By F. H. WALDEMAR NOLL
State University of Iowa

(Received September 16, 1932)

X-ray diffraction ionization curves were obtained for ethyl ether at 43.5 ± 0.7 kg/cm² pressure with temperatures in the range from 25°C to 210°C. The critical pressure and temperature of ether are 36.7 ± 0.2 kg/cm² and 194.6 ± 0.3°C, respectively. In the region of the higher temperatures the ionization curves are a combination of the liquid and polyatomic gas types, falling rapidly near 0° with increasing angle, then rising to a distinct peak and again falling. Liquid semi-orderly "cybotactic" groups are in evidence from room temperature to 199°C but not for specific volumes greater than the critical specific volume. It seems reasonable to expect vanishing of these groups at the critical point. The influence of the polyatomic gas type begins to appear at the low temperatures and increases with temperature. The liquid type decreases almost linearly until 155°C where it begins to fall off very rapidly. The observations are in excellent accord with the "cybotactic" view of the interior of a liquid.

THERE are many experiments which are most readily interpreted by the view of Stewart[1] that there are, within a liquid, molecular aggregates of sufficient size and orderliness to give marked x-ray diffraction bands. These "cybotactic" groups are not permanent and do not retain the same constituent molecules. It is interesting to ascertain if this condition of semi-orderly groups exists near the critical point, and if so, how it varies with temperature.

APPARATUS AND METHOD

The x-ray spectrometer used, and the method of procuring diffraction curves, is essentially the same as the apparatus and procedure described by Stewart and Morrow.[2] The diffraction effects obtained are produced by Mo $K\alpha$-radiation. The x-ray beam was made partially monochromatic by use of a zirconium oxide filter. The voltage applied was such as to produce a general radiation maximum at about 6°. Its influence is nevertheless noticed in the experiments, but does not interfere with the results and conclusions.

The liquid chosen was ethyl ether. The critical temperature[3] is $194.6° \pm 0.3$°C and the critical pressure is 36.7 ± 0.2 kg/cm². The pressure selected in this investigation, 43.5 ± 0.7 kg/cm², is not very near the critical pressure of 36.7 kg/cm². The higher pressure was necessary to prevent excessive density variations which could be produced by the slight unavoidable temperature fluctuations.

The liquid was contained in an aluminum tube with an external diameter of 1.0 cm and a wall thickness of 0.0176 cm. The optimum thickness of

[1] See articles by Stewart and co-workers, Phys. Rev., 1927–1932. For review of literature, Good, Helv. Physica Acta. p. 205 (1930); Debye, Ergebnisse der tech Röntgenkunde **2,** *1* (1931).

[2] Stewart and Morrow, Phys. Rev. **30,** 232 (1922).

[3] Schroer, Zeits. f. phys. Chem. **140,** 381 (1929).

ether under the selected pressure is 1.77 cm at 25°C and 6.3 cm at 210°C. The thickness of the ether column is thus always less than the optimum thickness. The aluminum tube was connected to a "U" tube, and thence to a Crosby dead weight gauge tester. The "U" tube was half filled with mercury, the gauge and connections were filled with oil, and the aluminum tube and connections were filled with ether. A special electric furnace with aluminum foil windows surrounded the aluminum tube. Temperature was measured with a constantan-copper thermocouple. All curves were corrected for scattering from the aluminum container, for decrease of density of the ether due to temperature increase, for cross fire slit penetration and for drift due to the penetrating radiation. No correction was made for the accentuation of general radiation by the aluminum container as this effect has no influence upon the conclusions.

Experimental Results

X-ray diffraction ionization current curves, pressure constant at 43.5 ± 0.7 kg/cm², were obtained for the following temperatures, 25°C, 137°C, 155°C,

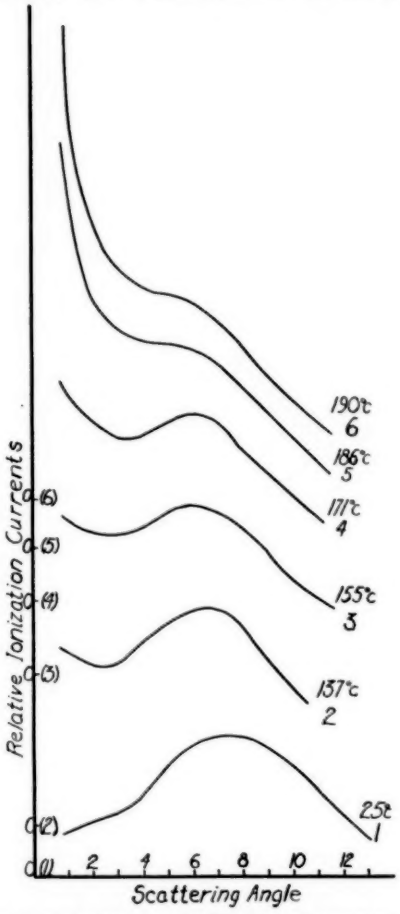

Fig. 1. Relative x-ray diffractions intensities of ethyl ether at a pressure of 43.5 ± 0.7 kg/cm².

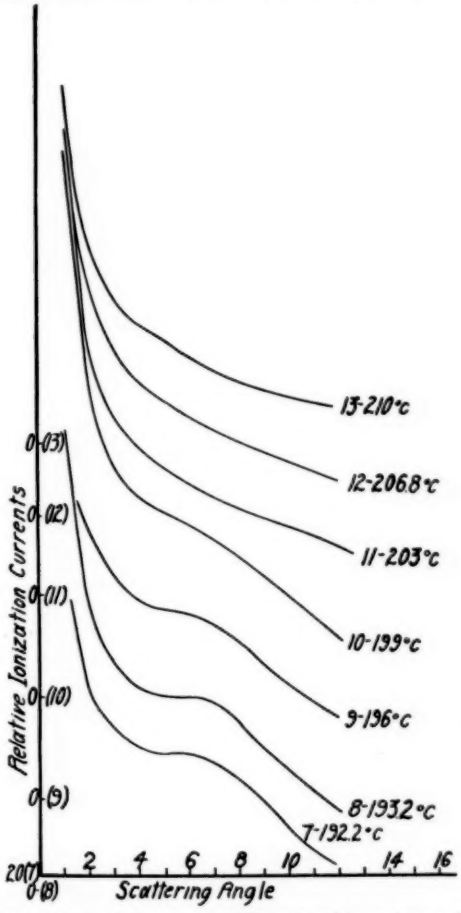

Fig. 2. Relative x-ray diffraction intensities of ethyl ether at a pressure of 43.5 ± 0.7 kg/cm².

171.4°C, 186°C, 190°C, 192.2°C, 193.2°C, 196°C, 199°C, 203°C, 206.8°C and 210°C. See Figs. 1 and 2.

A liquid type of curve is that obtained at 25°C.[4] A polyatomic gas type[5] is that obtained at 210°C. In the former case, there is a broad peak at 7.5° and 25°C with a decrease at both smaller and larger angles. In the gas type, the intensity is high near 0° but falls rapidly with increasing angle, the slope decreasing in magnitude. In point of fact, the 25°C curve shows an effect near zero that may be attributed to random molecules or molecules giving a gas type scattering. Indeed, the entire set of curves in Figs. 1 and 2 can be described by regarding the molecules as being either at random or in organized groups. Of course, this is not accurate, for there are conditions representing all gradations between these two extremes. If peak heights are plotted against temperature, Fig. 3 is obtained.

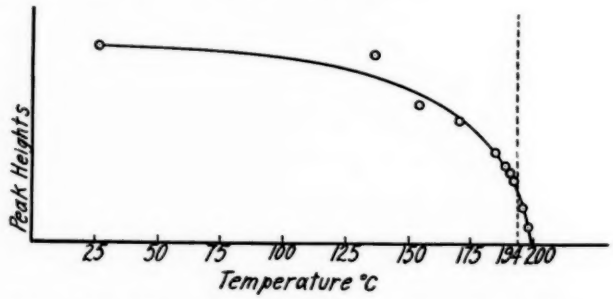

Fig. 3. Relative peak heights-temperature curve for ethyl ether.

The following results appear in the ionization curves as temperature is increased from 25° to 210°C, pressure being constant. (1) Peak heights decrease and finally disappear at about 5°C above the critical temperature. (2) Small angle scattering increases more and more rapidly as temperature increases. (3) Peaks become broader and the peak maximum shifts to smaller angles. However, the curves are too diffuse to obtain useful measurements on these two points. (4) In general, the curves may be described as changing from a liquid pattern to a gas pattern. (5) It is an interesting fact that no liquid peaks appear at a specific volume as great as the critical specific volume. A discussion of this point will appear in later publications from this laboratory.

Studies on the effect of temperature upon liquid x-ray diffraction have been made by Skinner,[6] Stewart,[7] Vaidyanathan,[8] Ramasubramanyan,[9] and Tanaka and Tsuji.[10] Results stated here are either in agreement with or not

[4] Similar curves can be found in the literature by Stewart mentioned in reference 1.

[5] This type can be found in various reports, for example, see Debye, Phys. Zeits. **31,** 419 (1930) and Wollan, Phys. Rev. **37,** 862 (1931).

[6] Skinner, Phys. Rev. **36,** 1025 (1930).

[7] Stewart, Phys. Rev. **37,** 9 (1931).

[8] Vaidyanathan, Ind. Jour. Phys. **3,** 391 (1929).

[9] Ramasubramanyam, Ind. Jour. Phys. **3,** 137 (1928).

[10] Tanaka and Tsuji, Kyoto Coll. Sci. Mem. **13,** 337 (1930).

contradictory to those obtained by the authors just mentioned. In respect to the increase of small angle scattering with increase of temperature, all observers are in agreement.

Discussion

With temperature increase, under the stated pressure, one might generally expect, (a) decreased molecular attractive forces because of increased separation resulting from thermal expansion and (b) increased thermal agitation. These should decrease the conditions favorable for the existence of the cybotactic groups. With temperature increase one might then expect that the percent of grouped molecules and regularity of space array within groups at any instant would decrease and that the percentage of "more random" molecules should increase. The former causes the peak heights to decrease. Because of increased irregularity of array peaks would become broader. The intensity of scattering from the "more random" molecules would increase and this means an increased small angle scattering. Assuming that Bragg's law here applied measures the distance between approximate planes of scattering centers, then expansion should shift the maximum to smaller angles. With continued increase of temperature the conditions favorable for the existence of groups would ultimately vanish and the liquid diffraction pattern cease to exist. The above interpretations based on the cybotactic theory are in accord with the experimental results already described.

At the critical point the liquid and vapor phases merge into one phase. It seems reasonable to suppose that the characteristic of the liquid phase, which is the cybotactic group formation, would cease to exist at this point. According to this view, if the substance were at a less specific volume and higher pressure, since the molecules are in closer proximity, the groups might exist at a temperature above the critical one. This is the experimental fact.

The general conclusion from these experiments is that the cybotactic view is corroborated and that the molecules of ethyl ether in these experiments may be roughly regarded as existing either in semi-orderly groups, or as approximately random molecules.

The writer wishes to express his appreciation to the members of the Physics Department for their assistance and his thanks to Professor G. W. Stewart who proposed the problem and under whose direction this study was made.

The Approximation of Geometric Optics as Applied to a Dirac Electron Moving in a Magnetic Field

By Otto Laporte
University of Michigan

(Received August 30, 1932)

The problem of a Dirac electron in a homogeneous magnetic field is integrated according to the recently published approximative method of Pauli. Homogeneous linear equations furnish, except for a multiplicative function, the eigenfunctions in zero approximation. An important condition of compatibility of the zero and first approximation determines these multiplicative functions. For the connection of the solution in the classically occupied regions with those that are classically not reached the Kramers connection formulae are used. The eigenvalue determination gives the result that the phase-integral is to be quantized not with half quantum numbers as is the case unrelativistically, but with whole quantum numbers, each level possessing a twofold degeneracy.

1.

THE advantages of the approximative method, due to Wentzel,[1] Brillouin[2] and Kramers[3] of solving the Schrödinger equation are well known. In the limiting case of large quantum numbers this "W.K.B. method" allows the asymptotic calculation of eigenfunctions and eigenvalues.

In a recent paper[4] W. Pauli has developed the corresponding approximative method for Dirac's relativistic wave equation of the electron. This problem differs from that of solving approximately the Schrödinger equation inasmuch as instead of one wave function ψ there are four $\psi_1 \cdots \psi_4$. If S is the classical relativistic action function of the problem, it is best to put

$$\psi_\rho = a_\rho e^{iS/h} \qquad \rho = 1 \cdots 4 \qquad (1)$$

and to develop the amplitudes a_ρ into a power series in h/i

$$a_\rho = a_\rho^{(0)} + (h/i)a_\rho^{(1)} + \cdots . \qquad (2)$$

It is well known that the W.K.B. method is analogous to the transition from wave optics to geometric optics in isotropic media; the Hamilton-Jacobi partial differential equation appears then as the equation for the eiconal function. In the case of a non-scalar wave function the Eqs. (1) and (2) give in zero approximation, as is to be expected, the equations of relativistic mechanics, or optically spoken, of geometric optics with polarization. However, and this is essential, the spin of the electron or its optical analog, double refraction, does not appear until the next approximation at the same time

[1] G. Wentzel, Zeits. f. Physik **38,** 518 (1926).
[2] L. Brillouin, C. R., July, 1926.
[3] H. A .Kramers; Zeits f. Physik **39,** 828 (1926); also Zwaan, *Diss. Utrecht.*
[4] W. Pauli, Helvetica Physica Acta **5,** 180 (1932).

as diffraction effects make themselves felt, since the spin moment is proportional to the Planck constant.

We shall here apply Pauli's method to the case of an electron moving in a homogeneous magnetic field. Eigenfunctions are obtained and connected by means of the "Kramers connection formulae." The eigen-value determination shows that the phase integral should be quantized with whole numbers, but that a double degeneracy occurs.

2.

We write the Dirac equations:

$$\left(\frac{h}{i}\frac{\partial}{\partial x_0} - e\phi_0\right)\psi_\rho + \alpha_{\rho\sigma}{}^k\left(\frac{h}{i}\frac{\partial}{\partial x_k} + \frac{e}{c}\phi_k\right)\psi_\rho + mc\beta_{\rho\sigma}\psi_\sigma = 0 \tag{3}$$

where $x_0 = ct$; $x_k = x, y, z$; ϕ_0 is the scalar, ϕ_k the vector potential of the external field. Roman indices run from 1 to 3, Greek ones from 1 to 4. Indices occurring twice are to be summed. The α^k and β are the well-known matrices which obey the usual conditions of anticommutability. Introducing (1) and (2) into (3) we obtain in zeroth and first approximation:

$$-\Pi_0 a_\rho{}^{(0)} + \Pi_k \alpha_{\rho\sigma}{}^k a_\sigma{}^{(0)} + mc\beta_{\rho\sigma} a_\sigma{}^{(0)} = 0 \tag{4}$$

$$-\Pi_0 a_\rho{}^{(1)} + \Pi_k \alpha_{\rho\sigma}{}^k a_\sigma{}^{(1)} + mc\beta_{\rho\sigma} a_\sigma{}^{(1)} = -\left(\frac{\partial a_\rho{}^{(0)}}{\partial x_0} + \alpha_{\rho\sigma}{}^k \frac{\partial a_\sigma{}^{(0)}}{\partial x_k}\right) \tag{5}$$

where

$$\Pi_0 = -\frac{\partial S}{\partial x_0} + \frac{e}{c}\phi_0; \quad \Pi_k = \frac{\partial S}{\partial x_k} + \frac{e}{c}\phi_k. \tag{6}$$

Corresponding equations hold for higher approximations. Condition for the solubility of the homogeneous system (4) for $a_\rho{}^{(0)}$ is that its determinant must vanish. This is equivalent with:

$$-\Pi_0{}^2 + \Sigma\Pi_k{}^2 + m^2c^2 = 0 \tag{7}$$

which is the Hamilton-Jacobi partial differential equation. Let us assume that as far as its classical-mechanical aspects are concerned, the problem has been solved, so that we know Π_0, Π_k as functions of the coordinates. It is then seen that the system (4) has *four* solutions $a_{\rho\tau}{}^{(0)}$ $(\tau = 1 \cdots 4)$. They are, except for a multiplicative constant to be determined later,

$$a_{\rho\tau}{}^{(0)} = \Pi_0 \delta_{\rho\tau} + \alpha_{\rho\tau}{}^k \Pi_k + mc\beta_{\rho\tau}. \tag{8}$$

It is easily seen by direct substitution that (8) satisfies (4) for any index τ. The above solutions are, however, not linearly independent, as there are the following four relations between them:

$$-a_{\rho\tau}{}^{(0)}\Pi_0 + a_{\rho\sigma}{}^{(0)}\alpha_{\sigma\tau}{}^k\Pi_k + a_{\rho\sigma}{}^{(0)}\beta_{\sigma\tau}mc = 0 \tag{9}$$

which form the adjoint system to (4). Each equation of this adjoint system connects three of the solutions (8); it is thus possible to express two of the

$a_{\rho\tau}{}^{(0)}$ by two others leaving only two linearly independent solutions (say $a_{\rho 1}{}^{(0)}$ and $a_{\rho 2}{}^{(0)}$) of (4). This is as it should be; the two independent solutions correspond to the two directions of the spin (or of the polarization). The general solution of (4) is then obtained by multiplying $a_{\rho 1}{}^{(0)}$ and $a_{\rho 2}{}^{(0)}$ with two as yet arbitrary functions C and C' of the coordinates and by adding:

$$a_\rho{}^{(0)} = C(x_0, x_k)a_{\rho 1}{}^{(0)} + C'(x_0, x_k)a_{\rho 2}{}^{(0)} \tag{10}$$

The determination of C and C' follows from (5), which is an inhomogeneous system whose homogeneous system has solutions. As is well known, the right-hand side of (5) and the solutions of the adjoint homogeneous system (9) have to be orthogonal, which condition can be put into the following form:

$$\bar{a}_{\rho\tau}{}^{(0)}\left(\frac{\partial a_\rho{}^{(0)}}{\partial x_0} + \alpha_{\rho\sigma}{}^k\frac{\partial a_\sigma{}^{(0)}}{\partial x_k}\right) = 0; \qquad \tau = 1, 2. \tag{11}$$

where we indicate by the bar, that the complex conjugate has to be taken (provided, as will be the case, that the Π themselves are real). Having determined C and C' by means of these differential equations,

$$a_\rho{}^{(0)}e^{iS/h}$$

represents in first approximation the wave functions everywhere except in the vicinity of the turning points of the classical orbit, where certain of the Π_0, Π_k vanish, and the approximation of geometric optics breaks down. How to deal with these exceptional points, will be seen later.

3.

We put the magnetic field H parallel to the z axis of a cartesian coordinate system. The scalar potential ϕ_0 is zero; the vector potential is chosen to be:

$$\phi_1 = -H_y;\ \phi_2 = 0;\ \phi_3 = 0. \tag{12}$$

The Hamilton-Jacobi differential Eq. (7) becomes:

$$-\left(\frac{\partial S}{\partial x_0}\right)^2 + \left(\frac{\partial S}{\partial x} - \frac{eH}{c}y\right)^2 + \left(\frac{\partial S}{\partial y'}\right)^2 + \left(\frac{\partial S}{\partial z}\right)^2 + m^2c^2 = 0. \tag{13}$$

Since x_0, x and z are evidently cyclic, we put:

$$S = -\Pi_0 x_0 + p_x x + \Pi_3 z + \sigma(y) \tag{14}$$

where Π_0, Π_3 and $p_x = m\dot{x}$ are constant. We introduce for the sake of brevity

$$\Pi_\tau{}^2 = \Pi_1{}^2 + \Pi_2{}^2 = \Pi_0{}^2 - \Pi_3{}^2 - m^2c^2 \tag{15}$$

the constant momentum in the x, y plane. For $\sigma(y)$ we have:

$$\sigma = \int^y \Pi_2 dy = \int^y \left[\Pi_\tau{}^2 - \left(p_x - \frac{eH}{c}y\right)^2\right]^{1/2} dy. \tag{16}$$

The radicand vanishes at the turning points $y_1 < y_2$.

$$(eH/c)y_{2,1} = p_x \pm \Pi_\tau.$$

It is seen that the orbits are circles with the radius $(c/eH)\Pi_r$ whose centers lie on a line parallel to the x axis and at a distance $(c/eH)p_x$ from it.

4.

It is now necessary to specialize the matrices α^k and β. We take the following well-known matrix system:

$$\beta = \begin{pmatrix} 1 & 0 & 0 & 0 \\ 0 & 1 & 0 & 0 \\ 0 & 0 & -1 & 0 \\ 0 & 0 & 0 & -1 \end{pmatrix}; \quad \alpha^1 = \begin{pmatrix} 0 & 0 & 0 & 1 \\ 0 & 0 & 1 & 0 \\ 0 & 1 & 0 & 0 \\ 1 & 0 & 0 & 0 \end{pmatrix};$$
$$\alpha^2 = \begin{pmatrix} 0 & 0 & 0 & -i \\ 0 & 0 & i & 0 \\ 0 & -i & 0 & 0 \\ i & 0 & 0 & 0 \end{pmatrix}; \quad \alpha^3 = \begin{pmatrix} 0 & 0 & 1 & 0 \\ 0 & 0 & 0 & -1 \\ 1 & 0 & 0 & 0 \\ 0 & -1 & 0 & 0 \end{pmatrix}. \tag{18}$$

Introducing these into (8) the $a_{\rho\tau}^{(0)}$ occurring in (10) are found to be:

$$\begin{aligned} a_{\rho 1}^{(0)} &= (\Pi_0 + mc, \quad 0 \quad , \quad \Pi_3, \Pi_1 + i\Pi_2) \\ a_{\rho 2}^{(0)} &= (\quad 0 \quad , \Pi_0 + mc, \Pi_1 - i\Pi_2, -\Pi_3). \end{aligned} \tag{19}$$

We then put (19) and (10) into (11) and get after a few elementary transformations:

$$\Pi_0 \frac{\partial C}{\partial x_0} + \Pi_1 \frac{\partial C}{\partial x} + \Pi_2 \frac{\partial C}{\partial y} + \Pi_3 \frac{\partial C}{\partial z} - \frac{1}{2}\left(\frac{\partial \Pi_2}{\partial y} - i\frac{\partial \Pi_1}{\partial y}\right) C = 0 \tag{20}$$

and the complex conjugate equation for C'.

It is most convenient to integrate these differential equations in the momentum space. We have

$$\partial C/\partial x_\sigma = (\partial C/\partial \Pi_\lambda)(\partial \Pi_\lambda/\partial x_\sigma)$$

which vanishes for $\sigma = 1, 2, 3$. Only the derivative with respect to y gives a contribution. Because of

$$\frac{d\Pi_1}{dy} = -\frac{eH}{c}; \text{ and } \frac{d\Pi_2}{dy} = \frac{eH}{c}\frac{\Pi_1}{\Pi_2} \tag{21}$$

one finds

$$\frac{\partial C}{\partial y} = \frac{eH}{c}\left(-\frac{\partial C}{\partial \Pi_1} + \frac{\Pi_1}{\Pi_2}\frac{\partial C}{\partial \Pi_2}\right).$$

By means of this formula and of (21) the differential Eq. (20) is readily transformed into:

$$-\Pi_2 \frac{\partial C}{\partial \Pi_1} + \Pi_1 \frac{\partial C}{\partial \Pi_2} + \frac{1}{2}\left(\frac{\Pi_1}{\Pi_2} + i\right) C = 0. \tag{22}$$

Introducing polar coordinates in the Π_1, Π_2 plane:

$$\Pi_1 = \Pi_r \sin\theta;\ \Pi_2 = \Pi_r \cos\theta$$

we get:

$$-\frac{\partial C}{\partial \theta} + \tfrac{1}{2}(\operatorname{tg}\theta + i)C = 0.$$

Since Π_r does not occur in this differential equation C is seen to be a function of the quotient Π_1/Π_2 solely. Straightforward integration gives:

$$C = \frac{K}{(\cos\theta)^{1/2}} e^{i\theta/2} = \frac{K'}{{\Pi_2}^{1/2}} \exp\left[\frac{i}{2} \operatorname{arctg} \frac{\Pi_1}{\Pi_2}\right] \tag{23}$$

or

$$C = K''\left(\frac{\Pi_1 - i\Pi_2}{\Pi_2}\right)^{1/2}. \tag{23'}$$

The latter form is obtained using the well-known connection between the arctg and the log. For C' the complex conjugate is found. Putting (23) and (19) into (10) we finally have:

$$\begin{aligned} {a_\rho}^0 = \frac{K'}{{\Pi_2}^{1/2}}\Big\{ & (\Pi_0 + mc) \exp\left[\frac{i}{2} \operatorname{arctg} \frac{\Pi_1}{\Pi_2}\right], \\ & (\Pi_0 + mc)e \exp\left[-\frac{i}{2} \operatorname{arctg} \frac{\Pi_1}{\Pi_2}\right], \\ & (\Pi_r + \Pi_3) \exp\left[\frac{i}{2} \operatorname{arctg} \frac{\Pi_1}{\Pi_2}\right], \\ & (\Pi_r - \Pi_3) \exp\left[-\frac{i}{2} \operatorname{arctg} \frac{\Pi_1}{\Pi_2}\right]\Big\} \end{aligned} \tag{24}$$

or from (23′):

$$\begin{aligned} {a_\rho}^{(0)} = K''/{\Pi_2}^{1/2}\big\{ & (\Pi_0 + mc)(\Pi_1 - i\Pi_2)^{1/2},\ (\Pi_0 + mc)(\Pi_1 + i\Pi_2)^{1/2}, \\ & (\Pi_r + \Pi_3)(\Pi_1 - i\Pi_2)^{1/2},\ (\Pi_r - \Pi_3)(\Pi_1 + i\Pi_2)^{1/2}\big\}. \end{aligned} \tag{24'}$$

With these amplitudes the current and the density take the form

$$(s_x, s_y, s_z, \rho) = 4K''\Pi_r(\Pi_0 + mc)\frac{1}{\Pi_2}(\Pi_1, \Pi_2, \Pi_3, \Pi_0)$$

in agreement with the proportion:

$$s_k : \rho = \Pi_k : \Pi_0.$$

5.

The last problem will be the determination of the multiplicative constant K. It was pointed out before that, according to the sign of ${\Pi_2}^2$ we have to distinguish three regions (compare 17):

(I) $y < y_1$ $\Pi_2 = \pm i(\Pi_1^2 - \Pi_r^2)^{1/2}$

(II) $y_1 < y < y_2$ $\Pi_2 = \pm (\Pi_r^2 - \Pi_1^2)^{1/2}$

(III) $y_2 < y$ $\Pi_2 = \pm i(\Pi_1^2 - \Pi_r^2)^{1/2}$.

II is the classically occupied interval between the two turning points. Since in I and III the action function $\sigma = \int \Pi_2 dy$ becomes imaginary they represent classically unreached regions. The approximate expressions for the wave functions have, according to (1), (14) and (16), different analytical character in the three regions: in I and III they will be exponential functions with real exponents, and in II they will be oscillating functions. In the three regions one is at liberty to multiply the wave functions with constants, the relation between which remains undetermined by our approximate method. However, these constants are determined by the requirement that our approximate wave functions in the various regions be asymptotic expressions of one and the same physically admissible solution of the rigorous Dirac equations.

In the nonrelativistic theory where the same difficulty occurs, the Kramers connection formulae show how to link up the constants inside the two turning points with those outside. The Schrödinger equation may be written in the form:

$$\psi'' + \frac{f(y)}{h^2}\psi = 0 \tag{25}$$

where $f(y)$ is a continuous function with two roots y_1 and y_2 so that for $y_1 < y < y_2$ the function $f(y)$ is positive, otherwise negative. The requirement that ψ be real and vanish for $y = \pm \infty$ restricts the choice of asymptotic solutions to those that vanish exponentially outside and oscillate like trigonometric functions inside. Now the connection formulae of Kramers state, e.g., for the turning point y_1, that for $y < y_1$, the function

$$K_{\mathrm{I}} \left| f^{-1/4} \right| \exp \left\{ \frac{1}{h} \int_{y_1}^{y} (-f)^{1/2} dy \right\} \tag{26}$$

and for $y_1 < y < y_2$ the function

$$K_{\mathrm{II}} \left| f^{-1/4} \right| \cos \left\{ \frac{1}{h} \int_{y_1}^{y} f^{1/2} dy + \epsilon \right\} \tag{27}$$

are then and only then, asymptotic representations of the same particular solution of the above differential equation if

$$K_{\mathrm{II}} = 2K_{\mathrm{I}} \text{ and } \epsilon = -\pi/4. \tag{28}$$

Similarly for the other turning point.

These considerations of Kramers can be applied to our case without change, because it is easily possible to bring our first order differential Eqs. (3) into the form of Eq. (25). For the second order Dirac equations

$$(-\Pi_0^2 + \Sigma \Pi_k^2 + m^2c^2)\psi_\rho = -(eh/2ic)(\alpha^k \alpha^l)_{\rho\sigma} F_{kl} \psi_\sigma$$

are in our case no longer simultaneous equations. The field tensor F_{kl} has only one component $F_{12}=H_z$, and the matirx $\alpha^1\alpha^2$ is diagonal, as is seen from (18). In order to get complete agreement with Kramers' form of the solutions we write the wave functions with the function C and C' in the form of (23). Then the Kramers amplitude is:

$$\left| f^{-1/4} \right| = \left| \Pi_2^{-1/2} \right| = \left| (\Pi_r^2 - \Pi_1^2)^{-1/4} \right| \tag{29}$$

and the phase is:

$$P_\rho = \frac{1}{h} \int_{y_1}^{y} \Pi_2 dy \pm \tfrac{1}{2}\left(\operatorname{arctg} \frac{\Pi_1}{\Pi_2} - \frac{\pi}{2} \right) \tag{30}$$

where according to (24) the upper sign is to be taken for $\rho=1, 3$ and the lower sign for $\rho=2, 4$. The phase constant was fixed so that P_ρ vanishes at y_1 in agreement with (26) and (27).

Since Π_2 is real within, and imaginary outside of, the interval y_1y_2, the wave function $\left|\Pi_2^{-1/2}\right| \exp iP_\rho$ will indeed oscillate in region II and will be exponentially decreasing or increasing in I and III.

Now the requirement that ψ_ρ vanish for $y=-\infty$ leaves as only choice for region I:

$$\psi_\rho^{\mathrm{I}} = K(\ )_\rho \left| \Pi_2^{-1/2} \right| \exp (+P_\rho). \tag{31}$$

As is seen from (24) the bracket with the index ρ is either Π_0+mc for $\rho=1, 2$ or $\Pi_r \pm \Pi_3$ for $\rho=3, 4$. The unessential factor $\exp i(-\Pi_0 x_0+p_x x+\Pi_3 z$ was left off.

The Kramers connection requires that this wave function is continued in II as

$$\psi_\rho^{\mathrm{II}} = 2K(\ )_\rho \left| \Pi_2^{-1/2} \right| \cos (P_\rho - \pi/4). \tag{32}$$

The analogous connection must now be carried out at the other turning point y_2. The phase Q_ρ which at y_2 plays the same rôle as P_ρ at y_1, is

$$Q_\rho = \frac{1}{h} \int_{y_2}^{y} \Pi_2 dy \pm \tfrac{1}{2}\left(\operatorname{arctg} \frac{\Pi_1}{\Pi_2} + \frac{\pi}{2} \right). \tag{33}$$

Introducing the abbreviation

$$I = \frac{1}{h} \int_{y_1}^{y_2} \Pi_2 dy = \frac{1}{2h} \oint \Pi_2 dy = \frac{c\pi}{2ehH} \Pi_r^2 \tag{34}$$

one may write (32):

$$\begin{aligned} \psi_\rho^{\mathrm{II}} &= 2K(\ )_\rho \left| \Pi_2^{-1/2} \right| \cos (Q_\rho - \pi/4 + I \pm \pi/2) \\ &= 2K(\ )_\rho \left| \Pi_2^{-1/2} \right| \left\{ \cos\left(I \pm \frac{\pi}{2} \right) \cos\left(Q_\rho - \frac{\pi}{4} \right) \right. \\ &\quad \left. - \sin\left(I + \frac{\pi}{2} \right) \cos\left(Q_\rho + \frac{\pi}{4} \right) \right\} \end{aligned} \tag{35}$$

Applying the connection formulae again, the first term inside the parenthesis gives rise to an exponentially increasing function in III, the second term to the desired exponentially decreasing function. We must therefore require

$$\cos (I \pm \pi/2) = 0$$

which gives for ψ_ρ^{III}:

$$\psi_\rho^{\mathrm{III}} = \pm K(\ )_\rho \left| \Pi_2^{-1/2} \right| \exp (-Q_\rho). \tag{36}$$

The above condition leads to:

$$I = (n + \tfrac{1}{2} \pm \tfrac{1}{2})\pi$$

or using (34)

$$\oint \Pi_2 dy = (n + \tfrac{1}{2} \pm \tfrac{1}{2})h_0 \tag{37}$$

where $h_0 = 2\pi h$ is the ordinary Planck constant. Eqs. (37), (34) and (15) determine the energy. Eqs. (31), (35) and (36) represent the eigenfunctions. Of course, they may also be written in a form analogous to (24′).

Kramers obtained the result that the influence of wave mechanics upon phase-integral quantization meant replacing the integer q uantization by half-integer quantization. As (36) shows, relativity and spin as embodied in the Dirac equations mean a return to whole number quantization but with each level possessing a twofold degeneracy. This result may be interpreted in the usual vector language that the spin moment $s = \frac{1}{2}$ is added in two directions to the orbital moment $l = n + \frac{1}{2}$. This used to be called the "branching-off principle."

The problem of an electron moving in a homogeneous magnetic field, was treated by various authors,[5] according to the rigorous Dirac equations. It is interesting to note that our result for the energy agrees rigorously with the energy determination on the basis of the complete Dirac equations.

The author is greatly indebted to Professor W. Pauli for helpful discussions.

[5] W. Alexandroff, Zeits. f. Physik **56,** 818 (1929); Ann. d. Physik **2,** 477 (1929). E. Fues and H. Hellmann, Phys. Zeits. **31,** 465 (1930). L. D. Huff, Phys. Rev. **38,** 501 (1931).

The Isotope Displacement in Hyperfine Structure

By G. BREIT
Department of Physics, New York University

(Received September 12, 1932)

With Goudsmit's extension of Landé's formula for $(\overline{1/r^3})$ it is possible to explain the order of magnitude of the isotope displacements in Hg, Tl, Pb arc and spark spectra on the hypothesis of small changes in nuclear radii. The nuclear radius is supposed to be proportional to the 1/3 power of the atomic weight. The effective nuclear charge is supposed to be distributed with a roughly uniform density through the interior of the nucleus. The spectra Hg I, Hg II, Tl I, Tl II, Pb II, are in agreement with the above theory. The larger displacements are due to the addition or removal of a $6s$ or $7s$ electron to the electron configuration. The direction of the shift is in agreement with the supposition that the nuclear radius increases with atomic weight, the heavier isotope having the looser binding for the s and $p_{1/2}$ electrons. In order to explain the shifts of the $6p^2$, $6p7s$, $6p8s$, $d6p$, $6p8p$ configurations of PbI it is supposed that in this case the displacements are due principally to changes in the penetration to the nucleus of the $6s^2$ subgroup. These changes are presumably caused by differences in screening of the two $6s$ electrons from the nucleus as the valence electron is excited from the $6p$ state to the ionization limit.

THE elements Hg, Tl, Pb show in their hyperfine structure a number of components which are ascribed to the different isotopes of these elements. The observed displacements are considerably larger than would be expected according to the simple mass correction to the Rydberg formula given by the factor $(1+m/M)^{-1}$. The suggestion has been made that these isotope displacements are due to deviations of the electric field of the nucleus from the inverse square law. Calculations by Racah[1] and also by Rosenthal and the writer[2] indicated however that on such a hypothesis the displacement would be expected to be several times larger than that observed. In addition, in the case of Tl, it appeared impossible[2] to reconcile the observed direction of the displacement in the spark with that in the arc spectrum.

It has since been found possible to interpret the troublesome terms of Tl in such a way that the direction of the displacement in its arc and spark spectrum fits in with that observed in Hg and Pb. For these three elements, the large displacements can be attributed consistently to differences of binding of s electrons and particularly those of the deeply penetrating $6s$ electron. It was furthermore found that a simple formula used by Goudsmit[3] in the calculation of hyperfine structure separations gives in these cases smaller values for the probability of finding an electron at the nucleus than the numerical calculations of Racah which have been used by Rosenthal and the writer as well. It appears possible that the numerical calculations may be sub-

[1] G. Racah, Nature **129,** 723 (1932).

[2] J. E. Rosenthal and G. Breit, Phys. Rev. **41,** 459 (1932).

[3] Pauling and Goudsmit, *Structure of Line Spectra*. See also J. C. McLennan, A. B. McLay and M. F. Crawford Proc. Roy. Soc. **A133,** 652 (1931).

ject to cumulative errors and it is at all events of interest that Goudsmit's application of the Landé formula for $\overline{(1/r^3)}$ leads to a reasonable agreement of the expected and observed isotope displacements.

In order to obtain an expression for the square of the Shroedinger function at $r=0$ we use Landés approximate formula

$$l(l+1)\overline{\left(\frac{1}{r^3}\right)} = \frac{R\alpha^2 Z_i Z_0^2}{\mu_0^2(2l+1)n_0^2} \tag{1}$$

where l is the azimuthal quantum number, R the energy corresponding to the Rydberg constant, $\alpha = 2\pi e^2/hc$, μ_0 is the Bohr magneton, Z_i is the effective nuclear charge in the inner part of the orbit, Z_0 is the effective charge in the outer part of the orbit and n_0 is the effective quantum number defined by equating the term energy to $-R\,Z_0^2/n_0^2$. This formula has been derived by Landé by means of classical considerations with penetrating orbits. One may expect it, however, to be at least qualitatively correct also in quantum mechanics. For s terms the meaning of the left side of (1) is known to be[4]

$$\overline{l(l+1)r^{-3}} = 2\pi\psi^2(0) \tag{2}$$

so that

$$\psi^2(0) = \frac{Z_i Z_0^2}{\pi a_H{}^3 n_0{}^3} = 2.16\times 10^{24}\frac{Z_i Z_0^2}{n_0{}^3}\ \text{cm}^{-3} \tag{3}$$

where a_H is the Bohr radius. It will be noted that *for Coulomb fields Eq. (3) is exact.* The fact that for $l=0$ the left side of (2) is indeterminate does not concern us because in the relativistic theory of hyperfine structure this expression is replaced by one having a perfectly definite meaning. Also Eq. (3) may be interpreted along the lines of Landé's penetrating orbits by regarding $(Z_0/Z_i)^2/n_0{}^3$ as the factor by which the normalization constant in the region of effective nuclear charge Z_i is decreased on account of the presence of the region with effective nuclear charge Z_0. Thus (3) is a reasonable approximation. We do not pretend, however, to regard it as exact and the ultimate test of its validity lies in comparing it with accurate numerical calculations. Computing $\psi^2(0)$ for the normal states of the alkalies by means of (3) we have the following comparison (Table I) with values of $\psi^2(0)$ obtained by means of numerical calculations of the eigenfunctions:

TABLE I.

Element:	Na	Cs	Rb
$\psi^2(0)$ by (3):	5.6×10^{24}	1.8×10^{25}	1.4×10^{25}
$\psi^2(0)$ according to Fermi[5]:	2.4×10^{24}	2.7×10^{25}	0.88×10^{25}
$\psi^2(0)$ according to Nile:		$1.7(5)\times10^{25}$	

[4] G. Breit, Phys. Rev. **37**, 51 (1931).
[5] E. Fermi, Zeits. f. Physik **60**, 320 (1930).

For the lighter elements $\psi^2(0)$ is smaller when computed numerically. For Cs the very careful as yet unpublished calculations of Nile agree very well with (3) while Fermi's value is appreciably higher.

It will be seen that in the case of Tl the comparison of the magnitude of the hfs splitting of the $7s$ state is in much better agreement[6] with that of the $6p_{1/2}$ using (3) than the numerical calculations of $\psi^2(0)$ for this state made by Racah. One may regard the hfs splitting as an empirical determination of $\psi^2(0)$ and it appears that this determination fits in with the magnitude of the isotope shift and with the value for $\psi^2(0)$ obtained by means of (3).

In mercury the isotope displacement has been observed both for the spark and the arc spectra. In the spark spectrum Schüler and Jones[7] arrive at an interpretation according to which the largest displacement is that of the $^2D_{5/2}$ term belonging to the $5d^9\ 6s^2$ configuration. The other terms belong to the $5d^{10}\ 6s$, $5d^{10}\ 6p$, $5d^{10}\ 7s$ arrangements. The displacement between Hg^{204} and Hg^{202} is 0.52 cm^{-1} and it is significant that the energy of Hg^{204} is higher than that of Hg^{202}. This shows that a change of an electron from the $5d$ to the $6s$ state produces a larger energy increase in Hg^{204} than in Hg^{202}. The $6s$ electron may be thus thought of as less tightly bound in Hg^{204} than in the lighter isotopes. Similarly in the arc spectrum[8] of Hg the largest displacement is assigned to $6s^2\ ^1S_0$, the shift between Hg^{204} and Hg^{202} being 0.15 cm^{-1} while that between Hg^{201} and Hg ^{199} is reported to be 0.21 cm^{-1}. The direction of the shift is again such that Hg^{204} has the highest energy. The $6s\ 7s$ configuration also shows a shift in the same direction but of a smaller magnitude, the displacement between Hg^{204} and Hg^{202} being 0.03 cm^{-1} both in the $^1S_0$ and $^3S_1$ states.

It has been observed by Shenstone and Russell[9] that the large displacement of the ^1P terms of this spectrum finds a natural interpretation in a perturbation of these terms by the $5d^9\ 6s^2\ 6p$ configuration. In particular the $8\ ^1P_1$ term[9] shows an isotope displacement of practically the same amount as the $6s^2\ ^1S_0$ term. The direction of the displacement is again the same and corresponds to a tighter binding of the $6s$ electron in the lighter isotope.

For Tl it appeared at first difficult[2] to interpret the displacement in terms of nuclear fields because the directions of the shift in the spark and arc spectrum did not agree. A further examination of the data[10] showed that the terms with large displacements are the X_2 and the term previously designated as $6s\ 7p\ ^1P_1$. According to McLennan and Crawford[11] this designation is incorrect and it is therefore called by them $1_1{}^0$. In this term as well as in X_2 the lighter isotope Tl^{203} has a tighter binding between the electrons and the nucleus than Tl^{205}. The analogy between this and Hg suggests that X_2 and $1_1{}^0$

[6] This has been observed first by Goudsmit who kindly informed the writer of the fact.

[7] H. Schüler and E. G. Jones, Zeits. f. Physik **76,** 14 (1932), see Fig. 1, p. 17.

[8] H. Schüler and J. E. Keyston, Zeits. f. Physik **72,** 423 (1931), see Fig. 16, p. 438. H. Schüler and E. G. Jones, Zeits. f. Physik **74,** 631 (1932).

[9] A. G. Shenstone and H. N. Russell, Phys. Rev. **39,** 415 (1932), see p. 427. The "$8\ ^1P_1$" term practically belongs to the $5d^9\ 6s^2\ 6p$ configuration.

[10] H. Schüler and J. E. Keyston, Zeits. f. Physik **70,** 1 (1931).

[11] J. C. McLennan and M. F. Crawford, Proc. Roy. Soc. **A132,** 10 (1931).

belong to a configuration involving two $6s$ electrons. Professor Goudsmit kindly examined the data on Tl II and Tl III, and it appears in fact quite logical to interpret the X_2 (McLennan and Crawford's $3_2{}^0$) and the $1_1{}^0$ terms of Tl II as belonging to the $5d^9\ 6s^2\ 6p$ configuration, the difference in term values of $5d^9\ 6s\ 6p\ {}^4F^0$ and $5d^{10}\ 6s$ of Tl III being $\geqq 124{,}000\ \text{cm}^{-1}$ while the difference in term values of $1_1{}^0$, X_2 from $5d^{10}\ 6s^2$ in Tl II is respectively 126,204 and 125,437 cm^{-1}. With this interpretation, the observed senses of the displacements in Tl I and Tl II are in agreement provided one supposes that $5d^{10}\ 6s^2\ 6p\ {}^2P_{3/2}$ of Tl I is undisplaced so that the largest displacement is to be assigned to $5d^{10}\ 6s^2\ 7s\ {}^2S_{1/2}$ and a somewhat smaller displacement to $5d^{10}\ 6s^2\ 6p\ {}^2P_{1/2}$. This view appears to be in disagreement with the reported fact that combinations of the higher ^2P terms with $5d^{10}\ 6s^2\ 7s\ {}^2P_{1/2}$ show no isotope shift. The experimental difficulties involved are apparently very high, however, as shown by the disagreement between Jackson and Schüler and Keyston on the isotope shift of λ3776. Since the direction of the displacement in Tl II is the same as in Hg I, II and Pb I, II, it would be surprising if Tl I were different. [See discussion of Pb I below.]

The displacements in Pb II have been discussed previously.[2] The view that the large shifts are to be attributed to the $6s$ electrons is seen to be in agreement with the similar cases in Tl and Hg both with respect to the direction of the shift and its order of magnitude.

The isotope displacements in Pb I fit into the above theory only partly. Taking the $6p^2\ {}^1D_2$ level as having no displacement, and letting $\Delta W = W(\text{Pb}^{208}) - W(\text{Pb}^{206})$ we obtain, using the data of Kopfermann,[12] Rose and Granath,[13] and of Schüler and Jones[14] the following approximate values for ΔW in cm^{-1}: $6p^2\ {}^1S_0 + 0.01$; $6p^2\ {}^3P_{0,1,2} + 0.01$; $7s\ 6p\ {}^3P_{0,1} + 0.09$; $d\ {}^3D_{2,1} + 0.07$; $d\ {}^3F_3 + 0.07$; $8s\ 6p\ {}^3P_{1,2} + 0.09$; $7s\ 6p\ {}^1P_1 + 0.07$; $6p\ 8p\ {}^3P_1 + 0.08$; $6p\ 8p\ {}^3P_0 + 0.07$. The fact that all levels of the $6p^2$ configuration have approximately the same isotope displacement indicates that ΔW for $6p_{1/2}$ is small and of the order of 0.01 cm^{-1} so that $\Delta W(6p_{3/2})$ can be neglected altogether. The relatively large displacement of the $d\ 6p$ terms is therefore rather puzzling. It may possibly be due to a perturbation by the $6p\ 7s$ configuration, and it may also be that there is as a consequence a perturbation with $6p\ 8s$. Such perturbations make it possible to explain why the displacements of $6p\ 7s$ and of $6p\ 8s$ are of the same order of magnitude. With the above mutual perturbations of $d\ 6p$ by $6p\ 7s$ and of $6p\ 8s$ by $d\ 6p$, the approximately equal shifts of the three configurations may be understood and should then be ascribed mainly to the influence of the $7s$ electron.

It is more difficult, however, to interpret the relatively large shifts of $6p\ 8p\ {}^3P_{0,1}$ which follow from the observed structure[14] of λλ6059, 6012, 5896. On the present theory we should expect the shifts to be of the same order as

[12] H. Kopfermann, Zeits. f. Physik **75,** 363 (1932); Naturwiss. **19,** 400 (1931); **19,** 675 (1931).

[13] John L. Rose and L. P. Granath, Phys. Rev. **40,** 760 (1932). With the later data of Schüler and Jones $a' = 0.012$, $a'' = 0.372$ for $6p^2$.

[14] H. Schüler and E. G. Jones, Zeits. f. Physik **75,** 563 (1932).

those of $6p^2\ {}^3P_{1,2}$ while actually they are approximately the same as those of the $6p\ 7s$ configuration. It is not possible that the $6p\ 8p$ configuration could be perturbed by $6p\ 7s$ or $d\ 6p$ so that another explanation must be looked for.

It should be remembered in this connection that the subgroup $6s^2$ is present in all of the Pb I spectrum. A change in the screening constant of the two $6s$ electrons would lead to an isotope shift. It appears possible, although it is not certain, that the screening of the nucleus by $8p$ is sufficiently weaker than the screening by $6p$ to produce a larger penetration of $6s$ and a consequent isotope shift. The existences of such effects is also suggested by the apparent absence of isotope shifts in the lines $7s\ mp$ of Tl I which would otherwise be expected to show the full shift of the $7s$ electron. As has already been mentioned in connection with Tl I we do not feel very confident that a shift of the $7s\ mp$ lines could have been detected with certainty since there appears to be some contradiction between different observers of λ3776. It appears nevertheless reasonable to suppose that in Pb I the $6s$ electrons have a smaller $\psi^2(0)$ when the valence electron is in a low energy state, because from the point of view of our theory this fits in with the presence of isotope shifts in all the higher terms in the Pb I spectrum. The mass effect considered by Hughes and Eckart for Li can hardly have much to do with the observed shifts in Pb I since there appears no reason why it should give the same shifts for the five ground levels and since it should give equal spacings between Pb^{206}, Pb^{207}, Pb^{208} which is not the case experimentally. It thus seems that changes in $\psi^2(0)$ of $6s$ and perhaps other underlying groups should be considered as mainly responsible for the isotope shifts in Pb I. In Pb II, however, we deal primarily with shifts due to the addition or subtraction of a $6s$ electron and we are thus not concerned with the smaller effects of differences in penetration.

Both the isotope shifts and the nuclear spin term splittings depend on the penetration of the electrons to the nucleus. We discuss, therefore, briefly the theoretical interpretation of the nuclear spin term splittings for Pb I in order to see whether it can be made consistently.

Using (jj) coupling and supposing that ${}^3P_0$ belongs to $6p_{1/2}\ 8p_{1/2}$ while ${}^3P_1$ belongs to $6p_{1/2}\ 8p_{3/2}$, we derive from the observed level splitting of -0.155 cm^{-1} the value[15] $A=-0.103$ cm^{-1} and $a''(6p)=A(6p_{1/2})=0.41$ cm^{-1} which compares reasonably well with the value[13] 0.37 cm^{-1} derived by means of the sum rule from the splittings of the $6p^2$ configuration. The interpretation of $6p\ 8p\ {}^3P_1$ as $6p_{1/2}\ 8p_{3/2}$ appears to be a natural one in view of the fact that it falls into the same series with $6p^2\ {}^3P_1$. Also the interpretation of $6p\ 7s\ {}^3P_1$ and $6p\ 8s\ {}^3P_1$ as $6p_{1/2}\ 7s$ $(j=1)$ and $6p_{1/2}\ 8s$ $(j=1)$ leads to reasonable values $a''(6p)+a(7s)=0.586$, $a''(6p)+a(8s)=0.386$ which gives on using $a''(6p)=0.372$, $a(7s)=0.214$ and $a(8s)=0.014$. Using the observed[14] splitting -0.060 cm^{-1} for $6p\ 7s\ {}^1P_1$ and interpreting this term as $6p_{3/2}\ 7s$ $(j=1)$, we obtain $A=-0.040$ cm^{-1}, $5a'(6p)-a(7s)=-0.160$ cm^{-1}. Using here $a(7s)=+0.214$ cm^{-1} we get $a'(6p)=0.011$ cm^{-1} in good agreement with $a'(6p)$

[15] S. Goudsmit, Phys. Rev. **37**, 663 (1931). For (jj) coupling
$A=\{[j(j+1)+j_1(j_1+1)-j_2(j_2+1)]a(j_1)+[j(j+1)+j_2(j_2+1)-j_1(j_1+1)]a(j_2)\}/2j(j+1)$.

$=0.007$ cm^{-1} which follows from the $6p^2$ configuration according to Rose and Granath's data[13] and 0.012 cm^{-1} according to Kopfermann's[12] and the latest of Schüler and Jones.[14] The $^3F_3$ level of the $d6p$ configuration must be interpreted as $d_{5/2} \cdot 6p_{1/2}$. For if the observed[12] splitting is 0.250 cm^{-1}, $A=0.0714$ cm^{-1} and $a''(6p)=0.43$ cm^{-1} again in fair agreement with 0.37 cm^{-1} from the $6p^2$ configuration. The hfs splittings do not call, therefore, for any change in the interpretation of the terms and we are thus unable to interpret the large displacements of the $6p$ $8p$ configuration[16,17] *except as a change in the effective screenings of* $6s^2$. Experimental material on other levels of the $6p$ mp series would be of value in arriving at a definite explanation.

The comparison of the observed and theoretically expected shifts is given in Table II.

TABLE II.

Element and spectrum	Electron state	$\psi^2(0)10^{-25}$	Method of computation	Shift as multiple of $A\Delta y_0/y_0$	Fractional change in nuclear radius $\Delta y_0/y_0$	Expected shift in cm^{-1}	Observed shift in cm^{-1}
Tl I	$7s$	0.17	Goudsmit		1/300	0.07	0.06
"	"	0.49	Racah	360	"	0.2	"
"	$7p_{1/2}$			49	"	0.03	0.01 ± 0.005
Tl II	$6s$	<1.6	Goudsmit from Tl III		"	<0.8	0.23
	"	2.8		2060	"	1.4	"
Pb I	$7s$				"		0.07
Pb II	$6s$		G. from Hg II		"	0.70	0.50
Hg I	$6s$				"		0.18
	$7s$	0.30	G. from Hg II		"		0.03
Hg II	$6s$	1.45	G. from Hg II	1060	"	0.70	0.52

$A=(n+1)/(2\rho+1)\,(2\rho+n+1) \backsim 1/5$ for $\rho=0.81$.

It will be noted that in the one electron spectra of Tl I, Hg II the agreement with Goudsmit's formula for $\psi^2(0)$ is quite satisfactory. Only in such cases is the use of this formula safe because the screening is then the same in the calculation of the effective quantum number and in the calculation of

[16] The *relative* values of the isotope shifts which should be expected for $7s$ and $6p_{1/2}$ of Pb I are approximately the same as in Tl I because for Pb I, $a(7s) \backsim 0.22$, $a''(6p) \backsim 0.37$ while for Tl I, $a(7s) \backsim 0.40$, $a''(6p) \backsim 0.71$ so that the ratio $a(7s)/a''(6p)$ is nearly the same for the two spectra.

[17] The small disagreements which exist in the above comparison between theory and experiment for the hfs of Pb I can be easily explained by the influence of the penetration of the electrons on the coupling to the nucleus and by the fact that the coupling is intermediate between Russell-Saunders and jj. For the $6p^2$ configuration the Zeeman effect g values determine the $^1D_2$ term as $0.93\ 6p_{3/2}\ 6p_{3/2}+0.38\ 6p_{3/2}\ 6p_{1/2}$ and $^3P_2$ as $0.93\ 6p_{3/2}\ 6p_{1/2}-0.38\ 6p_{3/2}\ 6p_{3/2}$. The deviation from jj coupling measured by $(0.38)^2=0.14$ is quite large enough to account for the difference between $A(^1D_2)=0.026$ and $a'(6p)=0.012$. Neglecting matrix elements of the type $(p_{3/2}/H'/p_{1/2})$ we derive theoretically $A(^1D_2)=0.024$, $A(^3P_2)=0.089$ in excellent agreement with experiment. It is not quite certain that these matrix elements are sufficiently small to be neglected. Nevertheless it is clear that the deviations from jj coupling may easily account for the remaining discrepancies.

$\psi^2(0)$. With Goudsmit's value[6] for $\psi^2(0)$ of $7s$ Tl I the hfs splitting of this term gives $\mu_0/\mu = (0.17/0.49)4050 = 1.4 \times 10^3$ which is in much better agreement with the value $\mu_0/\mu = 0.92 \times 10^3$ which follows according to Racah from the splitting of $6p_{1/2}$ Tl I than $\mu_0/\mu = 4.0 \times 10^3$. The isotope shift and the hfs splitting agree with Goudsmit's formula.

Summary

It is seen from the above discussion that the theory of isotope shifts as due to changes in nuclear radii is substantially in agreement with the observed facts. The apparent objections[1,2] to such a theory have been removed. The main changes with respect to previous work are: (1) changes in the probable values of $\psi^2(0)$; (2) the interpretation of electron configurations in Hg, Tl, Pb. The values of nuclear radii and their differences have a significance only so far as order of magnitude is concerned, on account of uncertainties in the values of $\psi^2(0)$.

The picture of the nucleus as having an approximately uniform charge density is expected to apply only to its action on extranuclear electrons and has presumably somewhat the same relation to reality as the Hartree central field has to the correct treatment of an atom in configuration space.

Absorption Spectrum of Iodine Bromide

By WELDON G. BROWN*
Ryerson Physical Laboratory, University of Chicago

(Received August 25, 1932)

It is shown by means of a vibrational analysis that the absorption spectrum of iodine bromide is analogous to that of iodine chloride and that an interpretation similar to that recently proposed by the writer and Gibson for ICl is applicable. The infrared bands of IBr discovered by Badger and Yost are classified as a $^3\Pi_1 \leftarrow {}'\Sigma$ transition. The $^3\Pi_{0^+} \leftarrow {}'\Sigma$ system is observed as a faint set of bands in the red, not hitherto reported, which exhibit the same type of predissociation as the corresponding bands of ICl. Transitions to a state which originates at the maximum of the $^3\Pi_{0^+}$ state and which dissociates to yield normal iodine and excited bromine atoms are observed as a strong system of partially diffuse bands. Cordes' assignment of these bands to two systems is not confirmed. In the present work the vibrational quantum numbering for each system is deduced from measurements of the isotope effect due to bromine. The heat of dissociation of IBr is 1.808 ± 0.001 volts. For the four molecules I_2, IBr, ICl, and Br_2 it is shown that the separation of the $^3\Pi_{0^+}$ and $^3\Pi_1$ states is roughly equal to two-thirds of the mean ^2P multiplet widths of the constituent atoms. The total $^3\Pi$ widths are then probably greater and the $^3\Pi_2$ state somewhat lower than has been supposed.

INTRODUCTION

THE close generic relationship between iodine bromide and iodine chloride furnishes good grounds for believing that their absorption spectra should be closely analogous. Thus, in accordance with the interpretation of the ICl spectrum recently proposed by the writer and G. E. Gibson,[1] one would expect to observe transitions from the normal $^1\Sigma$ state to $^3\Pi_1$ and $^3\Pi_{0^+}$ states, the latter exhibiting predissociation. A system of bands in the infrared is known from the work of Badger and Yost[2] who have shown that the dissociation products of the upper state are normal atoms. In this respect the system is like the strong visible system of ICl and is therefore probably the $^3\Pi_1 \leftarrow {}^1\Sigma$ system. In the visible, according to Cordes,[3] there are two systems of diffuse bands, the upper levels of which dissociate to give normal iodine plus excited bromine (a') and normal bromine plus excited iodine (a''). While one of these (a') may correspond to the peculiar 0^+ state of ICl, the other is quite unexpected, and transitions to the $^3\Pi_{0^+}$ state were not observed.

In the hope of making a detailed study of the spectrum, photographs of the visible and infrared regions were made with high dispersion (21′ Rowland grating). Lack of sufficient resolution has hindered the fine structure analysis,

* National Research Fellow in Chemistry.

[1] W. G. Brown and G. E. Gibson, Phys. Rev. **40**, 529 (1932). For the theory of the electronic states of the halogens, see R. S. Mulliken, Phys. Rev. **36**, 669, 1440 (1930); Rev. Mod. Phys. **4**, 17, 70 (1932).

[2] R. M. Badger and D. M. Yost, Phys. Rev. **37**, 1548 (1931).

[3] H. Cordes, Zeits. f. Physik **74**, 34 (1932).

however, and the following results are based on a study of the vibrational levels.

The strongest absorption bands are the partially diffuse bands in the visible which were studied by Cordes. At longer wave-lengths, in the red, a faint system of double headed bands is to be observed. This occurs in several v' progressions each of which terminates abruptly with an apparently diffuse band, and is obviously the $^3\Pi_{0^+} \leftarrow {}^1\Sigma$ system. The doublet nature of the heads is due to the equally abundant isotopes of bromine, 79 and 81. The infrared bands, as described by Badger and Yost, also appear in several v' progressions. A few members of the $v'' = 0$ and $v'' = 1$ progressions show the isotope effect sufficiently clearly for approximate measurement.

Vibrational Analysis

Badger and Yost carried out a vibrational analysis of the infrared system but as a consequence of not having resolved the isotope effect their values of the vibrational constants for the normal state are only approximately correct and those for the upper state are without significance because of the arbitrary

Table I. *Infrared system.*

v' \ v''	0	1	2	3	4	$\Delta G'$
9				12,464		103
10				567		96
11				663		94
12			13,021	757	12,496	88
13			107	845	584	86
14		13,459	194	931	670	79
15		537	275	13,010		73
16		609	348	084		68
17		677	414	155		65
18		745	478	219		59
19		806	537	275		54
20		858	593	330		51
21		906	645	382		46
22		953	691	427		43
23		995	734			40
24		14,038	771			34
25		071	806			36
26	14,373	107	842			29
27	404	135	871			30
28	434	165				25
29	459					23
30	482					22
31	504					21
32	525					19
33	544					19
34	563					16
35	579					14
36	593					12
37	605					10
38	615					9
39	624					9
40	633					8
41	641					5
42	646					4
43	650					4
44	654					

v' numbering. As mentioned above, however, the isotope effect is observed only for a few members of the $v''=0$ and $v''=1$ progressions, and, because of the presence of a Q branch which tends to confuse the head formed by the R branch, it is not accurately measurable. Nevertheless, the data serve to determine the order of magnitude of the correction to be applied to the arbitrary v' numbering, and this turns out to be an increase of 9 ± 1 units.

Some uncertainty in the value of ω_e' is introduced by the long extrapolation from $v'=9$. In obtaining the value, $\omega_e'=140\pm5$ cm^{-1}, we are guided to some extent by the assumption that the $\omega:v$ curve will have the same general shape as the corresponding curve for ICl which is known over its entire course. The heat of dissociation, on the other hand, can be determined with high precision, and the extrapolation gives for the convergence of the $v''=0$ progression the value $14{,}660\pm5$ cm^{-1}, or $D''=1.808\pm0.001$ volts. This is somewhat higher than the Badger and Yost value, $1.801\ \pm0.007$, but within their limit of error. The new value introduces a small discrepancy between the spectroscopic value for the heat of formation of IBr from I_2 and Br_2 and the thermal value determined by Yost and McMorris,[4] but is nicely confirmed by the convergence of the system III bands.

The analysis of the infrared bands given in Table I, from low dispersion measurements, undoubtedly confirms that of Badger and Yost who have not yet published their data, and is given here for the sake of completeness. Table II contains the measurements of the isotope shifts, from photographs taken in the first order of the 21′ grating.

TABLE II. *Isotope shifts, infrared system.*

v', v''	ν*	$\delta\nu$ obs.	$\delta\nu$ calc.	v', v''	ν	$\delta\nu$ obs.	$\delta\nu$ calc.
26,1	14,106.8 103.2	3.6	3.7	29,0	14,459.2 454.0	5.2	4.8
27,1	137.8 134.2	3.6	3.5	30,0	482.3 477.5	4.8	4.5
28,1	165.2 162.4	2.8	3.2	31,0	503.9 499.9	4.0	4.3
26,0	373.3 367.6	5.7	5.7	32,0	525.1 521.6	3.5	4.1
27,0	404.4 398.3	6.1	5.5	33,0	544.3 540.0	4.3	4.0
28,0	433.6 427.0	6.6	5.2	34,0	563.4 560.2	3.2	3.8

* First given in each pair is the IBr^{79} head.

More accurate data for the normal state are provided by the visible $^3\Pi_{0^+}\leftarrow{}^1\Sigma$ bands, the analysis of which is given in Table III. The v'' numbering is fixed with reference to the infrared system and the v' numbering is that obtained from the isotope shifts in the usual way. Only bands with sharp heads

[4] D. M. Yost and J. McMorris, J. Am. Chem. Soc. **53**, 2625 (1931).

are included in the table; in addition, bands with $v'=6$ have been observed in each progression. These bands are approximately 100 cm^{-1} distant from the corresponding $v'=5$ bands, and like the $v'=4$ bands of the corresponding ICl system, appear diffuse but with widely spaced series of lines superimposed.

TABLE III. $^3\Pi_{0^+}\leftarrow{}^1\Sigma$ *systems.*

v' \ v''	3		4		5		6		7
2					15,053.4				
					15,062.8				
					125.1				
					123.1				
3			15,438.7	260.2	15,178.5	*257.0*	14,921.5		
			15,444.4	*258.5*	15,185.9	*256.5*	14,929.4		
			116.8		*116.5*		*115.1*		
			116.3		*116.1*		*116.1*		
4	15,817.2	*261.7*	15,555.5	*260.5*	15,295.0	*258.4*	15,036.6	*257.1*	14,779.5
	15,820.7	*260.0*	15,560.7	258.7	15,302.0	*256.5*	15,045.5	*255.0*	14,790.5
	108.6		*108.3*		*108.4*		*107.7*		*106.7*
	108.4		*107.6*		*108.0*		*107.1*		*107.1*
5	15,925.8	*262.0*	15,663.8	*260.4*	15,403.4	*259.1*	15,144.3	*258.1*	14,886.2
	15,929.1	*260.8*	15,668.3	*258.3*	15,410.0	*257.4*	15,152.6	*255.0*	14,897.6

Since the data provide only three values of ω_v', which are not quite linear in v', the extrapolation to $v'=-\frac{1}{2}$ is again somewhat uncertain, the value of ω_e' being $\sim$140 cm^{-1}. Thus, as nearly as can be determined, the $^3\Pi_{0^+}$ an $^3\Pi_1$ states have the same value of ω_e. An extrapolation to the point of dissociation is much more uncertain but it is obvious that too low a value will be obtained. Even a linear extrapolation from the observed levels, which in most cases yields too high a value for the heat of dissociation, falls short of the limit I ($^2P_{3/2}$) + Br ($^2P_{1/2}$) by 1000 cm^{-1}. Clearly such an extrapolation is without significance except insofar as it shows the abnormality of the levels.

The remaining visible bands, which have their analogy in the system III bands of ICl, are remarkable not only for their intensity but also for the anomalous appearance of certain bands ($v'=8$ and 11). These bands are assigned in the analysis (Table IV) in a way that may seem arbitrary, for, unlike all other bands in this system, they possess sharp heads showing the isotope effect clearly. Attempts were first made to consider them as members of an independent system, that is, as successive members in v' progressions instead of differing by three in quantum number. This possibility was rejected for two reasons, first, there are no additional bands of like character to support such an assignment, and secondly, the isotope shifts calculated on this basis do not agree with the observed values. Supporting their assignment in Table IV is the observation of the intervening levels, 9 and 10, although these bands are totally different in appearance and are so ill-defined that they are not measurable.

TABLE IV. *System III*, $0^+ \leftarrow {}^1\Sigma$.

v' \ v''	0		1		2		3		4
8			16,947.8 16,947.3 *54*	*265.1* *263.5*	16,682.7 16,683.8 *63*	*263.7* *261.7*	16,419.0 16,422.1 *66*	*262.0* *260.5*	16,157.0 16,161.6 *58*
9			17,002* *68*	*256*	16,746* *60*	*257*	16,489* *55*	*271*	16,218* *66*
10			17,070* *61*	*264*	16,806* *59*	*262*	16,544* *57*	*260*	16,284* *57*
11			17,131 *57*	*266*	16,865.3 *60*	*263.7* *262.2*	16,601.6 16,603.1 *60*	*262.5* *260.1*	16,339.1 16,343.0
12			17,188* *49*	*263*	16,925 *53*	*263*	16,662 *57*		
13			17,237 *54*	*259*	16,978 *56*	*259*	16,719*		
14			17,291 *67*	*257*	17,034 *59*				
15			17,358 *53*	*265*	17,093 *58*	*264*	16,829		
16			17,411 *51*	*260*	17,151 *42*				
17			17,462 *44*	*269*	17,237 *44*				
18			17,506 *50*	*265*	17,237 *54*				
19			17,556 *47*	*265*	17,291 *50*				
20			17,603 *42*	*262*	17,341 *43*				
21			17,645 *35*	*261*	17,384 *40*				
22	17,942 *41*	*262*	17,680 *46*	*256*	17,424 *38*				
23	17,983 *46*	*257*	17,726 *42*	*264*	17,462 *38*				
24	18,029 *39*	*261*	17,768 *33*	*268*	17,500 *33*				
25	18,068 *33*	*267*	17,801 *29*	*268*	17,533 *32*				
26	18,101 *29*	*271*	17,830 *33*	*265*	17,565 *34*				
27	18,130 *27*	*267*	17,863 *30*	*264*	17,599 *28*				
28	18,157	*264*	17,893	*266*	17,627				

(*continued*)

v' \ v''	0		1	
28	18,157 *30*	*264*	17,893 *26*	
29	18,187 *22*	*268*	17,919 *23*	
30	18,209 *20*	*267*	17,942 *19*	
31	18,229 *19*	*268*	17,961 *22*	
32	18,248 *15*	*265*	17,983	
33	18,263 *15*			
34	18,278 *17*			
35	18,295 *12*			
36	18,307 *8*			
37	18,315			

* Cordes' measurements.

Cordes has described the bands of this system as diffuse, but in reality they are only partially so. Fine structure appears throughout and in certain regions is remarkably sharp. It is true, however, that the heads are not sharp, except for those with $v' = 8$ and 11, and cannot be measured at all accurately as the combination differences of Table IV will show. The sharpness of the heads varies greatly, improving somewhat at high quantum numbers, and also, bands with $v' = 15$ and 20 are somewhat sharper than their neighbors.

No evidence has been obtained for the existence of a second band system in this region, as reported by Cordes. The bands assigned by Cordes to this second system fit, within the experimental error, in the v', v'' matrix of Table IV.

The dissociation products of the upper state are obviously normal iodine and excited bromine atoms, since, by a short extrapolation, we obtain the value, $18{,}345 \pm 15$ cm^{-1}, for the convergence of the $v'' = 0$ progression. Subtracting the ^2P separation of bromine, 3685 cm^{-1}, gives for the heat of dissociation $D'' = 14{,}660$ cm^{-1}, in fortuitously good agreement with the value obtained from the infrared bands.

In attempting to determine the value of ν_e or of ω_e' we are again confronted with the uncertainty of a long extrapolation, as the lowest observed level is $v' = 8$. There is some evidence for a maximum in the $\omega : v$ in this case

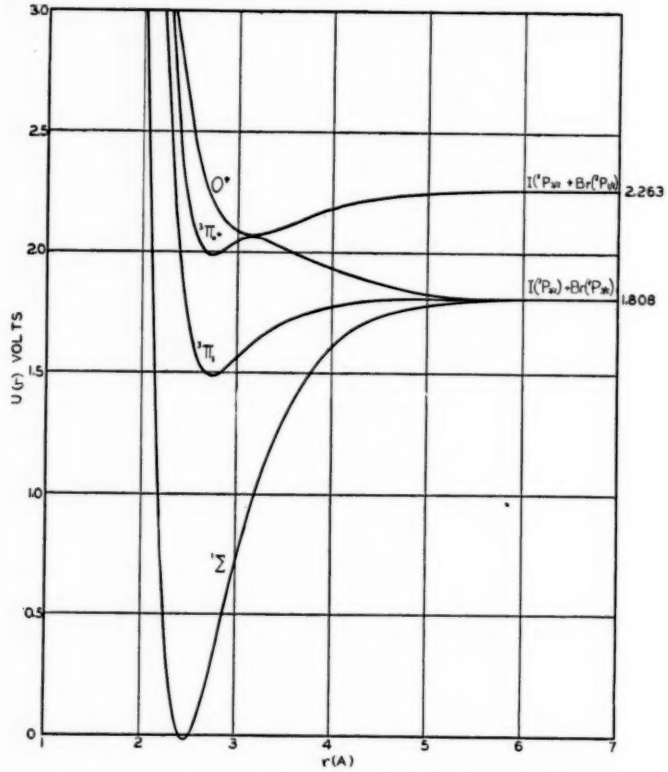

Fig. 1. Approximate potential energy curves for IBr. The r_e value for the normal state is assumed to lie midway between those for I_r and Br_r.

as well as in ICl. Assuming that ω does not change with v' up to $v' = 8$, the origin of the upper state would lie approximately at the height of the $^3\Pi_{0^+}$ $v = 5$ level, or perhaps 50 cm^{-1} higher if the $\omega : v$ curve actually has a maximum. The latter position is required by the interpretation. The fact that the upper state originates in the neighborhood of the last $^3\Pi_{0^+}$ level lends strong support to the interpretation, since it was not possible to prove this in the case of ICl.

It seems reasonable to suppose that the phenomena are essentially similar to those in iodine chloride, and that the upper state of system III arises in the same way, namely, by interaction of a repulsive 0^+ state derived from

normal atoms and the $^3\Pi_{0^+}$ state with the resultant formation of a quantized set of levels at the intersection. This state being formed from two 0^+ states also has the 0^+ character, and leads to dissociation into normal iodine and excited bromine atoms. The situation is illustrated in Fig. 1 by means of approximate potential energy curves for the various states. To interpret the character of the bands and the irregular fine structure we must suppose a certain degree of communism between the new 0^+ state and the $^3\Pi_{0^+}$ state so that transitions only to certain limited ranges of rotational quantum numbers, varying from level to level, can give rise to sharp lines. In some cases, as for $v=8$ and 11, the range of quantum numbers will be so low that a sharp head will be formed. In others the range will be higher so that the band appears shifted to the red and the progression accordingly irregular. Thus it can be seen that the interpretation proposed to account for the structure of the ICl bands provides a qualitative explanation for the unusual appearance of this system of IBr. It is unfortunate that on account of the overlapping of bands, the large mass of molecule, and the equally abundant isotopes of bromine, a detailed study of the structure is a problem of extreme difficulty.

Likewise, the relative intensities of the transitions $^3\Pi_1 \leftarrow {}^1\Sigma$ and $^3\Pi_{0^+} \leftarrow {}^1\Sigma$ are very much the same as in ICl when the Franck-Condon effects are taken into consideration. This involves the interpretation of the various regions of continuous absorption, and, because of the uncertainty as to the exact form of the potential energy curves, it is difficult to make an unambiguous assignment. The work of Cordes shows the existence of two regions of continuous absorption, with maxima at 4050A and 4950A, the latter being stronger. As drawn in Fig. 1 the potential energy curves indicate that transitions from the level $v''=0$ to the $^3\Pi_1$ state would be strongest in the region of the latter's discrete states but at high quantum numbers, while transitions to the $^3\Pi_{0^+}$ state would account for the strong maximum at 4950A. (Since the energy of this radiation is slightly more than enough to give excited bromine atoms on dissociation, a decision as to which path the $^3\Pi_{0^+}$ state actually follows, that is, whether normal or excited bromine atoms are the result, cannot be made.) The maximum at 4050A is then to be attributed to transitions to the 0^+ state, in harmony with the fact that iodine bromide does not exhibit a region of continuous absorption in the ultraviolet corresponding to that of iodine chloride.[5] The continuous absorption associated with the infrared system is probably that underlying the $^3\Pi_{0^+} \leftarrow {}^1\Sigma$ bands. According to this interpretation the $^3\Pi_{0^+} \leftarrow {}^1\Sigma$ system is actually very much stronger than the $^3\Pi_1 \leftarrow {}^1\Sigma$ transition, just as in ICl, although a comparison of transitions to discrete levels would yield an opposite conclusion.

Vibrational Constants

In obtaining the vibrational constants for the normal state, data from the three systems have been combined, the normal state being common, and selected to include only measurements of bands for which the isotope effect

[5] H. Cordes and H. Sponer, Zeits. f. Physik **63**, 338 (1930).

has been measured. The theoretical relations between the constants for isotopic molecules have also been taken into consideration. Owing to the long extrapolations the ω values for the $^3\Pi$ states are too uncertain to differentiate between the isotopic species.

TABLE V. *Vibrational constants.*

State	ν^{el}	ω_e	$\omega_e x_e$	D_0 (volts)
$^1\Sigma$	0	268.4 266.4	0.78 0.77	1.808
$^3\Pi_1$	12,230	140		0.31
$^3\Pi_{0^+}$	16,240	140		
O^+	16,880	60		0.19

$^3\Pi$ MULTIPLET WIDTHS

Unfortunately the $^3\Pi_2$ and $^3\Pi_{0^-}$ states cannot be observed in absorption since transitions to these states from the normal state are not allowed according to the selection rules,[6] and, therefore, one cannot determine the total multiplet width from the absorption bands alone. However, Van Vleck[7] has shown that the splitting of the 0^+ and 0^- levels at moderate values of r is small compared to the multiplet width, though not negligible. It may be assumed then that the separation of the 0^+ and 1 states gives an approximate measure of the half width of the multiplet and it is of some interest to consider how the values obtained in this way are related to the ^2P atomic separations.

Data are available for the four molecules, I_2, IBr, ICl, and Br_2. The value for Br_2 is based on new measurements of the isotope effect in the infrared system according to which the arbitrary v' numbering used by the writer[8] is to be increased by 6 units. Unfortunately, the v' numbering in the infrared system of iodine cannot be determined in this way as there are no isotopes of iodine. If one assumes that, as in IBr, ICl, and Br_2, the $^3\Pi_{0^+}$ and $^3\Pi_1$ states of iodine have the same value of ω, a reasonable extrapolation can be made from the observed $^3\Pi_1$ levels,[9] and a value for the separation obtained. The data are given in Table VI, together with the mean ^2P widths in the atoms.

TABLE VI.

Molecule	Mean ^2P width	$^3\Pi_{0^+}-{}^3\Pi_1$ obs.
I_2	0.94	0.68 ± 0.05
IBr	0.70	0.50
ICl	0.53	0.44
Br_2	0.46	0.27

[6] R. Schlapp, Phys. Rev. **39,** 806 (1932).
[7] J. H. Van Vleck, Phys. Rev. **33,** 484 (1929); **40,** 544 (1932).
[8] W. G. Brown, Phys. Rev. **38,** 1179 (1931).
[9] W. G. Brown, Phys. Rev. **38,** 1187 (1931).

The proportionality is obvious, the 0^+, 1 width being approximately two thirds the atomic multiplet width.

These results indicate that the total width of the $^3\Pi$ multiplets is greater by one-third than the mean ^2P separations in the atoms, or approximately twice the width estimated by Mulliken.[10] If true, this implies that the $^3\Pi_2$ state lies considerably lower than has been supposed. For I_2 this supposition of equal spacing of the components places the $^3\Pi_2$ component about 0.6 volts above the normal state. It would then be low enough to affect the dissociation equilibrium at high temperatures whereas Gibson and Heitler[11] have found very close agreement between the experimental values and those calculated by considering the normal state alone. It seems likely, therefore, that for the heavier halogens, at least, there is a considerable departure towards case *c* so that the spacing of the multiplet is no longer the usual equal spacing of molecular (case *a*) multiplets.[12]

[10] R. S. Mulliken, Phys. Rev. **36,** 1413 (1931).
[11] G. E. Gibson and W. Heitler, Zeits. f. Physik **49,** 465 (1928).
[12] R. S. Mulliken, Interpretation of Band Spectra, Part IIc, Rev. Mod. Phys. **3,** 117 (1931).

On the Interpretation of the Rotational Structure of the CO_2 Emission Bands

By ROBERT S. MULLIKEN
Ryerson Physical Laboratory, University of Chicago

(Received September 17, 1932)

Schmid's analysis of the rotational structure of a number of the ultraviolet CO_2 emission bands is discussed, and it is pointed out that in spite of uncertainties, some definite conclusions can be drawn, notably that the molecule in equilibrium is nearly linear, or probably strictly linear, in both initial and final states, that B' is nearly equal to B'', and that the values of both are approximately known (cf. Schmid). It is also shown that the bands are most probably of the type $^1\Pi \rightarrow {}^1\Pi$, but possibly $^1\Sigma \rightarrow {}^1\Sigma$ or (much less likely) $^2\Sigma \rightarrow {}^2\Sigma$ or some other type. If $^2\Sigma \rightarrow {}^2\Sigma$ the emitter must be CO_2^+, otherwise CO_2. It is proposed to designate by κ the quantum number corresponding to the angular momentum of rotation of the carbon atom relative to the O atoms around the O-C-O axis. It is pointed out that in electronic bands, one expects predominantly $\Delta\kappa = 0$. This rule is then applied to possible interpretations of the band structures. Some suggestions are also made concerning the vibrational analysis. Evidence from the values of B and ν_1 is stated, which supports Smyth's interpretation of the a and c series as v_1' progressions. It is suggested that the isolated bands $\lambda\lambda$2896, 2883 may be the (0,0) band of a $^2\Pi \rightarrow {}^2\Pi$ transition of CO_2^+ with B' and B'' almost equal.

RECENT work by Schmid[1] in this laboratory on the rotational structure of a number of ultraviolet CO_2 emission bands has revealed an unexpectedly simple structure. Schmid's work indicates that the spectrum contains at least three band systems. The bands whose analysis he has published probably all belong to one system. They consist of P-form and R-form branches of about equal intensity, each showing staggering, i.e., being composed of doublets but with alternately the high- and low-frequency component of each doublet missing.

The observed structures are consistent with a molecular structure which when at rest is linear in both initial and final states. Small departures from linearity would apparently not affect the qualitative nature of the energy level scheme nor, for most practical purposes, the selection rules, but a large departure in either or both states would surely give rise to a less regular and simple band structure.[2]

For a symmetrical linear molecule, the electronic states can be classed as $^1\Sigma_g^+$, $^1\Sigma_g^-$, $^3\Pi_u$, etc., just as for a diatomic molecule, and the selection rules for electronic quantum numbers should be the same. The existence of three characteristic vibrations (quantum numbers v_1, v_2, and v_3) does not affect in any essential way the structures of individual bands, although the fact that levels with given electronic and rotational quantum numbers change

[1] R. F. Schmid, Phys. Rev. **41**, 732 (1932).

[2] D. M. Dennison, Rev. Mod. Phys. **3**, 280 (1931) for the basis of these statements. Also Phys. Rev. **41**, 304 (1932).

from symmetrical in the nuclei to antisymmetrical, or *vice versa*, when v_3 changes from even to odd,[2] is essential in deciding which particular rotational levels and lines are present, which missing, in any given band.

The rotational energy is given for a diatomic molecule without electronic angular momentum by:

$$E^r/hc = \text{const.} + BK(K+1) + \cdots .$$

If $\Lambda > 0$ and $S > 0$ this is still essentially true, but every level is split up into a fine doublet (Λ-type doubling), the width of this increasing in general with K.[3] If the molecule has two equal nuclei without spin, one component of each double level, alternately the upper and the lower, is missing. If $S > 0$, the case is more complicated, unless the spin is very loosely coupled. (This is usually true only for $\Lambda = 0$.) For a linear triatomic molecule like CO_2 there is an added complication in the existence[2] of a quantum number κ associated with, roughly speaking, the rotation of the C nucleus around the line joining the two O atoms.[4] Λ and κ play similar roles. If $\Lambda = 0$, we expect κ-type doubling, with one component of each doublet missing, when $\kappa > 0$.[2] In analogy with Λ-type doubling, we might expect to find the doubling usually largest for $\kappa = 1$, much smaller for $\kappa = 2$, and so on. If $\Lambda > 0$ and $\kappa > 0$, the matter is more complicated (see below).

In general, Λ and κ are expected to obey the selection rules $\Delta\Lambda = 0, \pm 1$ and $\Delta\kappa = 0, \pm 1$. But since there is relatively little interaction, "coupling," between the nuclear motion connected with κ and the electron motions, one may expect in the case of an electronic band system to find practically only bands with $\Delta\kappa = 0$. This rule is similar to the rule $\Delta M_S = 0$ for atoms in the Paschen-Back effect and to the rule $\Delta\Sigma = 0$ for diatomic molecules in Hund's case *a*.[3]

With $\Delta\kappa = 0$, one expects band structures and intensity relations of exactly the same types as for diatomic molecules, except for some complications in the fine structure of $\kappa > 0$, $\Lambda > 0$. For instance, we can speak of cases, *a*, *b*, *c*, *d* of Hund.[3] The bands analyzed by Schmid can hardly be case *a* bands, since these would show multiplet structure (e.g., heads all in pairs, or in triplets with approximately constant spacing), and in all probability would show noticeable Zeeman effects at high quantum numbers, contrary to Schmid's observations. Nor are they of the type with one state case *a*, the other case *b*.[3]

The bands must then be case *b*, with $S > 0$, or else be singlet bands ($S = 0$). Other cases (*c* and *d*) can safely be excluded for a molecule such as CO_2. The observed *P*-form and *R*-form branches are then surely actual *P* and *R* branches ($\Delta K = \pm 1$). Bands having *P* and *R* branches and no *Q* branches (or very weak *Q* branches) have $\Delta\Lambda = 0$, and an electric moment vibrating parallel

[3] R. S. Mulliken, Rev. Mod. Phys. **3**, 89 (1931).

[4] The symbol κ has been chosen here after some consideration in preference to Dennison's *l*. Since it is likely to be of considerable importance, it seems desirable to have a unique symbol for this quantum number. The use of a Greek letter for a rotation around the figure axis of a molecule is in accordance with diatomic usage; the choice of κ suggests that, as with K, we are dealing with a nuclear rotation.

to the axis (here the O-C-O line). If $S>0$, the band lines should almost certainly show evidence of fine structure if $\Lambda>0$, and very probably even if $\Lambda=0$. Only in the higher energy states of very light molecules (H_2, He_2) is such fine structure so narrow as to escape observation (case b') for $\Lambda>0$. For $\Lambda=0$, $S=\frac{1}{2}$ ($^2\Sigma\rightarrow{}^2\Sigma$ transition) there might possibly be an unobserved fine structure for CO_2, since $^2\Sigma$ states of NO and CO^+ are known with separations that are barely detectable or not detectable. But it is much more likely that, if the bands were really $^2\Sigma\rightarrow{}^2\Sigma$, some evidence of fine structure would have been found among the many bands and band-lines examined. Actually there is no evidence whatever of splitting or broadening of the lines in the absence of a magnetic field,—other than the staggered-doubling, which cannot possibly be a spin effect, since with spin doubling both components of a double line would be present or absent together.[3] The possibility $^3\Sigma\rightarrow{}^3\Sigma$ can be practically excluded, since in diatomic molecules (O_2, NH, N_2, etc.), except He_2, this gives a fine structure too large to be missed.

One concludes then that very probably $S=0$, but that possibly the bands are $^2\Sigma\rightarrow{}^2\Sigma$. Of course if the emitter is CO_2, as Smyth considers probable,[5] the latter possibility is excluded. On the other hand, $S=0$, is excluded if it is CO_2^+.

The bands correspond, then, very probably to one of the types $^1\Sigma\rightarrow{}^1\Sigma$, $^1\Pi\rightarrow{}^1\Pi$, $^1\Delta\rightarrow{}^1\Delta$, etc. Schmid's result that no Zeeman splitting or measurable broadening is observed even in strong fields[1] excludes all but $^1\Sigma\rightarrow{}^1\Sigma$ and $^1\Pi\rightarrow{}^1\Pi$. His definite observation that the low-numbered P lines are probably broadened (*apparently* weakened) agrees with what would be expected for the Zeeman effect of $^1\Pi\rightarrow{}^1\Pi$. (The corresponding low-numbered R lines are obscured by other lines.) The fact that weak Q branches would be expected (just a few lines at low J values) for $^1\Pi\rightarrow{}^1\Pi$, etc., but not for $^1\Sigma\rightarrow{}^1\Sigma$, is no objection to the $^1\Pi\rightarrow{}^1\Pi$ interpretation, since Schmid could not have detected these Q lines amid the strong and crowded R lines. A possible real objection, connected with the expected simultaneous occurrence of Λ and κ-type doubling, will be mentioned later. $^1\Sigma\rightarrow{}^1\Sigma$ should show no Zeeman effect, or at most a slight broadening at *high* quantum numbers. The same is true of $^2\Sigma\rightarrow{}^2\Sigma$ if, as we must suppose here in order to consider this case at all as a possibility, the spin is very loosely coupled, since then $\Delta M_S=0$.

From the foregoing it would seem most probable that the bands are $^1\Pi\rightarrow{}^1\Pi$, with $^1\Sigma\rightarrow{}^1\Sigma$ as a second important possibility in case some unexpected explanation of the magnetic behavior of the low-numbered P lines can be found, and with $^2\Sigma\rightarrow{}^2\Sigma$ as a rather remote possibility.

The bands analyzed by Schmid all show exactly the same type of structure, except for differences in the magnitude of the staggering. The strongest bands analyzed are three bands of the a progression of Smyth ($\lambda\lambda$3247, 3370 and 3503) and three bands of Smyth's c progression ($\lambda\lambda$3254, 3377 and 3511). The c bands show staggering, the a bands none within the experimental error,

[5] H. D. Smyth, Phys. Rev. **38,** 2000 (1931); **39,** 380 (1932); cf. also H. J. Henning, Ann. d. Physik **13,** 599 (1932).

but as Schmid shows, we may assume that a very small staggering is actually present.

Now as will be seen by reference to reproductions given by Smyth,[5] and by Fox, Duffendack and Barker, each of the *a* bands above mentioned is the first, and also the strongest, member of a well-marked group of bands extending toward longer wave-lengths. No bands which could be associated with the group, except a few of much lower intensity, occur on the short wave-length side of the *a* band of each of these groups. Following each *a* band closely on its long wave-length side, and nearly as strong as the *a* band, is a *c* band. At longer wave-lengths in each group is a more or less irregular distribution of weaker bands (members of Smyth's series *b*, *d*, *n* and *j*). A few of these have been analyzed by Schmid; they include two examples with no observable staggering (λλ3546 and 3674), one with small staggering (λ3534), and one with rather large staggering (λ3839); one or two of these (especially λ3839) may, however, perhaps not belong to the same system as the others.

The most natural interpretation of the above results consistent with the rule $\Delta\kappa = 0$ and a $^1\Pi \rightarrow {}^1\Pi$ electronic transition is that the strong bands *a* and *c* correspond to low values, presumably 0 and 1, of κ and also of the related[2] quantum number v_2 ($\kappa = v_2$ for $v_2 = 0, 1$), the other bands to higher v_2 or κ values. Since $\kappa' = \kappa''$, the intensity distribution among different κ values would be determined by the initial (κ') distribution. The fact that each group starts suddenly with a strong band (*a*) is most easily understood if this band has $\kappa = 0$, and $v_2 = 0$. With $\kappa = 0$, we should have pure Λ-type doubling, with alternate components of each doublet missing, giving staggering. The fact that each branch (*P*, *R*) appears in the *a* bands to consist of a single series of lines without staggering is not unreasonable, since the Λ-type doublets might happen to be very narrow. (In the angstrom bands of CO, for instance the Λ-type doubling in the $^1\Pi$ states is too small to detect except for very high *J* values.) This is especially true (cf. Schmid's Fig. 2) since the observed band-line displacements depend on *differences* of displacements in the initial and final $^1\Pi$ states. With $\kappa = v_2 = 1$, assumed in the *c* bands, we might have κ-type doubling to explain the observed staggering; or the fact that κ, $v_2 > 0$ may increase the Λ-type doubling. [For a nonlinear molecule, a $^1\Pi$ state must split into two electronic states; and $\kappa > 0$ or $v_2 > 0$, since it throws the C atom out of line with the O atoms, should induce such a splitting, giving Λ-type doubling even without rotation. Such a constant splitting might, however, escape observation.] With $\kappa = 1$, $\Lambda = 1$, there should be a quadrupling of each rotational level but with two components of each level missing; and unless they should more or less accidentally coincide, it would seem that each of the observed band-lines should be double (i.e., each line theoretically quadruple but with two components missing, alternately one pair and the other pair in adjacent lines; it can easily be shown theoretically that quadruple levels should give here quadruple lines, not more complex groups). The fact that only a staggered series of simple lines, not of doublets, is observed, tends to discredit the present interpretation. But until theoretical calcula-

tions have been made on the nature of combined κ- and Λ-type doubling, it seems worth considering. Another difficulty, however, is the fact that one would expect bands for which $\kappa = v_2$ has the values 0, 1, 2, $\cdots$ to form a nearly uniformly-spaced series, since the levels associated with v_2' and v_2'' should have approximately the uniform spacings characteristic of the harmonic oscillator; actually, the bands a, c, and so on, in each group are irregularly spaced.

An alternative interpretation may be attempted as follows. Disregarding as not quite conclusive the Zeeman effect evidence in favor of ${}^1\Pi \rightarrow {}^1\Pi$, suppose the bands are ${}^1\Sigma \rightarrow {}^1\Sigma$ (or ${}^2\Sigma \rightarrow {}^2\Sigma$). In this case there is no Λ-type doubling, only κ-type doubling, and if $\kappa > 0$ everything is consistent with the observed band structures. But for $\kappa = 0$, with $\Lambda = 0$, the rotational levels must be single, and now the requirement that every other level shall be missing means that for every other J value no level at all exists (with $\Lambda > 0$ or $\kappa > 0$, at least one level is present for every J value). This would give bands with alternate missing lines, i.e., with a spacing apparently twice as large as for bands with $\Lambda > 1$ or $\kappa > 1$. But the bands without appreciable staggering, to which we have tentatively assigned $\kappa = 0$, are in all other respects the same as the bands with staggering, so that the idea of alternate missing lines must be rejected (cf. also Schmid's evidence based on intensity measurements).[1] Hence if $\Lambda = 0$ for the a bands, we must rule out $\kappa = 0$. If $\kappa = 0$ does not apply to the a bands, then presumably there are other bands somewhere with $\kappa = 0$, since there is no theoretical reason why the transition $\kappa = 0 \rightarrow \kappa = 0$ should not occur. One might assume, for instance, $v_2 = 3$, $\kappa = 3$, for the a bands, $v_2 = 3$, $\kappa = 1$ for the c bands, and suppose that $v_2 = 2$, $\kappa = 2$; $v_2 = 2$, $\kappa = 0$; $v_2 = 1$, $\kappa = 1$; $v_2 = 0$, $\kappa = 0$ are among the weaker bands in the group. But this would require a rather surprising initial distribution (v_2', κ'), as well as an improbable arrangement of the initial and final energy levels associated with v_2 and κ, such as to form a kind of band-group head just at the a band, with both lower and higher numbered bands at longer wave-lengths. Everything considered, the ${}^1\Pi \rightarrow {}^1\Pi$ interpretation seems more probable than a $\Sigma \rightarrow \Sigma$ interpretation, but both interpretations are tentative and far from satisfactory.

We may turn next to some other points connected with Schmid's analysis. Usually when a diatomic spectrum is analyzed, the correctness of the analysis is not considered as proved until conclusive combination agreements, i.e., agreeing sets of ΔT values, have been found for both initial and final electronic states. But when one is sure that the bands belong to a definite type, or to one of a few closely similar types, these requirements can be relaxed in some respects. In the case of Schmid's analysis of three of the c bands, combination agreements within experimental error are found for any of two or three different interpretations. According to these all the c bands may have a common initial state, or all may have a common final state in agreement with Smyth's vibrational analysis,[5] or two may have a common initial, two a common final state. Corresponding statements hold for the three a bands analyzed by Schmid. One might think then that the analysis proves nothing, but this is far from being true. Schmid's results determine

within one or at most two units the correct rotational quantum numbers (K) of the band lines, and also determine the values of the rotational constants B' and B'', and the moment of inertia and dimensions of the excited molecule, within a few percent. That is, we know that the correct values of B' and B'' must be chosen from just a few possible sets whose values do not differ much. Also, the *difference* $B'-B''$ is accurately known from the band structure, so that with the B values themselves approximately known, we can definitely conclude that B' and B'' are *nearly equal*. Further, Schmid's work shows definitely that neither B' nor B'' can be *exactly* the same in any of the a as in any of the c bands, but also that they are certainly very *nearly* the same in the a and c series. Schmid's work also indicates, but somewhat less conclusively, that the B' and B'' values are nearly the same in all the bands he has analyzed. These results are in agreement with the present interpretation according to which the a and c bands, since $\Delta\kappa=0$, must differ in both initial and final states in respect to v_2 and κ at least. They do not support Smyth's assignment of a common final level to the a and c series but are not inconsistent with his formulation of the a and c series each as a v_1' progression.

Of the three or four possible combinations (ΔT sets), of which just one must be correct, indicated by Schmid's analysis for the series a and c, certain ones give almost exact integers for the effective rotational quantum numbers, the others almost exact half-integers.[1] The best agreement comes for one of the half-integral sets in each case. But the agreement is only slightly poorer for one of the integral sets. Since for a diatomic or linear polyatomic molecule the theory appears absolutely to demand integral K values for case b and for singlet transitions ($^1\Sigma\rightarrow{}^1\Sigma$, $^2\Sigma\rightarrow{}^2\Sigma$, $^1\Pi\rightarrow{}^1\Pi$, or any other singlet or $\Sigma\rightarrow\Sigma$ transitions), it seems necessary to rule out the possible combinations which would give half-integral rotational quantum numbers. (In speaking of integral K values, we are using the formula $BK(K+1)+\cdots$ for the rotational energy.) Half-integral values would be expected only for J values, in case a with S half-integral, but as has been mentioned above, the bands show no evidence of the multiple-headed structure necessary for this case, nor of the Zeeman effects probably to be expected (because of partial going-over to case b at high J values). Nevertheless, in view of the difficulties experienced in interpreting the bands as singlet or case b bands, it may be well not to exclude absolutely the possibility of case a bands. The most likely case a type, consistent with the observed P, R structure, would be $^2\Pi\rightarrow{}^2\Pi$.

Ruling out half-integral numbers would restrict the possible combinations considerably. If one could be perfectly sure from the vibrational analysis that the a bands all have a common final state and constitute a v_1' progression, and the c bands likewise, as indicated by Smyth's tentative analysis, the correct combinations could be given with considerable confidence. New evidence in favor of the interpretation of the a and c bands as v_1' progressions, in spite of the difficulty in understanding an intensity distribution involving a range of v_1' values and only one v_1'' value, can be given as follows.

The well-known empirical relation that the quantity ω_e/B_e is very nearly

a constant for all states of a single diatomic molecule might reasonably be expected to be capable of extension to the linear CO_2 molecule, at least if we use ν_1/B, where ν_1 refers to the symmetrical vibration. Taking ν_1/B for the normal state of CO_2,[6] one finds almost the same value as one obtains for the upper level of the ultraviolet emission bands using $\nu_1' = 1137$ (cf. Eq. (1) below) and using the most probable B' value of Schmid. No such good agreement is obtained if one uses Schmid's B'' and uses for ν_1 a value secured by reinterpreting the a or c series as v_1'' progressions. Hence Smyth's interpretation of these v_1' progressions receives strong support.

The reader may wonder why, in spite of his very accurate measurements, Schmid's analysis does not permit a decision between several different possible sets of combination differences. This is because of the fact, shown by Schmid's analysis, that if for instance we agree with Smyth that the a (or c) bands constitute a v_1' progression, then the constant B' varies only very slightly with v_1'. That is, if we write $B = B_0 - \alpha_1 v_1 - \alpha_2 v_2 - \alpha_3 v_3 + \cdots$ in analogy with the diatomic relation $B = B_0 - \alpha v + \cdots$, we find that the ratio α_1'/B' is very much smaller than the usual values of α/B for diatomic molecules,—although it has the same sign as is usual in the diatomic case. The former fact causes several sets of possible combination differences to agree so closely that the differences between them cannot be certainly distinguished from experimental error.

If we should assume that the a (or c) bands have a common *upper* level and a set of lower levels differing by unit steps of v_1'', we would conclude that α_1''/B'' is very much smaller than α/B for diatomic molecules, so that the same difficulty as before would arise for the analysis. In this case α'' has the opposite sign to that usual in diatomic molecules, i.e., α in the above equation is negative.

With the assumption of a common lower level for the bands of the a (or c) series, the vibrational analysis[5] gives an equation of the form

$$\nu = \text{const.} + 1136.85v' - 1.85v'^2. \qquad (1)$$

Here the ratio x of the coefficients of v'^2 and v' is much smaller than in diatomic molecules, in agreement with the behavior of the ratio α/B. In diatomic molecules too the ratios x and α/B are closely related, and in the only two known diatomic cases where x has a negative sign, and only in these cases, α also has a negative sign. If, contrary to Smyth's analysis, and in spite of the evidence given above based on the value of ν_1/B, the a and c series should turn out to be v_1'' progressions, x and α would have negative signs. Although this case is rare in diatomic, there is evidence that it is less so in polyatomic molecules. That the a and c series are *either* v' progressions or v'' progressions, and that the variable v is v_1, seem to have been fairly well established.[5]

Since Schmid's analysis shows that B' and B'' are nearly equal, so that the dimensions of the molecule change very little in emitting the ultraviolet

[6] Martin and Barker, Phys. Rev. **41**, 291 (1932). For ν_1 we may take the *average* of the two observed frequencies which result from the interaction of ν_1 and $2\nu_2$ ($v_2 = 2$, $\kappa = 0$).

bands, we can make by means of the Franck-Condon principle some predictions in regard to the intensities for various vibrational transitions. The most probable changes should be those conforming to $\Delta v_1 = 0$, $\Delta v_2 = 0$, $\Delta v_3 = 0$, except in case one or more of the v's has a large initial value or large initial values. Apparently this is true of v_1. The fact that the band system is not more complicated than it is suggests that perhaps $v_3' = 0$ mostly, and $\Delta v_3 = 0$, that v_2' (and κ') are confined mostly to a few small values, and that $\Delta v_2 = 0$ only (incidentally, $\Delta\kappa = 0$ *requires* $\Delta v_2 =$ even, in view of the fact that κ is limited to the values $v_2, v_2 - 2, \cdots 0$ or 1).

An initial distribution involving one or several fairly large v_1' values can be understood if it is produced[5] by electron impacts on unexcited molecules having mostly $v_1 = 0$, $v_3 = 0$, $v_2 = 0$ or 1 (the frequency ν_2 is the smallest of the three, and molecules with $v_2 > 0$ might be moderately abundant in the unexcited gas). Since the equilibrium dimensions of the molecule, which is linear in both states, are considerably different before and after electron impact in this case,[1,6] the latter should tend mainly to excite v_1, but v_3 not at all, and v_2 only indirectly through coupling of v_1 and v_2.

Something further needs now to be said about the Λ-type or κ-type doubling found by Schmid. As Schmid has shown for the band λ3839, the combination differences ΔT are surely of one of two classes. (Since λ3839 has no state in common with any of the other bands analyzed, it is impossible to make tests of the possible combination differences by comparison with other bands; but by analogy considerations the numbering of the lines can be established within a few units;[1] all the possible combinations then fall into these two classes.) Corresponding remarks apply, Dr. Schmid has informed the writer, to the other bands measured by him but not belonging to the a and c series. In one of the two classes, the effective rotational quantum numbers are approximately integral (exactly so where the staggering is small), in the other approximately or exactly half-integral. If the analysis is carried through assuming integral quantum numbers, it shows that the Λ-type or κ-type doubling is moderately large, but if half-integral quantum numbers are assumed, it must be much smaller. In view of theoretical considerations presented above, showing that the rotational quantum numbers ought almost certainly to be integers, it appears necessary to accept one of the sets of possible combination differences which involve integral quantum numbers. But whether one of the integral or of the half-integral sets is adopted, Schmid's work shows perfectly definitely that the Λ-type or κ-type doublet-widths are not greatly different in the initial and final states, also that the departures of the positions of the two doublet components x and y from the positions given by $BK(K+1)$ are of the form const.$_i + a_iK + b_iK(K+1)$, with $a_x = -a_y$; and that b_x and b_y differ considerably, although only $b_x - b_y$ is determinable from the data. These details may prove of considerable value for the analysis of the system.

The definite fact, established by Schmid's work, that the doubling is nearly the same in the initial and final states suggests that the two states are closely similar in respect to the wave functions and energy levels dependent

on v_2 and κ, in agreement with conclusions stated above based on the near-equality of B' and B''. A difficulty in the way of this conclusion, however, is the fact that there is a considerable interval (about 65 cm^{-1}) between each a band and the nearest c band. If ν_2 is about 600 cm^{-1}, as in the infrared or Raman spectra of CO_2, and if for the a bands $v_2 = \kappa = 0$ for both initial and final states while for the c bands $v_2 = \kappa = 1$, then ν_2 must be about 10 percent different for the initial and final states, which is rather surprisingly large. Consideration of the bands in each group other than a and c increases this difficulty (cf. above).

In conclusion, it may be remarked that a great deal remains to be done before the problem of the structure of this system of CO_2 bands will be completely solved.

A rather casual suggestion concerning the interpretation of the two strong CO_2 bands near λ2896 and 2883 may be worth making. The evidence of those who have worked on these bands shows rather clearly that they do not belong to the same system as those discussed above. Duncan's measurements,[5] and those of Schmid, show probable P, Q and R branches, and Schmid's work shows also that all the band lines have pronounced Zeeman effects. The doublet structure (λλ2896, 2883) can be interpreted by a transition $^2\Pi \rightarrow {}^2\Pi$ (or possibly by some other transition between doublet states) in CO_2^+. The doublet width has a reasonable value for a molecule like CO_2^+. The fact that only a single isolated double band is found can be understood by the Franck-Condon principle if the constants of the molecule (assumed linear) are practically identical in initial and final states. The band is then to be interpreted as having $v_1' = v_2' = v_3' = 0 = v_1'' = v_2'' = v_3''$, probably with weaker bands superposed having one or more quantum numbers greater than zero. This interpretation is supported by the band structure, which is of a type expected when B' and B'' are very nearly equal. Several cases like this are known among diatomic band spectra, e.g., the NH band at λ3360, which is a strong (0,0) band with a (1,1) and other weaker bands superposed.

On the Lifetime of the Metastable $^3P_2$ Neon Atom

By E. MATUYAMA
Physical Institute, Tohoku University, Sandai, Japan

(Received August 23, 1932)

To measure the lifetime of the metastable $^3P_2$ neon atom, the light from a Plücker tube was passed through the absorption tube which contained neon gas at various pressures ranging between 5.2 and 0.25 mm Hg. The gas was excited by external electrodes connected to the secondary coil of a high-frequency oscillator. By adopting the method of the rotating disk the percentage of absorption of the line $^3P_2-{}^3D_3$ at various stages after the interruption of the excitation of the gas in the absorption tube, was measured. The result obtained was that the life of the $^3P_2$ neon atom at a pressure of 5.2 mm Hg is about 0.005 sec., which is very near that already reported by Dorgelo, but several times longer than that obtained by Meissner and Graffunder. The effects of impurity and of temperature were also investigated.

THE most reliable experimental data up to date regarding the lifetime of the neon atom in the metastable $^3P_2$ and $^3P_0$ states have been reported in papers published by Meissner,[1] and Dorgelo[2] and Meissner and Graffunder,[3] but there are still some discrepancies in their results.

Dorgelo, using the phosphoroscopic method of a rotating disk, has measured the time elapsing after the interruption of the electrical excitation until the neon tube shows no measurable absorption. The results found by him for the lifetime of the $^3P_2$ state is 1/240 seconds, while that of the $^3P_0$ state is much shorter being about 1/2000 seconds. He has also verified his results by using the method of an alternate current. After rectification, one half-wave is sent through the discharge tube and the other half through the absorbing tube. Meissner and Graffunder used two coupled generators of equal period but of variable phase difference, one of them for the excitation of the Plücker tube and the other for the excitation of the absorbing tube. With any desired phase differences between them, they have measured the rate of decrease in the absorption of the lines above described for gas pressures ranging from 0.2 to 5.6 mm Hg and have found that the half period for $^3P_2$ is 7×10^{-4} sec., and that the lifetime of this state has a distinct maximum for pressures between 1.5 mm and 2 mm Hg.

The present writer has been working on the same subject using the method of exciting neon atoms with a high-frequency oscillatory current, and the results of the measurements on the rate of decrease of the absorption of the line $^3P_2-{}^3D_3$ (6402) will be here described.

The method used is also the same in principle as those of previous investigators which have been briefly described. An absorption tube contain-

[1] K. W. Meissner, Ann. d. Physik **76**, 124 (1925).
[2] H. B. Dorgelo, Zeits. f. Physik **34**, 766 (1925).
[3] K. W. Meissner and W. Graffunder, Ann. d. Physik **84**, 1009 (1927).

ing neon is electrically excited for a time and the excitation is then cut off. After the lapse of any interval of time, the light from an emission neon tube is passed through the absorbing tube and the absorption of the line $^3P_2-^3D_3$ is measured quantitatively. The variations in the time intervals between the excitation of the absorption tube and the light flash from the emission tube were effected by means of a rotating disk with a small hole near the periphery of the disk and an electric contact, in a somewhat different manner from that used in Dorgelo's method. He varied the time intervals by altering the rotational velocity of the disk. However, this gives rise to alterations in the time intervals during which the light passes through the hole, and it will be very inconvenient for comparing the variations in the absorption due to the change of concentration of the metastable $^3P_2$ atom in the absorbing tube. It seems preferable to use the method of varying positions of electric contact without altering the rotational velocity of the disk. To ascertain whether the

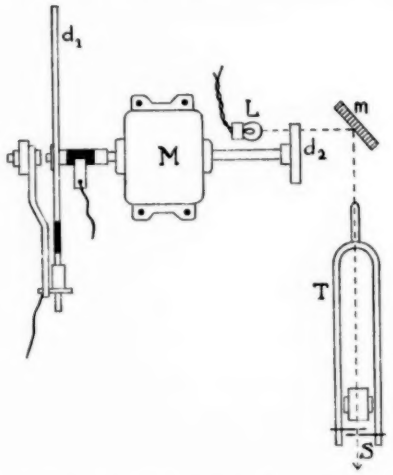

Fig. 1. Rotating disk and stroboscopic device.

disk d_1 while rotating always preserves a constant angular velocity, the following stroboscopic device was used as shown in Fig. 1. The light from an incandescent lamp L falls on the slit s after passing through a small hole in another disk d_2 which is attached to the axis of the motor M whch carries disk d_1, and is reflected by a mirror m. The slit s consists of two brass plates laying close to each other, each of which is attached firmly to each arm of an electrically-operated tuning fork T. By watching carefully the light from the lamp L through the slit s, the current to the motor M was so adjusted that the image of the light was always to be seen at rest. The rotational speed of the motor M was measured directly with a tachometer and was estimated as 1495 revolutions per minute. The rotating disk d_1 is made of a Bakelite plate 40 cm in diameter. A copper piece 6 cm in length, which serves as one of the terminals, is fixed along its periphery, and is connected electrically to a ring on the axis of the motor. The brush making contact with the disk d_1 is of copper, coated with a thin sheet of platinum to reduce the abrasion at

the contact. It is so placed as to be always able to turn around the same axis as that of the motor M. In addition to the precautions above described, the spring of the brush was made as strong as permissible and was adjusted to maintain the same condition of contact in every position of the brush.

The current for exciting the absorption tube was supplied by the secondary circuit of a high-frequency oscillator, which was constructed on the same principle as that of Gill and Donaldson. Its frequency was 3×10^7 cycles. The disk d_1 is inserted in series in the plate circuit of the oscillator and the current was kept at a constant value by slightly varying the filament current. The exciting duration was 0.0019 sec. per one revolution of the disk.

The optical system of the arrangement is shown in Fig. 2. The light from the emission tube p, which is fed with a high voltage d.c. generator, after passing through the lens l_1 and the absorbing tube A, focussed on the hole in the disk d_1. It then passes through the lens l_3, falls parallel on the six-stepped reducer b and is projected on the slit of the spectrograph by the lens l_4. By

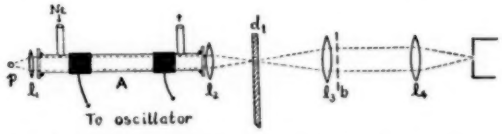

Fig. 2. Optical system for measuring absorptions quantitatively.

measuring the blackness of the plate before inserting the absorbing film it was proved that the illumination of the light falls uniformly on the stepped reducer. To maintain the constancy of the light intensity of the emission tube for the whole course of the experiment, a bulb of great capacity was attached to the emission tube. To prevent fluctuations of the light intensity which are liable to occur for a short time after the circuit has been made, the spectrogram was taken after a lapse of three hours from the beginning of excitation. In order to ensure the constancy of the light intensity of the emission tube, the other conditions being unchanged, the spectrogram, without exciting the absorbing tube, was taken on the same plate before and after the experiment. From this the blackness of the plate is corrected if necessary.

The neon gas used contained 1 percent of helium. It was circulated by means of a condensation pump through the absorbing tube, the tube filled with cocoanut charcoal immersed in liquid air, and the tube containing palladium black. The absorbing tube for the excited neon atom was of glass, 2.5 cm in inner diameter and 30 cm in length. The distance between the external electrodes was 15 cm. Since the light from this absorbing tube was very weak there were no appreciable error introduced into the spectrogram obtained.

The results obtained are diagrammatically shown in Fig. 3, in which the percentage absorption, reckoning the value at the instant of cutting off the excitation of the absorbing tube as 100, are plotted in logarithmic scale against the time which elapsed after the interruption of the excitation. The percentage absorption for the gas pressures 5.2, 1.2, 0.7 and 0.25 mm Hg at 13°C are represented by the curves 1, 2, 3, and 4, respectively, and for the

sake of comparison the results obtained by Meissner and Graffunder for the gas pressures 5.6, 1.42, and 0.50 mm Hg are also shown in the 1′, 2′, and 3′ curves in the same diagram. It will be evident from the diagram that though Meissner and Graffunder have already found that the metastable atom in the $^3P_2$ state has a maximum life for a gas pressure of about 1.5 mm Hg, the lifetime obtained as the result of this experiment in all cases of pressure is markedly greater than the values found by these investigators. Indeed they seem much more nearly the same as those observed by Dorgelo. For instance, the half-life of the metastable atom for the pressure 1.2 mm Hg is 2.3×10^{-3} sec. from curve 2, while that from curve 2′ which represents Meissner and Graffunder's measurement for the gas pressure 1.42 mm Hg gives 7×10^{-4} sec. which amounts only to one-third of the former. In addition, the whole lifetime, assuming this to be the time required to diminish the absorption to 3 percent of its initial value, is, in the case of a pressure 5.2 mm

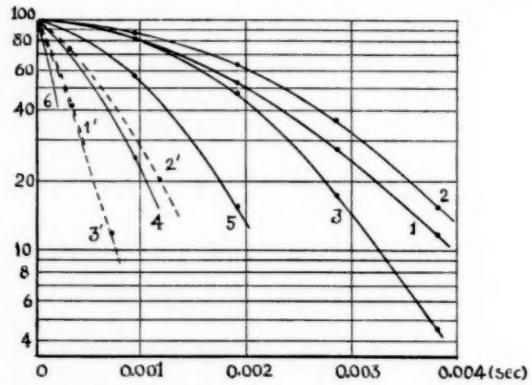

Fig. 3. Curves showing the decrease of the absorption. Curves 1, 2, 3 and 4 are for pressures 5.2, 1.2, 0.7, and 0.25 mm respectively at 13°C. Curve 5 is for neon mixed with hydrogen. Curve 6 is for neon heated at 216°C. Curves 1′, 2′, 3′, are for pressures 5.6, 1.42, and 0.50 mm respectively, measured by Meissner and Graffunder and are plotted for the purpose of comparison.

Hg estimated as nearly 1/200 sec. This fairly coincides with the value 1/240. sec. observed by Dorgelo, at a pressure of 8 mm Hg, while the extrapolation of the curve 2′ gives 1/500 sec.

Next, the percentage absorption when hydrogen gas is present at a very low pressure in the absorbing tube was investigated. For this purpose the palladium tube was removed from the system and neon mixed with a small quantity of hydrogen was introduced. Under these conditions hydrogen is slowly adsorbed in the charcoal. The results obtained when a very small quantity of hydrogen is mixed with the neon at a pressure of 1.5 mm Hg are represented in curve 5. The curve shows that the rate of decrease of the absorption of the line $^3P_2-{}^3D_3$ is considerably increased in spite of the fact that the quantity of hydrogen mixed is so small that it was not possible to observe its secondary spectrum with a small direct vision spectroscope. L. Eckstein[4] has already measured variations of the absorbing power of excited

[4] L. Eckstein, Ann. d. Physik **87**, 1003 (1928).

neon when the neon is mixed with various foreign gases as impurities. He found that the addition of helium in an increasing quantity causes only a slow decrease in the absorption while gases such as hydrogen, nitrogen and argon having lower excited levels than that of the $^3P_2$ and the $^3P_0$ neon states, produced the same effect but about 1000 times greater than helium. As one example in this investigation of the impurity effect, the addition of hydrogen at a pressure of 5.2×10^{-3} mm to the neon at 2.18 mm caused the reduction of the percentage absorptions of the line $^3P_2-{}^3D_3$ from 61.4 to 10 percent. This result is in good agreement with that shown in curve 4.

Thirdly, the effect of temperature was observed. It is already known that the energy difference between the $^3P_2$ and the $^3P_1$ neon atoms is 0.05 volts. The translational kinetic energy of the atom due to the heat motion at room temperature is estimated as 0.003 volts. To increase the mean kinetic energy of the neon atoms over 0.05 volts, the absorption tube was placed in the glass concentric cylinder, through the intervening space of which was circulated the vapor of diethyle aniline. The neon in the absorption tube was thus maintained at 216°C during the whole period of the experiment and the pressure was 5.6 mm Hg. It was observed that the absorption decreases so rapidly that no trace of it could be detected 0.001 sec. after the interruption of the excitation of the absorption tube.

The dependence of the decay of the metastable state on the gas pressure, on the diffusion of the metastable atoms, on the relative dimension of the absorption tube and the light flux through the tube, and on the collisions between the metastable atoms and other entities in the absorption tube have been fully considered by Meissner and Graffunder. Recently, Zemansky[5] has again treated the problem with the data obtained by Meissner and Graffunder on the basis of several assumptions, and has calculated the radius of the excited neon atom. But his result, *viz.*, that the excited atom has a smaller radius than the normal one, conflicts with that expected from theory. Meissner and Graffunder have inquired why the lifetime they have obtained for neon can be several times smaller than that obtained by Dorgelo. The lifetime here obtained is, as already mentioned, much longer than Meissner and Graffunder's value, and falls very near that obtained by Dorgelo. Comparing the experimental conditions with those of Meissner and Graffunder, the absorption tube they used was a much wider and shorter one than that used here, and the light flux in both experiments filled the full section of the absorbing tube. But in the case of this experiment, before entering the spectrograph, some portions of the light are cut off by the aperture in the disk and the stepped reducer, therefore the effective light flux relative to the tube is unknown. From the dimensions of the absorbing tube used, it might be expected that the rate of decrease of absorption in the case of the narrow tube used would decrease more rapidly than in the wider tube, but in spite of this, contrary results were observed. In this experiment, the gas in the absorbing tube was excited with external electrodes and therefore was quite free from contaminations due to the sputtering of electrodes as well as to other gases

[5] M. W. Zemansky, Phys. Rev. **34**, 213 (1929).

occluded in these. By taking into consideration the percentage absorptions when only a trace of other gases are added, it seems very probable that the metastable neon atoms under these circumstances will have a lifetime longer than that in the case where the inner electrodes were used. There is also, in this case, some possibility that the recombination of ions must be considered. The reason the rise of temperature causes considerable increase in the rate of decrease of absorption may conceivably be that this increase is a simultaneous effect of increase of probability of transfer into the higher energy state $^3P_1$, of increase in frequency of collisions between metastable and the normal atoms, and of increase in the coefficient of diffusion.

In conclusion, the writer wishes to express his indebtedness to Professor J. Okubo for advice given during the course of the experiment.

The Molecular Scattering of Light from Ammonia Solutions. The Fine Structure of a Vibrational Raman Band

By JOHN WARREN WILLIAMS AND ALEXANDER HOLLAENDER
Laboratory of Physical Chemistry, University of Wisconsin

(Received September 2, 1932)

The Raman band of the ammonia molecule corresponding to the infrared absorption at 3 μ has been partially resolved into its fine structure. The experiments have been made not with gaseous or liquid ammonia but with aqueous solutions of relatively high concentration. The lines have been assigned to Q, P, R, PP, and RR branches, corresponding to changes in rotational quantum number $\Delta k=0$, ± 1, and ± 2. The moment of inertia about a line normal to the axis of symmetry calculated from the spacing of the lines is $I=2.82\times 10^{-40}$ g cm^2. As far as the present, somewhat incomplete results may be taken to indicate the structure of the NH_3 molecule is largely uninfluenced by the force fields of the solvent molecules.

A NUMBER of investigators have utilized the study of the Raman effect to indicate the changes taking place when an inorganic electrolyte is dissolved in water. The purpose of these studies has usually been to investigate the eventual possibility of obtaining a quantitative measure of the degree of dissociation of the dissolved electrolyte into ions. On the other hand the use of solvents to make it practical to work with simpler substances which do not dissociate upon solution has not met with general favor, it being assumed that perturbations arising from the mutual interaction of solvent and solute molecules will cause difficulties. Also in the case of pure liquids it has been stated[1] that similar interaction produces a lack of sharpness in the rotational states, so that rotational transitions give rise to continuous Raman spectra instead of sharply defined lines. In addition there are presented in this article data whose intent are to show a well-defined difference in the vibrational Raman shifts between gaseous and liquid ammonia.[2] Our experience with solutions in water has led us to believe such views to be unfortunate, at least in the case of the particular system we are about to describe, ammonia plus water. A very incomplete report of the work has already been published as a preliminary communication to the Editor of this Journal.[3]

The molecular scattering of light from gaseous ammonia has been studied by Wood,[4] by Dickinson, Dillon and Rasetti[1] and, more recently and com-

[1] Dickinson, Dillon and Rasetti, Phys. Rev. **34**, 582 (1929).

[2] Experimental error cannot account for the difference in Raman shift in the case of the liquid, $\Delta\nu=3298$, and that for the gas, $\Delta\nu=3334$. However, the "somewhat weaker" shift reported for the liquid, $\Delta\nu=3215$, may be the strong vibration-rotation line, $\Delta\nu=3216$, in our Table I. If this is true, liquid ammonia and the aqueous solution give the same result in this case.

[3] Hollaender and Williams, Phys. Rev. **37**, 1367 (1931).

[4] Wood, Phil. Mag. **7**, 744 (1929).

pletely, by Amaldi and Placzek.[5] There are here reported a vibrational line corresponding to $\Delta\nu = 3311$, and rotational lines which could be measured on both sides of the mercury exciting line λ2536. The experiments with liquid ammonia[6,7,1] have revealed the presence of the frequency differences $\Delta\nu = 3311$, $\Delta\nu = 1580$ and $\Delta\nu = 1070$, corresponding to three of the four fundamental frequencies of the pyramidal formula usually assumed for ammonia. Other weaker lines present in these spectra have either been described as having been caused by the association of single ammonia molecules to form double and triple molecules or have not been mentioned at all.

Carrelli, Pringsheim and Rosen[8] were the first to study solutions of ammonia in water, reporting frequency shifts of $\Delta\nu = 3314$ and $\Delta\nu = 3385$. The next work, as far as we are aware, is contained in the preliminary note referred to above,[3] in which it could be stated "that all the lines which have been reported from gaseous and liquid ammonia have now been found in the concentrated solution (16 normal) as well." There was also included here the microphotographic record of one of the plates which had been exposed in a small Steinheil glass spectrograph. This record shows not only the presence of the vibrational band corresponding to the infrared absorption at $3\,\mu$[9] but also unmistakable evidence of a fine structure due to its combination with the rotation spectrum of the ammonia molecule. The dispersion of the instrument was such that the position of the vibration-rotation lines could not be determined with a sufficient degree of accuracy to assign the proper rotational quantum numbers, so that further experiments with an instrument having a much greater dispersion were necessary. The work to be reported here was done with a Steinheil GH glass spectrograph. Satisfactory exposures were made with ammonia solutions varying in concentration from four normal to sixteen normal, but publication of the results had been postponed in the hope that exposures and microphotographic records suitable for reproduction might be included. It has just now come to our attention that in an article published last month Langseth,[10] working with ammonia solutions of like concentration, has also been able to resolve the Raman band corresponding to the infrared absorption band at $3\,\mu$. The positions of the lines in the two researches agree very well with each other except that we have as yet been unable to find sufficient positive evidence for the combination frequency differences which would make possible the calculation of the moment of inertia characteristic of the rotation about the axis of symmetry. The moment of inertia calculated for the rotation about an axis at right angles to the line of symmetry is almost identical in the two experiments. Under these circumstances it is felt that immediate submission of our present results is advisable even though they are incomplete in certain respects.

[5] Amaldi and Placzek, Naturwiss. **20**, 521 (1932).
[6] Daure, Trans. Farad. Soc. **25**, 825 (1929).
[7] Bhagavantam, Ind. Jour. Phys. **5**, 35 (1930).
[8] Carrelli, Pringsheim and Rosen, Zeits. f. Physik **51**, 511 (1928).
[9] Stinchcomb and Barker, Phys. Rev. **33**, 305 (1929).
[10] Langseth, Zeits. f. Physik **77**, 60 (1932).

Apparatus and Technic

The experimental arrangement was similar to that described by Kohlrausch[11] in his recent book. The ammonia gas, taken from a commercial cylinder, was thoroughly washed before it was passed into conductance water to form the solution. The solution to be investigated was placed in a long tube, illuminated along its length with a commercial mercury arc, and the spectrum of the scattered light which passed through a plane window in the end of the tube was recorded by using the spectrograph mentioned above. The tubes were cooled by means of a jacket through which a continuous stream of cold water was pumped. A comparison spectrum from a copper arc was recorded on each plate. The mercury lamps were cooled by an electric fan. The Raman lines reported were all excited by Hg 4047. The filter technic used was essentially that described by Wood. In the calculation of the frequency differences the frequency of this line was taken as 24,705 cm^{-1}.

The plates were photometered with a Moll recording microphotometer. The frequencies of the Raman lines were obtained by interpolation on a calibration curve prepared from the microphotometric record of the copper spectrum. All lines reported were observed on several of the plates taken, with different concentrations of ammonia and different times of exposure. The intensity of the lines, while difficult to establish in any quantitative way, always became weaker as the concentration of the solution was decreased, indicating that the excitation of the water bands was not a source of difficulty and that the structure observed was actually characteristic of the ammonia molecule.

Experimental Results

The results of the experimental determinations are summarized in Table I. The columns of this table give, from left to right; the frequency of the excited line in reciprocal centimeters, the corresponding frequency difference between exciting and excited line, the assignment of rotational quantum number for the transition $\Delta k \pm 1$, and the assignment of rotational quantum number for the transition $\Delta k = \pm 2$. In a number of cases the microphotometric record shows the head of the line to be somewhat broadened rather than sharp, therefore the exact positions of the weaker lines will be somewhat in doubt. Nevertheless, it is believed that most of them have been located to within ± 3 cm^{-1}. It is interesting to note that the transitions $\Delta k = +1$ and $\Delta k = -1$ are required to account for the positions of some of the observed Raman lines. As Placzek[12] has pointed out this is to be expected in the case of a nonlinear molecule like ammonia. A graphical analysis of the k-structure assigned shows no irregularity or inconsistency.

In Table II there are compared the frequency differences of the several levels for ammonia found by Badger and Cartwright from their study of the infrared rotation bands, by Amaldi and Placzek from the Raman effect for

[11] Kohlrausch, *Der Smekal-Raman Effekt*, Springer, Berlin, 1931.

[12] Placzek, *Molekülstruktur*, Leipziger Vorträge, Hirzel, 1931; Amaldi and Placzek, Naturwiss. **20**, 521 (1932).

TABLE I. *Raman spectrum from aqueous ammonia solution showing fine structure of vibrational transition band corresponding to infrared absorption at 3μ.*

ν in cm^{-1}	$\Delta\nu$ (4047A) in cm^{-1}	Transition $\Delta k = \pm 1$	Transition $\Delta k = \pm 2$
21096	3609	14→15	6→8
21125	3580	13→14	
21161	3544	11→12	
21215	3490	8→9	3→5
21230	3475	7→8	
21254	3451	6→7	2→4
21280	3425	5→6	
21296	3409	4→5	1→3
21315	3390	3→4	
21332	3373	2→3	0→2
21356	3349	1→2	
21394	3311	—	—
21430	3275	2→1	
21450	3255	3→2	2→0
21469	3236	4→3	
21489	3216	5→4	3→1
21510	3195	6→5	
21532	3173	7→6	4→2
21567	3138	9→8	5→3
21586	3119	10→9	
21607	3098	11→10	6→4
21631	3074	12→11	
21656	3049	13→12	7→5
21685	3020	15→14	8→6
21709	2996	16→15	
21743	2962	18→17	

the gas, and by us from our work with aqueous solutions. The agreement, while it cannot be claimed to be excellent, is satisfactory when one considers the difficulties associated with the proper location of the lines and with a possible slight deformation of the ammonia molecule when dissolved to such high concentration.

TABLE II. *Comparison between Raman and infrared spectrum of ammonia.*

Concentrated water solution at 10°C Raman effect*			Gas under pressure Raman effect†			Rotation spectrum infrared absorption‡		
$\Delta k = \pm 2$	$\Delta k = \pm 1$	Frequency	$\Delta k = \pm 2$	$\Delta k = \pm 1$	Frequency	$\Delta k = \pm 1$	Frequency observed	Frequency calculated
	1⟷2	41		1⟷2	—	1⟷2	—	—
0⟷2	2⟷3	59	0⟷2	2⟷3	—	2⟷3	—	59.1
	3⟷4	77		3⟷4	79.5	3⟷4	79.8	79.5
1⟷3	4⟷5	97	1⟷3	4⟷5	99.5	4⟷5	99.1	99.2
	5⟷6	115		5⟷6	119.5	5⟷6	118.6	118.6
2⟷4	6⟷7	139	2⟷4	6⟷7	140.2	6⟷7	—	138.0
	7⟷8	164		7⟷8	159.6	7⟷8	156.8	157.1
3⟷5	8⟷9	176	3⟷5	8⟷9	179.0	8⟷9	176.1	175.9
	9←10	192		9⟷10	199.0	9⟷10	—	194.5
4←6	10←11	213	4⟷6	10⟷11	219.0	10⟷11	—	—

* Present experiments.
† Amaldi and Placzek, Naturwiss. **20,** 521 (1932).
‡ Badger and Cartwright, Phys. Rev. **33,** 692 (1929).

In the microphotometric record mentioned above[3] the fine structure corresponding to the *R* and *RR* branches was less distinct than that on the low wave-length side of the line corresponding to no change in rotation. There is

Fig. 1.

included as Fig. 1 a portion of a microphotograph which shows the resolution of the high wave-length side of the band to greater advantage. Another record, Fig. 2, taken from a plate for which a considerably higher dispersion was

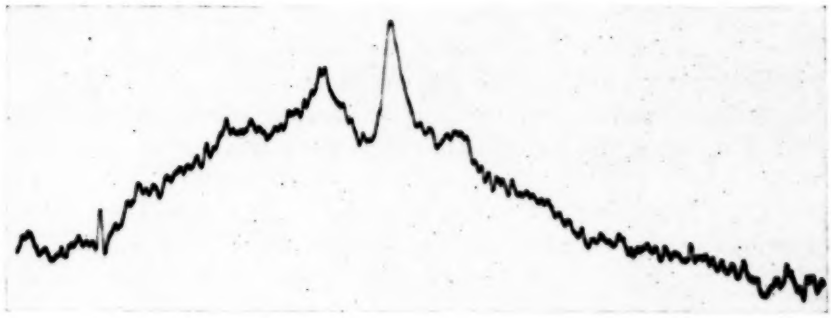

Fig. 2.

used, gives the general structure of the band and permits an estimate of the relative intensities of the lines to be made.

Discussion

The structure of the ammonia molecule is now known to resemble a regular pyramid in form. This is definitely indicated both by potential energy

calculations[13] and by observations of the molecular spectra. In neither case have the mathematical analyses and experimental results been sufficiently refined to enable the assignment of universally acceptable dimensions to the model. However, there is now agreement that the 3μ band in the near infrared is associated with a vibration of the electric moment parallel to the symmetry axis, and that it has been successfully resolved into one zero branch and a simple rotation series.[9] From this band the moment of inertia of the molecule about a line normal to the symmetry axis has been obtained. Values lying between $I=2.77\times10^{-40}$ and $I=2.83\times10^{-40}$ have been reported by a number of investigators of the infrared spectra, so that the agreement here is excellent.

This absorption band has now been resolved by means of the Raman effect, the spacing of the lines corresponding well with that reported by Stinchcomb and Barker. From this spacing it is possible to calculate the moment of inertia.

As indicated in Table I the Raman lines have been assigned to an R branch, $\Delta k=+1$; to an RR branch, $\Delta k=+2$; to a P branch, $\Delta k=-1$; and to a PP branch, $\Delta k=-2$. The frequencies of the lines can be quite exactly expressed by means of the following formulae:

$$\Delta k = +1, \quad \nu = 3311 + 2B(k+1) \quad \text{where } 2B = 19.7 \text{ cm}^{-1},$$
$$\Delta k = +2, \quad \nu = 3311 + 2B(2k+3) \quad \text{where } 2B = 19.8 \text{ cm}^{-1},$$
$$\Delta k = -1, \quad \nu = 3311 - 2B(k) \quad \text{where } 2B = 19.4 \text{ cm}^{-1},$$
$$\Delta k = -2, \quad \nu = 3311 - 2B(2k-1) \quad \text{where } 2B = 19.4 \text{ cm}^{-1}.$$

The values for the constant $2B$ vary but little within each series, in addition the values determined for each series show only slight differences from each other. Taking 19.6 cm^{-1} as an average the moment of inertia may be calculated from the well-known formula, $B=h/8\pi^2cI$, with the result that, $I=2.82\times10^{-40}$ g cm^2. This value is almost identical with that given by Stinchcomb and Barker.[9] It is evident that the dissolved ammonia molecules have not been deformed to any appreciable extent by the continual bombardment and electrical force fields of the solvent molecules otherwise the moment of inertia could have been expected to deviate somewhat from this value.

There has been much discussion with respect to a shift in the characteristic frequency differences given by an ion such as $CO_3^=$ or $SO_4^=$ when it is dissolved in water. Embirikos[14] could detect shifts of approximately 10 cm^{-1} in sulphate solutions when the concentration was changed from one normal to two normal. Even larger shifts were observed by Woodward[15] in the case of lines associated with the $SO_4^=$ ion in his studies of sulphuric acid solutions. These systems differ from the type considered in this article because the scattering is caused by a doubly charged ion instead of by a neutral mole-

[13] Debye, *Polar Molecules*, Chemical Catalog Co., New York, 1929.
[14] Embirikos, Zeits. f. Physik **65**, 266 (1930).
[15] Woodward, Phys. Zeits. **32**, 212 (1931).

cule. The ability of an ion to segregate and orient water molecules about it is well known.

Ammonia gas when dissolved in a large excess of water will first neutralize the acid H_3O^+ and then begin to remove protons from the water itself according to the reactions,

$$H_3O^+ + NH_3 \rightarrow NH_4^+ + H_2O,$$

and

$$H_2O + NH_3 \rightarrow \underset{\uparrow\downarrow}{NH_4^+} + OH^-.$$
$$NH_4OH$$

But as the concentration of the gas is increased greater and greater amounts of ammonia molecules which have not reacted in a chemical way must be present. In such cases the concentration of the ammonia molecules may become so great that observations of the light scattered by them may be made with relative ease. It might be well to mention that the concentration as determined by ordinary analytical methods includes both the NH_3 and the NH_4OH formed.

One might reasonably expect similar experiments in which hydrochloric acid gas was dissolved in water to be successful. Undissociated hydrochloric acid molecules are known to exist in aqueous solutions of concentration as low as one normal, and it is possible to obtain solutions containing more than ten times this amount of hydrochloric acid. However, Woodward[15] and others have reported failure to find any Raman lines using a solution saturated with the gas. The concentration of the undissociated HCl molecules should be sufficient for the purpose. In spite of such experiences, it is to be hoped that there may be accomplished the resolution of the other bands of ammonia and the similar treatment of the spectra of many other simpler gaseous substances using the solution method to obtain a sufficient molecular concentration.

It is a pleasure to acknowledge the material assistance of Professor J. G. Winans of this University in connection with the interpretation of the results.

Raman Spectra of a Series of Normal Alcohols and Other Compounds

By R. W. Wood and George Collins
Rowland Hall, Johns Hopkins University

(Received September 14, 1932)

The Raman spectra of benzene, cyclohexane, cyclohexene, carbon disulfide, butyl bromide and the normal alcohols from CH_3OH to $C_{12}H_{25}OH$ were investigated. The technique recently developed by Wood was used in conjunction with a praseodymium filter. New lines were found in all cases and for some compounds the number was nearly doubled. Two new frequencies at 2660 and 2730 cm^{-1} were found in the spectra of essentially all the alcohols and butyl bromide. They appear to be characteristic of the saturated hydrocarbons. The lines which appear in the Raman spectra of the aliphatic hydrocarbons at 1450 and 1300 cm^{-1} have been attributed respectively to the transverse vibrations of the hydrogens of the CH_3 and CH_2 groups. The line appearing in the Raman spectra of the alcohols at 1270 cm^{-1} is attributed to the transverse vibrations of the hydrogens of the CH_2OH groups. It is pointed out that the Raman spectra of $C_{12}H_{25}OH$ is that of an infinitely long normal alcohol. The new lines of benzene reported by Weiler and Krishnamurti were verified with the exception of the 806 cm^{-1} frequency. In addition a new line at 1690 cm^{-1} was found. The two relatively strong lines of CS_2 at 650 and 800 cm^{-1} were each found to be doublet, thus completing the analogy with CO_2. The separation of the components in each case was 10 cm^{-1}. The existence of a line at 391 cm^{-1}, originally reported by Bhagavantam, was verified.

THE Raman spectra of a number or organic compounds were investigated by an experimental arrangement recently developed by Wood.[1] New lines were found in all cases, and in some the number was nearly doubled. This emphasizes the importance of repeating much of the earlier work that was done before the technique of Raman spectra reached its present stage of development. Most of the recent improvements have been in the direction of improved methods of excitation, and it is perhaps well to call attention to the advantages of using spectroscopes of relatively high dispersion. This is shown by the present investigation in which a glass prism spectrograph with dispersion of 22A per mm in the blue was used. It was found that many of the bands reported in the literature actually possess structure. Likewise Langseth[2] using a one meter grating, found that the Raman lines of CCl_4 were double, and in some cases even triple. There is no doubt but that incomplete and inaccurate data have greatly retarded the interpretation of Raman spectra.

We have investigated the Raman spectra of a series of normal alcohols beginning with methyl (CH_3OH) and ending with dodecyl alcohol ($C_{12}H_{25}OH$). This series was loaned to us by Professor E. Emmet Reid of this University, and was complete up to $C_{17}H_{35}OH$. It proved to be unnecessary, however,

[1] R. W. Wood, Phys. Rev. **38**, 2168 (1931).
[2] Langseth, Zeits. f. Physik **72**, 350 (1931).

to investigate those above $C_{12}H_{25}OH$ as the higher members showed no differences in their Raman spectra. Benzene, cyclohexane and cyclohexene were taken since very pure samples of these were available. As they have already been rather extensively investigated, they served to indicate the efficiency of the apparatus. Carbon disulfide was investigated in order to verify the existence of a line at 390 cm^{-1} which is of vital importance in the analysis of the Raman and infrared spectra.

Experimental

All excitation was by Hg 4358. The experimental arrangement was essentially that described by Wood, modified in that two filters were employed in two Pyrex tubes placed one above the other over the mercury arc. The diameters of these tubes were 5 cm and 2.3 cm, the larger being placed below. With this arrangement a large part of the exciting light from the arc was concentrated into a narrow beam passing vertically through the Raman tube. In most cases a 30 percent aqueous solution of praseodymium ammonium

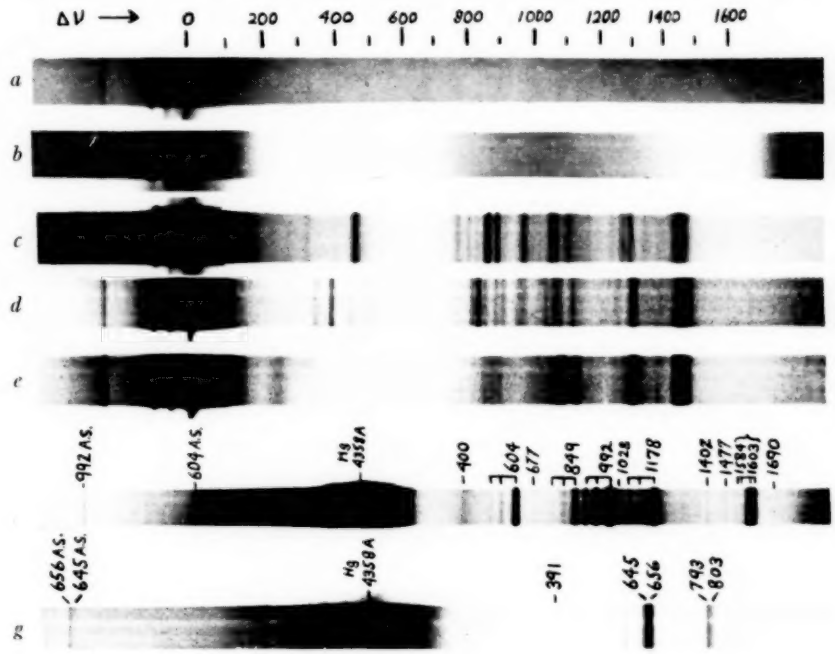

Fig. 1. a, Hg arc; b, Hg arc through praseodymium filter; c, C_3H_7OH (n); d, C_4H_7OH (n); e, $C_{10}H_{21}OH$ (n); f, benzene; g, carbon disulfide.

nitrate was placed in the smaller tube. Praseodymium has a strong and very sharp absorption band on the long wave-length side of, and very close to, Hg 4358, and when used as a filter absorbs the strong continuous spectrum of the mercury arc in this region, leaving a clear background for the Raman lines. Such a filter is particularly advantageous in obtaining Raman lines of low frequency when the excitation is by Hg 4358. Figs. 1a and 1b show the effec-

tiveness with which this filter removes the background. This filter has the disadvantage of reducing the intensity of Hg 4358 to about one-half when used in the above concentration. A rather strong solution of crystal violet was substituted for the praseodymium when investigating Raman lines of frequency greater than 2000 cm^{-1}. The larger tube contained a quinine solution of sufficient concentration to absorb Hg 4047 and Hg 4077 and was protected against photochemical change by a sheet of noviol glass, as previously described. With this arrangement it was possible to make exposures of 70 hours or more before the general background appeared with appreciable intensity.

The wave-lengths of the Raman lines were determined by interpolation on a large dispersion curve obtained from the iron lines of the comparison spectrum. The frequencies given are accurate to about ± 3 cm^{-1} for moderately sharp lines.

The alcohols from $C_8H_{17}OH$ to $C_{12}H_{25}OH$ were prepared by Dr. Jane Meyers of this University. Those from CH_3OH_4 to $C_7H_{25}OH$ were obtained from other reliable sources, and all were carefully purified by distillation. The benzene, cyclohexane, and cyclohexene were from samples especially purified for specific heat and melting point determinations. The remaining liquids investigated were from standard C. P. sources.

Raman Spectra of Alcohols

A chart of the Raman lines of the normal alcohols from CH_3OH to $C_{12}H_{25}OH$ is given in Fig. 2. The lines of frequency greater than 1500 cm^{-1} are not included, but may be found in the complete list of Table I. $C_{11}H_{23}OH$ is omitted from this series as it was not obtainable in sufficient quantities. Enlargements of some of the original plates may be found in Fig. 1.

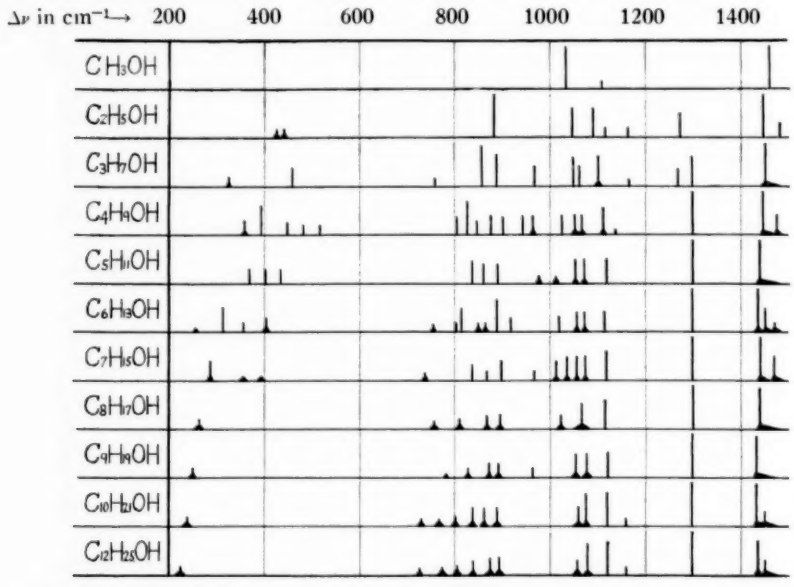

Fig. 2. Diagram of Raman frequencies of alcohols showing relative intensity and breadth of lines.

TABLE I. *Raman frequencies in cm⁻¹.*

CH_3OH	1028(10) 1107(2) 1457(10) 2729(1) 2831(10) 2942(10)
C_2H_5OH	426(5) 443(2) 883(20) 1047(10) 1091(10) 1115(1) (1162)(1) 1273(8) 1449(10) 1481(4) 2637(0) 2714(1) 2823(2) 2783(10) 2925(10) 2972(10)
C_3H_7OH(n)	324(2) 458(4) 757(4) 856(10) 887(8) 967(4) 1049(5) 1064(4) 1100(6) 1268(4) 1296(6) 1451(10) 2663(1) 2731(2) 2873(15) 2905(10) 2931(10) 2963(10)
C_4H_9OH	350(3) 394(6) 448(3) 483(2) 514(2) 805(4) 825(8) 845(3) 877(4) 901(4) 944(4) 963(4) 1025(4) 1051(4) 1067(4) 1104(6) 1135(1) 1296(1) 1147(10) 1476(4) 2660(1) 2733(1) 2865(10) 2903(10) 2932(10) 2963(15)
$C_5H_{11}OH$	366(3) 401(3) 434(3) 835(3) 858(4) 889(4) 975(1) 1013(1) 1053(5) 1072(5) 1116(5) 1299(10) 1442(10) 2653(1) 2721(1) 2868(10) 2908(10) 2935(5) 2961(5)
$C_6H_{13}OH$	253(1) 311(5) 355(2) 402(3) 754(2) 802(2) 814(5) 850(2) 864(2) 888(8) 915(3) 1019(3) 1056(4) 1072(4) 1113(4) 1297(10) 1435(10) 1451(5) 1472(2) (Band 2842 to 2932 (10)) 2958(3)
$C_7H_{15}OH$	287(3) 357(1) 392(1) 735(2) 836(3) 866(2) 897(4) 966(2) 1012(4) 1035(5) 1054(5) 1074(5) 1116(6) 1297(10) 1442(10) 1471(5) (Band 2842 to 2952(10))
$C_8H_{17}OH$	263(2) 759(1) 809(2) 867(3) 894(3) 1023(3) 1066(5) 1120(6) 1300(10) 1442(10) (Band 2848 to 2941 (10))
$C_9H_{19}OH$	250(2) 784(1) 830(2) 872(3) 891(3) 963(2) 1055(5) 1078(5) 1118(5) 1297(10) 1432(10) (Band 2842 to 2932(10)) 2958(2)
$C_{10}H_{21}OH$	238(2) 727(1) 768(1) 801(2) 838(3) 863(3) 889(4) 1059(4) 1076(7) 1116(7) 1159(2) 1295(10) 1430(10) 1449(3) 2643(1) 2719(1) (Band 2836 to 2929(10)) 2954(2)
$C_{12}H_{25}OH$	224(2) 722(1) 771(1) 805(2) 838(4) 874(4) 893(4) 1056(4) 1079(7) 1119(7) 1159(2) 1297(10) 1433(10) 1449(10) 2847(10) 2887(10) 2925(8) 2958(3)
Benzene	400(2) 604(10) 677(1) 849(5) 982(2)* 992(20)* 1028(0) 1178(10) 1402(2) 1477(2) 1584(10) 1603(5) 1690(1) 2291(0) 2452(1) 2542(1) 2618(2) 2920(0) 2948(3) 3051(5)* 3065(5)* 3163(2)* 3186(2)*
Cyclohexane	380(2) 422(3) 801(10) 1026(8) 1154(4) 1264(8) 1342(2) 1442(10) 2626(0) 2661(1) 2693(0) 2750(0) 2849(10) 2880(1) 2920(10) 2934(10)
Cyclohexene	171(2) 282(3) 390(5) 445(1) 487(2) 635(1) 715(3) 821(10) 873(2) 904(3) 963(3) 1034(3) 1062(5) 1134(1) 1218(10) 1238(2) 1263(4) 1426(10) 1443(3) 1650(10) 2634(9) 2660(1) 2833(10) 2856(10) 2873(10) 2908(10) 2934(10) 3020(10)
Carbon disulfide	391(1) 645(10) 656(20) 793(8) 803(3)
Butyl bromide	218(3) 235(3) 276(5) 345(1) 387(2) 411(2) 457(5) 559(20) 640(10) 736(5) 796(6) 833(0) 865(5) 893(4) 909(2) 967(1) 993(2) 1011(2) 1048(8) 1097(8) 1214(5) 1260(4) 1294(5) 1441(10) 2660(0) 2733(1) 2833(2) 2868(10) 2902(5) 2934(10) 2963(10) 3008(3)

* Weiler's values.

Two new Raman lines, hitherto unreported, were found in the spectra of C_2H_5OH, C_3H_7OH, C_4H_9OH, $C_5H_{11}OH$ and $C_{10}H_{21}OH$. They lie at about 2660 and 2730 cm^{-1}. CH_3OH shows only the one at 2730 cm^{-1}. To determine whether these frequencies are associated with the OH groups, the Raman spec-

tra of C_4H_9Br were taken. The position of these new lines was found to be the same in C_4H_9Br and C_4H_9OH showing that they are independent of the radical attached to the end of the molecule. This, combined with the fact that these frequencies appear in so many of the alcohols, makes it seem likely that they are characteristic of the saturated hydrocarbons. New lines, in addition to those discussed above, are now considered.

In methyl alcohol a new frequency was found at 1107 cm^{-1}.

In ethyl alcohol the 426 cm^{-1} frequency as reported in Kolhrausch[3] was resolved into two components, 426 and 443 cm^{-1}, and an additional lines was discovered at 1115 cm^{-1}.

In normal propyl alcohol new lines were found at 324, 757, 1064, 1165 and 1268 cm^{-1}. The frequency 1364 cm^{-1} reported by Duare[4] and by Gamesan and Venkateswaran[5] was not verified. Trumpy likewise failed to find this line.

Six new lines were found in the spectrum of normal butyl alcohol (C_4H_9OH) and six lines previously considered single were resolved into two components. The Raman spectra of normal alcohols above butyl have not been investigated previously.

Lines whose frequencies remain unchanged, or which change in a systematic way from molecule to molecule, are of course the easiest to interpret. Attention is called to five of this type which occur in the spectrum of the alcohols. There is the broad, often unresolved, line at 1450 cm^{-1}, the strong lines at about 1300 and 1120 cm^{-1}, the double line at 1055 and 1075 cm^{-1} (unresolved in $C_8H_{17}OH$), and the group of lines below 500 cm^{-1}. Something may be said in regard to these frequencies.

Kohlrausch[3] and Trumpy[6] have attributed the 1450 cm^{-1} frequency to vibrations of the hydrogens of the

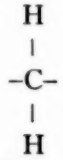

groups (referred to in the future as CH_2 groups). They have at the same time attributed the 1300 cm^{-1} frequency to vibrations of the end CH_3 groups against the remainder of the molecule. This assignment appears unlikely, since, if the line at 1300 cm^{-1} were due to vibrations of the CH_3 group against the remainder of the molecule, its frequency should diminish with increasing mass of the molecule. Fig. 2 shows clearly that this is not the case, and another explanation must be looked for. Andrews has pointed out that the line at 1450 cm^{-1} appears whenever a CH_3 group is present in a molecule, and that the line at 1300 cm^{-1} is usually associated with the presence of CH_2 groups. These two lines presumably arise from a transverse or bending motion

[3] Kohlrausch, *Der Smekal Raman Effekt*, p. 309.
[4] Duare, Ann. d. Physik **12**, 375 (1929).
[5] Gameson and Venkateswaran, Ind. Jour. Phys. **4**, 196 (1929).
[6] Trumpy, Zeits. f. Physik **62**, 806 (1930).

of the hydrogen atoms with respect to the carbons. The fact that these frequencies are so constant would indicate that the influence of the hydrogen bending motions does not extend to adjacent atoms. The 1270 cm^{-1} line which appears in the spectrum of ethyl and propyl alcohol is then explained as arising from transverse vibrations of the hydrogens of the

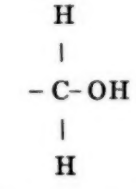

groups (referred to as a CH_2OH group). The hydrogens of this group would be expected to have a different frequency from those of the CH_2 group as their bond strength should be changed by the presence of the OH radical. In support of this contention, attention may be called to the following.

Methyl alcohol (H_3COH) and isopropyl alcohol[3] ($H_3C \cdot HC \cdot OH$) CH_3 contain no CH_2OH or CH_2 groups, and do not show the 1270 and 1300 cm^{-1} frequencies. Ethyl alcohol ($H_3C \cdot H_2COH$) contains a CH_2OH group, and no CH_2 group, and shows only the 1272 cm^{-1} frequency. Normal propyl alcohol ($H_3C \cdot H_2C \cdot H_2OH$) contains a CH_2OH group and shows both the 1270 and the 1300 cm^{-1} frequencies. Butyl ($H_3C \cdot H_2C \cdot H_2C \cdot H_2COH$) and the higher alcohols, however, have both CH_2OH and CH_2 groups, and show only the 1300 cm^{-1} frequency, indicating a possible discrepancy. The explanation may be, however, that the 1270 cm^{-1} frequency exists in the higher alcohols, and is simply too weak to be recorded. The decreased number of CH_2OH groups with respect to the CH_2 groups in the higher alcohols makes this explanation plausible.

The double frequency at 1055 and 1070 cm^{-1} probably arises from a sidewise compressional motion of the carbon chain suggested by Collins.[7] These values are close to the calculated one of 1075 cm^{-1}. In calculating this frequency the influence of the hydrogen atoms attached to the carbons was neglected. Their influence may produce two frequencies instead of one, resulting from the hydrogens vibrating with or against the carbon atoms. A compressional vibration of the type considered is optically inactive, and would account for the high intensity of these lines. It is to be noted that the Raman spectra of $C_{10}H_{21}OH$ and $C_{12}H_{25}OH$ are identical and these two spectra differ but slightly from that of $C_9H_{19}OH$. A further increase in the length of the carbon chain above that of $C_{12}H_{25}OH$ should then produce no change in the Raman spectra. This being the case the Raman spectra of $C_{12}H_{25}OH$ may be considered that of an infinitely long hydrocarbon chain with an OH group at one end.

Raman Spectrum of Benzene

The Raman spectrum of benzene has been examined recently by Weiler[8]

[7] Collins, Phys. Rev. **40**, 829 (1932).
[8] Weiler, Zeits. f. Physik **69**, 586 (1931).

and Krishnamurti,[9] who have reported new frequencies at 687, 806, 1407 and 1477 cm^{-1}. The existence of all these frequencies with the exception of 806 cm^{-1} was verified. The position of the latter frequency when excited by Hg 4358 coincides closely with that of the strong 848 cm^{-1} Raman line excited by a weaker line of the mercury triplet (Hg 4347.5), and it was found impossible to distinguish between the two. Inasmuch as Krishnamurti used Hg 4358 as the exciting line, the existence of 806 cm^{-1} is perhaps doubtful. A hitherto unreported frequency was found at 1690 cm^{-1}. This Raman line falls within one of the praseodymium absorption bands, and otherwise would probably be masked by the continuous background of the arc. An enlargement of one of the benzene plates is given in Fig. 1b with the Raman frequencies, both stokes and antistokes marked. The effect of the praseodymium filter in reducing the continuous background is very noticeable.

Raman Spectra of Cyclohexane and Cyclohexene

The samples of cyclohexane and cyclohexene were of extreme purity, and benzene-free. There was no evidence of the cyclohexane line at 992 cm^{-1} reported by Krishnamurti, and since this frequency corresponds to the strongest benzene line, the inference is obvious. The existence of the new lines in cyclohexane reported by Krishnamurti at 2630, 2662, 2889 and 2963 cm^{-1} was verified, with small discrepancies in their exact frequencies.

Cyclohexene, due no doubt to its unsymmetrical ring structure, shows many more Raman lines than either benzene or cyclohexane. In addition to those already reported by Weiler,[8] new lines were found at 445, 715, 1134, 1238, 2634, and 2660 cm^{-1}; the latter not appearing in benzene and having perhaps the same origin as the lines of similar frequency which occur in the Raman spectra of the alcohols.

Raman Spectrum of Carbon Disulfide

A special effort was made to obtain the complete spectrum of CS_2. The lines at 645 and 793 cm^{-1} were resolved into two components, the separation in both cases being 10 cm^{-1}. An enlargement of one of the plates is shown in Fig. 1g. From this is can be seen that the weaker component of the 800 cm^{-1} line is on the long wave-length side while the weaker component of the 650 cm^{-1} line is on the short wave-length side. As is to be expected, this condition is reversed in the antistokes member of the 650 cm^{-1} line. Of the three lines reported by Bhagavantam[10] at 412, 1229 and 1577 cm^{-1} only the first was verified. The observation of 793–803 as a doublet is of especial interest. It has been previously reported single but a doublet is required to make the analogy with the spectrum of CO_2 complete.

[9] P. Krishnamurti, Ind. Jour. Phys. **4**, 543 (1931).
[10] Bhagavantam, Nature **126**, 995 (1930).

Magnetic Spectra of Secondary Electrons from Silver

By S. CHYLINSKI
Ryerson Physical Laboratory, University of Chicago

(Received August 29, 1932)

By means of a magnetic analyzer and electrometer, the spectra of secondary electrons from silver, when bombarded with cathode rays of energies in the range of 2.1 to 30 equivalent k.v., were determined. Each of the kinetic energy distribution curves shows one prominent peak the location of which varies somewhat with the primary voltage. For voltages up to about 10 k.v. it is located between 0.6 and 0.7 eV_0, where eV_0 is the primary energy; for voltages between 15 and 30 k.v. it is located between 0.7 and 0.8 eV_0. The slopes of the curves on the high energy side of the peaks increase with increasing primary voltages, becoming discontinuous at a point which, within experimental error, corresponds to the primary energy. On the low energy end the peaks decrease less rapidly, reaching half maximum values around 0.3 eV_0 for voltages up to 10 k.v. and around 0.5 eV_0 for the higher primary voltages. The curves have a shape similar to that of the continuous x-ray spectrum curves.

I. INTRODUCTION

WHEN x-rays strike a substance they give rise, among other phenomena, to an electronic radiation. This so-called x-ray photoelectric effect, has been placed upon a secure basis by the experiments of M. de Broglie.[1] His work established the fact, that when a monochromatic beam of x-rays of frequency ν is incident on a substance, a number of groups of secondary electrons are expelled, the energies of which are given by Einstein's equation,

$$\tfrac{1}{2}mv^2 = h\nu - h\nu_0 \qquad (1)$$

where $h\nu_0$ stands for the quantities $h\nu_K$, $h\nu_{L_3}$, $h\nu_{L_2}$ $\cdots$, the work of extraction for the corresponding levels K, L_3, L_2, etc., of the atom. Knowing v, the velocity of each group of electrons, the several values of $h\nu_0$ and from them the absorption limits ν_K, ν_{L_3}, ν_{L_2} $\cdots$, can thus be obtained. The different groups of electrons were isolated by the magnetic spectrograph.

de Broglie's experiment and other similar experiments provided an almost direct method of proving that electrons exist at various energy levels and that there are one K level, three L levels, five M levels, etc.

It is also known, since the work of Lenard[2] and his collaborators, that electrons striking a metal surface cause an emission of secondary electrons.[2] The early work in this field is full of contradictory statements. Since ionization, characteristic radiations etc., are produced by electron bombardment as well as by x-rays, one might expect to find magnetic spectra of secondary electrons such as those observed by de Broglie in the case of the x-ray photoelectrons. Such spectra have actually been observed in the case of certain

[1] M. de Broglie, Comptes Rendus **1**, 274, 527, 746 and 806 (1921).

[2] P. Lenard, *Quantitatives über Kathodenstrahlen*, 1925 Ed. The name "secondary" electrons is used by Lenard and his school in a very restricted sense. In this article we mean by secondary all those electrons that issue from a target when it is bombarded by primary electrons.

gases, for instance, by Dymond,[3] Harnwell[4] and others for helium, and by Eldridge[5] for mercury vapor. In the case of solids no such clear-cut results have been obtained. One might think the reason for this to be partly due to the use of the electric counterfield method of analysis, which was used by the early investigators in this field. This method gives essentially integrated results and hence the existence of any special groups of electrons should be indicated merely by bends or inflections of the velocity distribution curves. The author[6] applied the magnetic analyzer method which is described in detail below. Lorenz[7] made an indirect study of secondary electrons from a tungsten target by comparing the spectra of the focal spot and the so-called stem radiations. The stem radiation is supposed to be produced by the electrons which leave the target and fall back on it due to the negative field of the glass walls and the positive field of the target. The two spectra are similar but that of the stem radiation is displaced towards longer wave-lengths. The difference between the short wave-length limits of the two types of radiation Lorenz identifies as corresponding to the work of extraction of the electrons from definite levels within the atom. Reasoning in this manner he concluded that the secondary electrons were electrons that had been knocked out from the different atomic levels by the primary electrons. Wagner[8] criticized these conclusions and by a photographic magnetic spectrum analysis showed that no such groups of electrons as Lorenz had found, actually existed. He studied the magnetic spectra of high-speed secondary electrons emitted by gold, silver and aluminum targets when bombarded with cathode rays of 16 to 40 k.v. He found the velocity distribution curves to be everywhere continuous except possibly at the high velocity end; also that most of the secondary electrons had speeds close to those of the primary electrons, as the author[6] had found for silver in the range of 5 to 20 k.v. These electrons were evidently of the type that in Lenard's old terminology were named "re-diffused," that is, those electrons which issue from the solid after undergoing deflections by a penetration of relatively few atomic layers.

The present work was undertaken with a view of settling the question of whether or not energy relations exist between the primary and secondary electrons analogous to those that de Broglie found in the case of x-rays and photoelectrons. It was decided to study the electronic emission proceeding in a definite direction from a silver target bombarded with electrons of speeds in the range of 2 to 30 k.v., which region contains all of the critical potentials necessary to excite the various x-ray spectra of silver. It is well known that a certain minimum potential is necessary to excite the K-series spectrum of an element. An increase in the primary potential beyond that minimum might be supposed to detach a K-electron which should then issue with an

[3] E. G. Dymond, Phys. Rev. **29**, 433 (1927).
[4] G. P. Harnwell, Phys. Rev. **33**, 559 (1929).
[5] J. A. Eldridge and H. F. Olson, Phys. Rev. **28**, 1151 (1926).
[6] S. Chylinski, Phys. Rev. **28**, 429 (1926).
[7] E. Lorenz, Zeits. f. Physik **51**, 71 (1928).
[8] P. B. Wagner, Phys. Rev. **35**, 98 (1930).

energy equal to the difference between the energy of the primary electron and that required for K-ionization, the thermionic work function being negligible. The same should be true for the other levels. For instance, with a primary potential of 2 k.v. all of the N and M levels of silver should be excited and we might expect groups of secondary electrons given by the following relations:

$$P - W_{N_7} = 2000 - 106,\ P - W_{M_5} = 2000 - 723, \text{ etc.}$$

where P stands for the primary potential and the W's represent the energy in electron-volts corresponding to the different absorption limits. In addition to the removal of these electrons by inelastic collisions, one might expect photoelectrons to be released from higher levels, due to the x-rays originating in the deeper levels of the same atom or other atoms. Thus, if the analysis is correct, there should appear on the velocity distribution curves distinct peaks, some of which, namely those due to electron impact, should shift their position towards the high velocity end with increasing primary potentials, while those due to x-ray photoelectrons should remain fixed. After a primary potential of about 4 k.v. is reached new peaks should appear, since the L absorption limits of silver correspond to about 3.8 k.v. The K-excitation would not be reached until a voltage of 25.5 k.v. was passed. The intensity of x-ray lines is known to vary approximately as $(V_0 - V)^2$, where V_0 is the primary voltage and V is the minimum voltage required to excite a given series. Hence one might expect the N, M and L electrons to be continuously more numerous as the K-voltage is approached.

Webster,[9] in his studies of the production of characteristic x-rays from silver concludes that they are largely of direct origin, that is produced by the ejection of K-electrons from atoms by the impact of the primary electrons on those atoms, rather than of indirect origin, which may be ascribed to the ejection of K-electrons by the photoelectric effect of continuous x-rays excited by cathode rays in other atoms. The ratio of direct to indirect rays he finds equal to about 2 at 50 k.v. for silver.

Certain considerations are rather discouraging as far as the expectation of the appearance of definite groups of secondary electrons is concerned. Chief among them is the very low line-emission efficiency of cathode rays. This amounts to only a fraction of one percent. Also, as Wagner[8] has pointed out, most of the atoms from which, for example, the L electrons are ejected are not at the surface of the target, and hence there are energy losses along the paths of both the primary and secondary electrons; and that the probability of a cathode ray transferring all of its energy to a given orbital electron is small.

II. Apparatus

The principal parts of the apparatus are shown diagrammatically in Fig. 1. B is a brass cylinder two inches long and of eight inches outside diameter. The cover is fitted to it by means of a ground joint. A little sealing wax around the outside edge makes it air tight. Soldered to the cover is a

[9] D. L. Webster, Proc. Nat. Acad. Sci. **14**, 330, 339 (1928).

small brass pipe having a ground taper into which is fitted the glass cone which supports the cathode. The bottom of B consists of a brass plate which is permanently soldered to it. This plate holds the water-cooled silver target T, an amber plug through which passes the connection to the Faraday cylinder F and a brass pipe leading to the vacuum pumps.

Electrons from the hot cathode pass through a small circular hole in the cover and strike the target. The silver is 2 cm in diameter and 2 mm thick. The target surface is located at 45 degrees with the plane of the drawing, the normal to the surface making an angle of 45 degrees with the primary beam. Electrons escaping from the target at right angles to the primary beam and

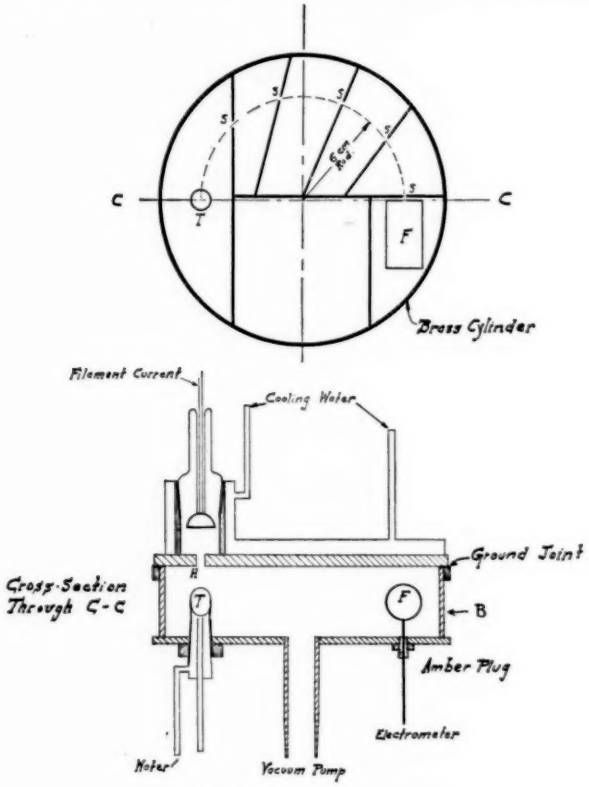

Fig. 1. Diagram of apparatus.

the normal to the target are bent into a semi-circle by means of a uniform magnetic field, which is parallel to the primary rays. The circle has a radius of 6 cm. The beam that enters the Faraday cylinder is reduced by a series of five slits S to a cross section much less than 1 mm^2.

The distance between cathode and cover was 3 cm and that between cover and target was 2 cm. The accelerating potentials were applied between cathode and cover, which, together with the rest of the brass cylinder and the target, was at ground potential. The target is thus located in a space that is practically free from electrostatic disturbances, especially so since the electron current was small, not greater in most instances than 1 m.a. Measure-

ments were made by means of a Dolezalek electrometer, having a sensitivity of 500 divisions per volt. To reduce stray (tertiary) electrons, the walls of the brass chamber were covered with a layer of soot.

The vacuum was obtained by mercury diffusion pumps. These were in continuous operation during the progress of the work. The vacuum was at all times less than 10^{-5} mm of mercury. Preliminary experiments showed no evidence of any ionizing effects due to residual gas. Before use, the apparatus was strongly heated to drive out all occluded gases; the target was heated by electron bombardment lasting several days. To insure steady conditions the apparatus was in operation for about four hours before any measurements were taken.

The magnetic field was supplied by a solenoid which slipped over the vacuum chamber, the latter being mounted on a wooden pedestal. The solenoid was 36 inches long, having about 2700 turns of insulated copper wire. In the middle of the solenoid, where the vacuum chamber was located, the field was found to be very uniform. It was calibrated by means of the usual search-coil ballistic galvanometer method. For any given magnetic intensity H, the voltages equivalent to kinetic energies of the electrons entering the Faraday cylinder could then be computed from the relation

$$V = \tfrac{1}{2}e/mr^2H^2 \qquad (2)$$

where the symbols have the usual signification. The solenoid current was supplied by a large storage battery.

A diagram of the principal electrical connections is given in Fig. 2. The 60-cycle alternating current was rectified by the two kenotrons K and smoothed out by the condenser C, which had a capacity of 0.32 microfarads. The high potential was measured by means of a specially constructed electrostatic voltmeter. This was calibrated against a spark gap. The cathode filament was heated by a current from the secondary of a 110 volt 60-cycle transformer. Throughout each run the current to the target, as measured by a milliammeter, was kept constant by a rheostat. In the case of the 2.1 k.v. run the potential was supplied by a storage battery.

III. Experimental Procedure and Results

The procedure consisted in applying a definite potential to the cathode and obtaining readings on the electrometer for different values of the solenoid current, everything else being kept constant. From these data curves were plotted, of which that shown in Fig. 3 is a typical example. The crosses represent experimental points for a primary voltage of 5 k.v. The electrometer readings are plotted as ordinates, against abscissas that are proportional to the magnetic field intensities and consequently to the square root of the energy. From these, by an application of relation (2) another set of curves was constructed, the abscissas now being proportional to voltages equivalent to kinetic energies. To get the velocity distribution or kinetic energy distribution curves, such as those shown in Figs. 4 and 5, each ordinate of the intermediate curve was divided by the corresponding value of V. This had to be

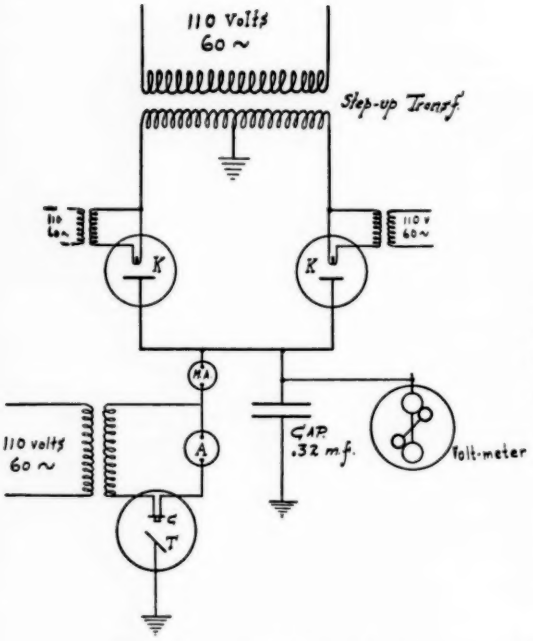

Fig. 2. Diagram of connections.

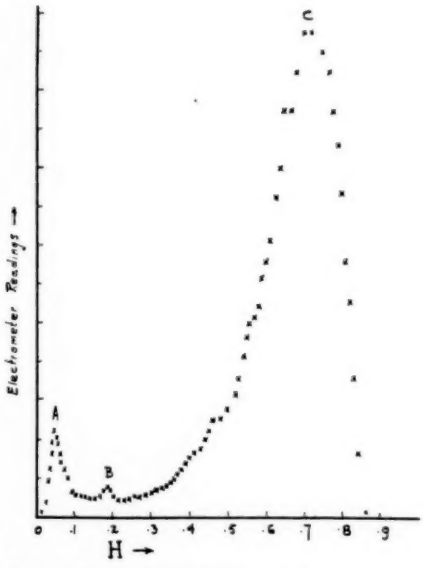

Fig. 3. Experimental curve for primary voltage of 5 k.v.

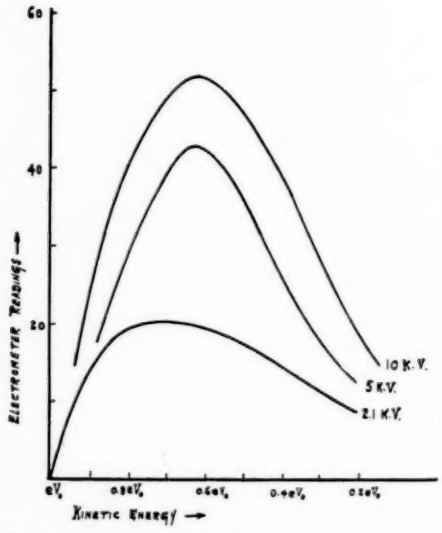

Fig. 4. Velocity distribution of secondary electrons for primary voltages V_0 of 2.1, 5 and 10 k.v.

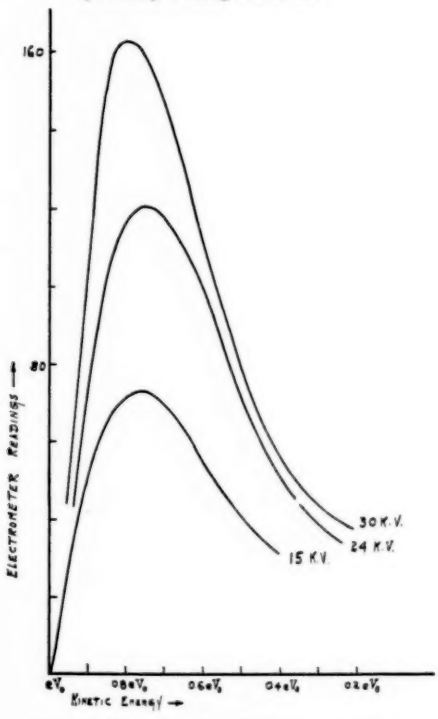

Fig. 5. Velocity distribution curves for primary voltages V_0 of 15, 24 and 30 k.v.

done in view of the change of resolving power of the magnetic analyzer from one part of the scale to another. For any given value of H the electrons entering the collector have values of V in the range of $V \pm \Delta V$, and ΔV is not a constant, but proportional to V.

In this manner the kinetic energy distributions of secondary electrons for primary potentials ranging from 2.1 to 30 k.v. have been investigated. This was done in steps of about 2.5 k.v., but only six representative distributions are shown in Figs. 4 and 5, the rest having exactly similar characteristics.

IV. Discussion

An examination of the curves in Figs. 4 and 5 reveals no such discontinuities as might have been expected if there had been energy relations between the primary and the secondary electrons of the type discussed in the introduction. For voltages up to about 10 k.v. there appear two small peaks, A and B in Fig. 3, which grow less prominent with increasing primary voltages, until at 12.5 k.v. they can no longer be detected. They appear at practically the same places in all curves, A at 8 volts and B at 220 volts. Little if any importance should be attached to the peak at 8 volts. The method of analysis is unreliable for values of V near zero. The low speed electrons do not get away from the target because of the space charge field, or if they do get away they are dispersed by their mutual repulsions and fail to reach the collector. It is not clear what the meaning of the B peak is.

All curves are characterized by the prominent peak at C. For primary voltages up to 10 kilovolts the location of this peak is, in terms of kinetic energy of the primary beam eV_0, between 0.6 and 0.7 eV_0; for voltages between 15 and 30 kilovolts it is located between 0.7 and 0.8 eV_0. The slopes of the curves on the high energy side of the peaks increase with increasing primary voltages, seemingly becoming discontinuous at a point which, within experimental error, corresponds to the primary energy eV_0. On the low energy end the peaks decrease less rapidly, reaching half maximum values around 0.3 eV_0 for the set shown in Fig. 4 and around 0.5 eV_0 for those in Fig. 5. The curves show plainly that most of the secondary electrons have very high speeds.

In conclusion one may say that, while undoubtedly some of the secondary electrons must have come from the inner orbits, their number must also be relatively so small as to be of no detectable influence upon the shape of the velocity distribution curves. The general shape of these curves merits perhaps a remark. They are of the same form as the continuous x-ray spectrum curves. It is not clear, however, what significance, if any, should be attached to this similarity.

It is a pleasure to express my appreciation of the kind interest and help extended to me by Professor Arthur H. Compton during the course of this work.

Experimental Establishment of the Relativity of Time

By Roy J. Kennedy and Edward M. Thorndike
University of Washington and Polytechnic Institute of Brooklyn

(Received July 9, 1932)

None of the fundamental experiments on which the restricted principle of relativity is based requires for their explanation that the classical concept of absolute time be modified; the present experiment was devised to test directly whether time satisfies the requirements of relativity. It depends on the fact that if a pencil of homogeneous light is split into two components which are made to interfere after traversing paths of different length, their relative phases will depend on the translational velocity of the optical system unless the Lorentz-Einstein transformation equations are valid. Hence, such a system at a point on the earth should give rise to an interference pattern which varies periodically as the velocity of the point changes in consequence of the rotation and revolution of the earth. The effect to be expected for a small velocity is so very small that it has been necessary to devise a special source of light, an interferometer of great stability and a refinement of the technic of measuring displacements in the interference pattern. With the apparatus finally employed, we have shown that there is no effect corresponding to absolute time unless the velocity of the solar system in space is no more than about half that of the earth in its orbit. Using this null result and that of the Michelson-Morley experiment we derive the Lorentz-Einstein transformations, which are tantamount to the relativity principle.

AMONG the several classical experiments which suggested the restricted principle of relativity there appears to be none in which any question as to the nature of time is involved. That is, in any of them, time as indicated by an ideal clock moving with the earth might be related in any way to that indicated by a hypothetical fixed clock without at all affecting their results, at least insofar as can be inferred from such theories of the experiments as we are at present able to construct. In experiments such as those of Rayleigh and Brace, of Trouton and Noble, and of Fizeau, all of which yielded null results, there is present the theoretical difficulty that unknown properties of matter are involved. The Michelson-Gale experiment gives a positive result, which is consistent with the concepts of either relative time or absolute time. In fact, it seems that the only experiment heretofore reported that permits of any definite interpretation is that of Michelson and Morley; and the null result of this experiment is completely explained if we suppose that space dimensions in the direction of motion are contracted by an amount depending upon a suitable function of velocity; so here, too, no question as to time is raised. Hence, although such experiments have suggested the relativity theory, they do not form a sufficient basis for the logical derivation of it.

It appears, then, that the theory has needed confirmation, particularly in its most revolutionary aspect; i.e., its denial of a significance for absolute time. Such confirmation has been obtained in the work reported in this paper, and by combining our results with those of the Michelson-Morley experiment, we derive the Lorentz-Einstein transformations which are well known to embrace the whole theory.

The principle on which this experiment is based is the simple proposition that if a beam of homogeneous light is split at a half-reflecting surface into two beams which after traversing paths of different lengths are brought together again, then the relative phases of the superposed beams will depend upon the velocity of the apparatus unless the frequency of the light depends upon the velocity in the way required by relativity. Furthermore, the phase-difference can be made to determine the positions of fringes in an interference pattern, so that by measuring these positions for various velocities of the system, the question whether the frequency follows the relativity requirement can be decided. The variation of the velocity of the system comes about because of the motions of rotation and revolution of the earth.

The theory of this experiment requires the following two assumptions: (a) There exists at least one coordinate system in which Huyghen's principle is valid and the velocity of light is the same in all directions. This assumption is unobjectionable from the standpoint either of relativity or of any plausible hypothesis involving an ether; for relativity, it is true for all uniformly moving systems, and in the latter case for any system at rest in the ether. (b) The Michelson-Morley experiment indicates that a system moving with uniform velocity v with respect to such a system has dimensions in the direction of motion contracted in the ratio $[1-v^2/c^2]^{1/2}$ as compared to dimensions in the fixed system, while dimensions perpendicular to this direction are unchanged. This is in part assumption, for although there can be little doubt that the experiment yields a strictly null result, nevertheless it actually shows only that dimensions in the direction of and perpendicular to the motion are in the ratio mentioned; either of these dimensions might be any function of the velocity so long as that ratio is preserved.

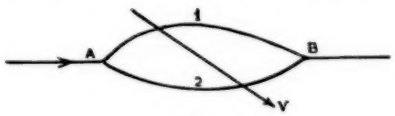

Fig. 1.

Let us consider one such system S', and suppose that a system S (attached, for instance, to the surface of the earth) moves practically uniformly with velocity v with respect to it. In S is set up an arrangement for producing interference; i.e., one in which a pencil of homogeneous light is divided as mentioned above into two pencils which are recombined after traversing paths of different lengths. We can simplify the discussion by treating the general case instead of the particular arrangement used in the experiment, and by adopting a rule regarding expressions for the distances, angles and times in system S that will be of interest; i.e., the magnitudes of these quantities will be expressed by unprimed letters when they are referred to standards moving with S, and by the same letters primed when referred to standards fixed in S'.

The path of a typical ray with respect to S can be represented schematically as in Fig. 1 where the ray coming from the left is divided at A into rays 1 and 2 which recombine at B. The courses of the same rays with respect to

S' are evidently determined by the requirement that to each element ds' of a ray is to be added an elementary vector vdt' where dt' is time required for light to traverse the element, and c is the velocity of light with respect to S'. The length of the resulting element is evidently cdt'; hence $c^2(dt')^2 = (ds')^2 + v^2(dt')^2 + 2v\,ds'dt'\cos\theta'$. Hence,

$$dt' = \frac{ds'}{c(1-\beta^2)}[\beta\cos\theta' + (1-\beta^2\sin^2\theta')^{1/2}] \tag{1}$$

where $\beta = v/c$ and θ' the angle between v and the element ds'.

If for the moment we consider a set of rectangular coordinates in S and S' with corresponding axes parallel and x-axes parallel to velocity v, we have from assumption (b)

$$ds' = [(dx')^2 + (dy')^2 + (dz')^2]^{1/2} = [(dx)^2(1-\beta^2) + (dy)^2 + (dz)^2]^{1/2}$$

$$= ds\left[1 - \beta^2\left(\frac{dx}{ds}\right)^2\right]^{1/2} = ds(1-\beta^2\cos^2\vartheta)^{1/2}$$

$$\cos\theta' = \frac{dx'}{ds'} = \frac{dx(1-\beta^2)^{1/2}}{ds(1-\beta^2\cos^2\theta)^{1/2}} = \cos\theta\left(\frac{1-\beta^2}{1-\beta^2\cos^2\theta}\right)^{1/2}$$

$$\sin^2\theta' = \sin^2\vartheta/(1-\beta^2\cos^2\theta).$$

When these expressions are substituted in Eq. (1), it reduces to

$$dt' = [ds/c(1-\beta^2)^{1/2}](1+\beta\cos\theta), \tag{2}$$

the right side of which equation involves only quantities referred to standards moving with S. The time for light to traverse the whole ray AB along path 1 is therefore

$$t_1' = \int_1 dt' = 1/c(1-\beta^2)^{1/2}\int_1 (1+\beta\cos\theta)ds$$

and a similar expression holds for path 2. Hence difference of time for the two paths is

$$t_1' - t_2' = 1/c(1-\beta^2)^{1/2}\left\{\int_1 ds - \int_2 ds + \beta\left[\int_1 \cos\theta\,ds - \int_2 \cos\theta\,ds\right]\right\}.$$

The term in brackets multiplied by β vanishes, since in order to interfere the rays must intersect, and therefore their projections on the line joining A and B are equal; these projections are the integrals in brackets. Hence

$$t_1' - t_2' = (s_1 - s_2)/c(1-\beta^2)^{1/2} = \Delta s/c(1-\beta^2)^{1/2}, \text{ say},$$

and the number of waves corresponding to this difference of time is

$$n = \nu'(t_1' - t_2') = \nu'\Delta s/c(1-\beta^2)^{1/2} \tag{4}$$

where ν' is the frequency of the light employed as measured by an observer in S'. This number n is seen to be independent of orientations, lengths and

dispositions of paths, but to depend upon difference of path-lengths, the relative velocity of S and S' (through β) and the frequency.

The foregoing treatment is strictly valid only if the moving system is regarded as not subjected to forces, but is undoubtedly sufficient for the purpose in the small constant field of gravitation and acceleration at the surface of the earth. Moreover, although the rotation of the apparatus with the earth involves a slight effect on the time difference computed above (whether regarded from the standpoint of relativity or classical theory), it turns out to be altogether negligible in amount. This effect is a function of rotational velocity, not of orientation of apparatus.

We have now to consider the effect of a change in the velocity v on the number n expressed by Eq. (4). In that equation c is evidently a constant, while the difference Δs, because it is referred to standards moving with the system, is constant unless the courses of the rays between the points of separation and recombination are dependent on the velocity; that this is not the case can be shown by Huyghens' principle. A direct consequence of this principle is that the course of the ray is determined by the condition that the time required for traversing the path is a minimum compared with the time for any neighboring path. Now, Eq. (3) expresses the time in terms of coordinates moving with S, and if minimized in the usual way would yield the equations of the paths. For the present purpose, however, it is unnecessary to carry out this operation. Rewriting (3) we have

$$t' = 1/c(1 - \beta^2)^{1/2}\left\{\int_A^B ds + \beta \int_A^B \cos\theta \, ds\right\}.$$

It will be observed that although the expression involves the velocity of the moving system, nevertheless the course of the ray is quite independent of it. That this is so is evident from the following considerations: the second integral is equal to the projection of the path on the line joining A and B, and being the same therefore for all paths, cannot contribute to the determination of the minimizing path. The first integral is expressed in terms of distances referred to standards moving with the system and so is independent of the velocity. Hence the actual courses of the rays, which are got by minimizing integrals of this form, are independent of the velocity, and Δs is a constant. This proof is essentially that of Lorentz extended by the inclusion of the contraction hypothesis.

The quantity ν' in Eq. (4) is the only one whose possible variability with velocity remains to be considered. From the standpoint of relativity, $\nu' = \nu(1-\beta^2)^{1/2}$ where ν is the constant value of the frequency which would be determined with standards moving with S; this value of ν' would evidently make n a constant. Furthermore, it will be shown later that insofar as the atom is to be regarded as a typical clock, the Lorentz-Einstein transformations can be derived from this relationship and assumption (b). If, on the other hand, $\nu' \neq \nu(1-\beta^2)^{1/2}$ these transformations do not apply and it turns out that there exists but one system S' satisfying assumption (a); this unique system would be the absolute reference frame postulated in the classical

ether theory. In this case n is evidently a function of the velocity of S with respect to the absolute reference frame. Evidently, then, the relativity hypothesis can be tested by determining whether n is constant as v changes in consequence of the motions of rotation and revolution of the earth.

For the present purpose the total velocity of the apparatus can be got by adding vectorially a presumably constant velocity v_0 of the sun, the orbital velocity v_1 of the earth and the circumferential velocity v_2 due to the rotation of the earth (taking account of latitude). Its square can be reduced to

$$v^2 = v_0^2 + v_1^2 + v_2^2 + 2v_\alpha v_1 \sin(\theta_1 - \omega_1) + 2v_\beta v_2 \sin(\theta_2 - \omega_2) + 2v_1 v_2 \cos(\theta_1 - \theta_2),$$

where v_α is the projection of v_0 on the orbital plane, v_β is projection of v_0 on the equatorial plane, ω_1 and ω_2 are constants related to the direction of v_0, and θ_1 and θ_2 are angles expressing the position of the earth in its orbit and its orientation on its axis with respect to the fixed-stars.[1] This procedure assumes only that the fixed-star system has no great angular velocity with respect to the fundamental system S'; there is an unimportant approximation in the last term.

In order to get an idea of the magnitude of the effect that might be expected, let us assume that $\nu' = \nu$ and replace ν by c/λ; then (4) becomes $n = \Delta s/\lambda(1-\beta^2)^{1/2}$. Expanding this, ignoring terms in β above second degree, substituting for the velocity from the expression above, and gathering constant terms into one,

$$\begin{aligned} n &= (\Delta s/\lambda)(1 + \tfrac{1}{2}(v^2/c^2) + \cdots) \\ &= (\Delta s/\lambda c^2)\left[v_\alpha v_1 \sin(\theta_1 - \omega_1) + v_\beta v_2 \sin(\theta_2 - \omega_2)\right] + \text{a constant} \\ &= \delta n + n_0. \end{aligned} \tag{5}$$

Here the variable part of n is represented by δn and the constant by n_0 and we assume v_α and v_β to be large compared with the orbital and circumferential velocities v_1 and v_2. Hence δn should be proportional to the sum of a term with a period of a year and one with a period of a sidereal day.

In performing the experiment, we wish, of course, to make δn as large as possible. The only factor that can be controlled is the ratio $\Delta s/\lambda$, the largest feasible magnitude of which is a measure of the homogeneity of the light. For various reasons the most suitable light seems to be the mercury line of wave-length 5461. With this, sufficiently clear interference fringes could be got when Δs was as large as 318 mm (the value finally used) and on substituting this in the expression for n it turns out that the rotation of the earth would produce a daily variation of a thousandths of a fringe for 200 km per

[1] More specifically, θ_1 is the angle between the projection of v_0 on the orbital plane and a direction in that plane determined by the angle ω_1 which depends on the position of the earth in its orbit or the time of year at which θ_1 is taken as zero. Similarly, θ_2 is the angle between the projection of v_0 on the equatorial plane and a direction in that plane determined by the angle ω_2 which depends on the time of day at which θ_2 is taken as zero. In the reduction of the data, the θ's are taken as zero at the beginning of each run, so the ω's depend on the times of starting runs. In the comparison and final summary of data, the θ's are of course referred to the same sidereal time.

second, while the orbital motion would produce the same variation in six months for 3 km per second.

Because of the probable minuteness of these effects it was necessary to contrive new ways of detecting them. In the rather complicated method first proposed[2] the phase variation would show itself in the rotation of the plane of polarization of a beam resulting from the superposition of two oppositely circularly polarized beams. This scheme, although theoretically capable of great precision, was abandoned in favor of the much simpler one finally employed. In the latter, ordinary interference rings were formed and photographed, and the problem became one of measuring very small changes in the diameters of the rings. It was satisfactorily solved by devising a special comparator which will be discussed later.

Evidently, it was necessary to take every precaution to keep the experimental conditions constant; we were able, in fact, to reduce the average daily periodic error in $\Delta s/\lambda$ to about two parts in 10^{10}. This great stability was attained mainly by using interference apparatus made almost entirely of fused quartz and kept in a vacuum at a temperature constant to within about a thousandth of a degree. The apparatus was furthermore (partly accidentally) compensated for temperature to such an extent that one degree change produced a shift of only about a hundredth of a fringe. The vacuum was employed as simplest way to eliminate variations in pressure, which would have caused variations in index of refraction of optical paths, and, by mechanical action, variations in lengths of paths.

Several disturbing factors producing spurious effects had to be dealt with. Perhaps the most troublesome was the variability in density of the photographs due (in the earlier green-sensitive plates) to rapid aging which affected the emulsions in varying degrees. Since the photographic effect of light is not proportional to its intensity, it follows that a spurious displacement of an interference pattern of the type used is to be expected if the density of the photographs is not constant. The methods adopted to eliminate this and other difficulties are discussed elsewhere in the paper.

Apparatus and Experimental Procedure

The general arrangement of the experimental apparatus is sketched in Fig. 2. Light from source S passes through a small circular opening in screen S_1, is rendered approximately plane-parallel by lens L_1 is dispersed in direct vision prism P and the green (λ5461) image of first opening is focused over a second one in screen S_2 by lens L_2. The water-cell C is to absorb stray heat radiation. The green light from second opening is polarized by nicol prism N so that the electric vector is horizontal, and then enters the vacuum chamber V through a window and is concentrated by lens L_3 to the extent required to produce the greatest intensity in interference pattern. The light is then split into two pencils at the half-reflecting mirror M_1 which is inclined at such an angle (Brewster's angle) that reflection of the polarized light occurs only at its platinized face; the faces of the compensating plate M_4 are equally

[2] Kennedy, Phys. Rev. **20**, 26 (1922).

inclined. Hence no stray (non-interfering) light can be superposed at these faces on the two pencils from M_1; these pencils are reflected by mirrors M_2 and M_3 back to M_1, at which one is partially transmitted and the other partially reflected through lenses L_4 and L^5 which focus the light as a system of interference rings on a wide horizontal slit just in front of a photographic plate in the holder H. The slit is 5 or 6 mm wide, so the plate receives a symmetrical central section of the interference pattern of that width. The plate is held by a spring in the holder lightly against the metal tube T which is sealed against the window W of the vacuum chamber. Most of the length of the tube as well as the vacuum chamber is within the tank V containing

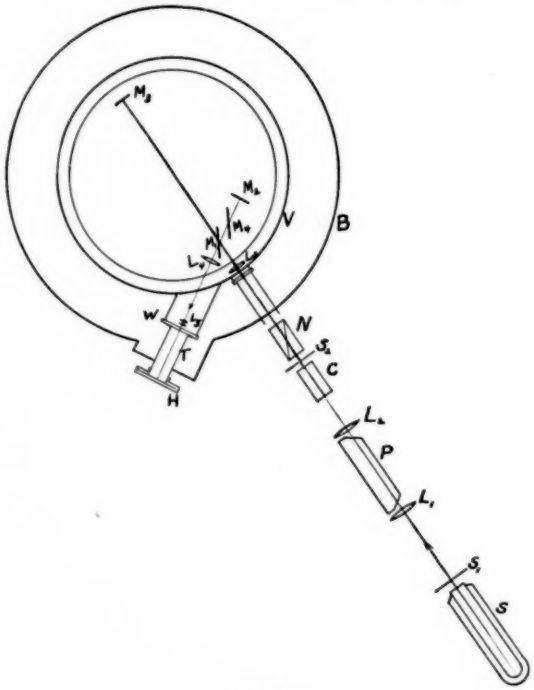

Fig. 2.

water at a temperature constant to within less than 0.001°C; hence slight variations in room temperature cannot affect focusing and thereby diameters of rings. The plate holder, which is kept from contact with the vacuum chamber in order to preclude the possibility of jarring the latter when the holder is operated, is arranged to let the plate slip down two slit-widths automatically every half hour. On each plate six photographs are taken consecutively in this way, and twelve hours after the start of the first series six more are taken in the spaces left vacant during first exposure of the plate; hence the developed plate will contain a series of photographs alternately taken twelve hours apart. The purposes served by this procedure will be explained later. Four such plates are taken during a day's run.

The temperature of water-bath was easily kept nearly constant for many weeks in succession. The temperature was chosen only slightly above that of

room, the water was circulated continuously and the mercury-toluene thermostat was arranged to control the potential of the grid of a vacuum tube which actuated the relay in the heating circuit—in this way only a minute current is broken at the mercury surface and it does not become contaminated with a film of oxide. The optical part of the apparatus was enclosed in a small dark room within a larger one. The temperature of the inner room was kept constant to within a few hundredths of a degree, that of outer room to within about a tenth.

The interference apparatus consisted essentially of a set of four interferometer plates of the best quality obtainable, mounted on a circular fused quartz base 28.5 cm in diameter by 3.8 cm thick. The method of mounting the plates is perhaps worth describing: the support of each plate was cut from a flat plate of fused quartz, and fused to a tapered plug of the same material which, after being ground to fit a tapered hole in the base, was etched away

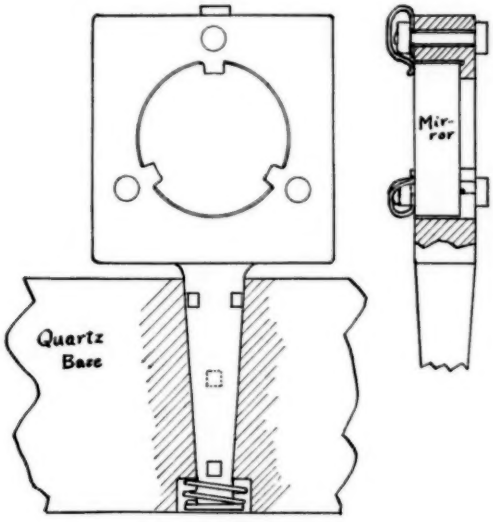

Fig. 3.

over the whole conical surface except in four spots of two or three square millimeters area, which were therefore the sole points of contact of the plug with the base. This procedure was necessary to insure a definite fixed position of plug, since if it were merely ground into the plate it would probably fit the hole only in a region near its middle. The positions of the bearing spots are indicated by the small squares in Fig. 3, the dotted one being on the opposite side of plug from the others. The plugs were held down by light springs as shown in the figure. The end mirrors were circular etalon plates 25 mm in diameter. Their supporting frames were fashioned so as to provide three projections of quartz against which the mirror was held by a light spring opposite each projection. The faces of the projections were ground flat and so as to be very nearly in a vertical plane when the frame is in place on the base. Final adjustment of mirrors was made by rotating them about their horizontal axes; it will be evident that in this way (because of slight in-

clination to each other of the faces of the mirror) a very fine adjustment can be made. It was sufficient simply to rotate the mirrors with the unaided fingers, to correct for the departure from the vertical, while viewing the interference rings with a telescope. The reflecting surfaces were of platinum applied by cathode deposition. It was impossible to use silver for the purpose because traces of mercury vapor in the vacuum chamber would quickly dissolve it. The light lens system which formed the rings on the photographic plate was attached to the base by means of invar plugs similar to those described above.

The quartz base rested on a piece of uniform velour, the back side of which was cemented to a heavy flat brass plate which was supported in an accurately horizontal position at three points. Each fiber of the nap of the velour thus served as a tiny spring so that the weight of the quartz plate was evenly distributed; this is important, since a fused material of this sort is essentially only semi-solid. The friction between the velour and the rough bottom face of the base sufficed to hold the latter accurately in position.

In order to produce interference under the existing condition of large difference of paths of the two beams, the image in the half-reflecting mirror of the face of either end-mirror must be nearly parallel to the face of the other end-mirror; it will be shown that such an adjustment of the mirrors gives rise to a pattern consisting of a series of concentric circular rings. In order that the effective diameter of each ring may be sensibly independent of accidental variations in distribution of light intensity over the faces of mirrors and with respect to direction in the beam, it is necessary to make this parallelism very accurate. The accuracy of adjustment could be tested by the simple procedure of moving a broad slit in various directions across the pencil incident on the half-reflector while the rings were observed in a telescope or photographed; when the diameters of rings were constant for all positions of slit the adjustment was the best obtainable.

The particular spectral line employed in the experiment was chosen on basis of several requirements. As has been pointed out, it must be capable of producing interference with large path-difference; it must also be entirely controllable as to intensity, the intensity must be fairly large, and the line must be easily separable from adjacent ones. On the whole, these conditions seemed best satisfied by the line $\lambda 5461$ of mercury. The homogeneity of any light is roughly proportional to the inverse square root of absolute temperature of source; hence the first source employed was a water-cooled mercury arc. This produced excellent interference rings, but it was soon noticed that their diameters depended on the part of the arc from which the light was taken; this suggests a Doppler effect due to motions of evaporating molecules from the hot liquid surface where the arc was brightest. Such an effect due to velocities variable by only a few centimeters per second would evidently be objectionable in view of the stability required.

The source finally used was an electrodeless discharge in unsaturated mercury vapor. The tube is sketched in Fig. 4. The inner tube in which the discharge took place was connected to a continuously operating pumping

system through a capillary tube (heated to prevent condensation in it) of such length and diameter as to keep the pressure of the vapor just below that of saturated vapor at the existing temperature. The vapor was supplied by the mercury well at the rear of tube, and the small amount escaping through the capillary would condense and return by way of the other vertical tube. The temperature of the source, and thereby the pressure of vapor, were kept constant by means of carbon-tetrachloride in the jacket surrounding the inner tube; the liquid was maintained at its boiling-point by heat from the discharge, and its vapor was condensed and returned by the water-cooled condenser connected to top of jacket. It will be evident that with the discharge occurring at some distance from the mercury well, first-order Doppler effects would be eliminated since no mercury condenses in the forward part

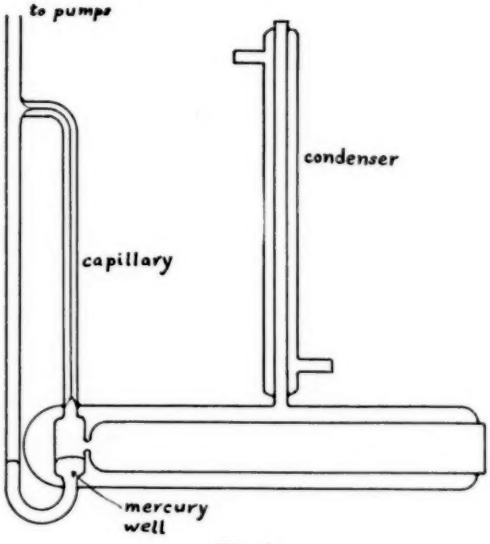

Fig. 4.

of the tube and therefore velocities of vapor molecules are on average same in all directions. Electrical energy was supplied by a coil of some thirty turns of wire around the outside of the jacket, in which oscillations of 20 meters wave-length were produced by a 75-watt transmitting tube. This discharge produced a uniform steady glow over nearly the whole diameter of the inner tube, and the interference rings were completely free from the fluctuations in brightness and diameter which were visible with the ordinary arc. During a run, and for some time in advance of it, the tube was kept in continuous operation in order that all conditions should be steady. It was found that the frequency of the light depended on the temperature of the cooling liquid and the voltage applied to oscillator, so these factors had to be closely controlled. These effects probably arise from the complicated structure of the green line; its "frequency," as inferred from the interference pattern, is of course a sort of mean of the frequencies of its components, weighted according to their intensities. It is to be mentioned that each of several attempts to

use sealed-off tubes failed; after a few minutes of operation with such tubes the rings would disappear, presumably because the oscillatory discharge readily excited a green band in traces of oxygen which probably remain in tube.

In view of the theorem of Lorentz previously discussed, the usual theory of interference for stationary systems can be applied directly to the present situation. In Fig. 5, A represents the surface of one end-mirror and B the

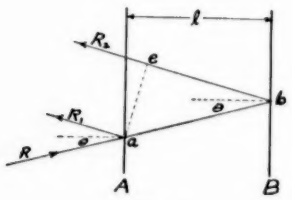

Fig. 5.

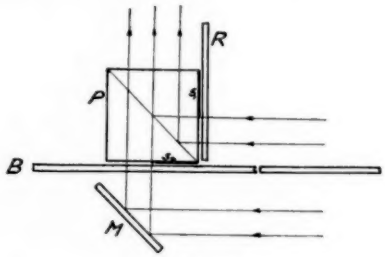

Fig. 6.

image of the other at distance l from A. Since A and B are parallel, the ray R impinging on both at angle θ produces on reflection the two parallel rays R_1 and R_2. If these are brought to a focus, the difference between the lengths of their paths will evidently be $ab+be$. Now

$$ab = l/\cos\theta,\ be = ab\cos 2\theta.\ \ ab + be = (l/\cos\theta)(1 + \cos 2\theta) = 2l\cos\theta.$$

For constructive interference, this path-difference must contain an integral number of waves; hence the cones of rays for which $2l\cos\theta_i (i = 1, 2, 3, \cdots)$ equals a series of consecutive integers[3] can be brought to a focus as a series of concentric rings of radii $r_i = (\sin\theta_i)/k_1$, where k_1 is a constant depending on magnification of lens system producing the interference pattern. Now $ab+be$ is the quantity Δs in Eq. (4); hence $\Delta s_i = 2l\cos\theta_i = 2l(1-k_1^2r_i^2)^{1/2}$ and $n = 2\nu' l(1-k_1^2r_i^2)^{1/2}/c(1-\beta^2)^{1/2}$. It is convenient to consider only the central ray, and to express its phase in terms of the radii of the rings. For this ray $r=0$, so

$$n = 2\nu' l/c(1-\beta^2)^{1/2} = n_0 + \rho \tag{6}$$

where n_0 is an integer and ρ a fraction. In general, for constructive interference $n = n_0 - i$. Then

$$n_0 - i = [2\nu' l/c(1-\beta^2)^{1/2}](1-k_1^2r_i^2)^{1/2} = (n_0+\rho)(1-k_1^2r_i^2)^{1/2}.$$

$$\therefore\quad \rho = (n_0 - i)/(1-k_1^2r_i^2)^{1/2} - n_0 = n_0 - i + \tfrac{1}{2}(n_0 - i)k_1^2r_i^2 - n_0 \cdots$$

$$= (k/2)r_i^2 - i, \tag{7}$$

approximately; here k is a new constant. The approximations are justified since n is of order $10^5 \times i$ and $k_1 r_i$ has a maximum value of about 10^{-2} for the rings measured. From Eq. (7) we find on differentiating

[3] When the distances are expressed in wave-lengths.

$$\delta\rho = kr_i\delta r_i = kr_j\delta r_j = \cdots . \tag{8}$$

If measurements $\overline{\delta r_i}$ of the values of the variations in r_i are made for each of a number of rings of orders m to p, the mean value of $\delta\rho$ computed from them is

$$\delta\rho = \frac{k}{p - m + 1} \sum_{m}^{p} r_i \overline{\delta r_i}. \tag{9}$$

It will be convenient to have $\delta\rho$ in another form. In the final summary of data there are many values of $\delta\rho$ to be averaged for each value of the hypothetical velocity. It is clear, then, that the final average will be unaffected if we replace the variations δr_i in (8) by their individual measured values $\overline{\delta r_i}$, so that $r_i\overline{\delta r_i} = r_j\overline{\delta r_j}$. Multiplying and dividing the right side of Eq. (9) by $\sum_m^p 1/r_i$ it becomes

$$\delta\rho = \frac{k}{\sum(1/r_i)} \sum\overline{\delta r_i} \tag{10}$$

when the expressions $(r_i/r_j)\overline{\delta r_i}$ that appear in the product are replaced by $\overline{\delta r_j}$. Since we are dealing with extremely small variations in the radii, the radii can be measured and $\Sigma 1/r_i$ computed once for all for a given adjustment of apparatus; then the variations $\delta\rho$ are simply proportional to the sums of the variations in the several radii. This possibility greatly expedites the labor of measurement of plates; the way in which it was employed is discussed in connection with the description of the comparator designed for the purpose. It should be remarked that in this procedure insufficient weight is given to the somewhat greater precision of measurements on the larger, sharper, rings; however the final weighting of data is based on mean deviations of the computed values of $\delta\rho$, and the conclusions as to precision are not vitiated by this approximation.

The principle of the comparator is as follows:

A diametral section of each photograph to be measured is made to appear juxtaposed with a similar section of a nearly identical photograph which is used as a standard of reference for the whole series. In this way very small differences between reference and measured plates reveal themselves. The juxtaposition is along a diameter of each of the systems of concentric rings, and the comparison is made by moving the standard until one side of a ring on one plate appears to be continuous with the corresponding ring on the other plate, and then noting the distance along the line of demarcation which the standard must be moved in order to make the other sides of same rings coalesce similarly. This distance is evidently the difference between the diameters of the two rings. On the shaft of a fine micrometer screw which moves the reference plate, and concentric with it, is mounted a graduated slip-ring arranged so as to be held stationary when the portions of interference rings on one side of center are matched, and to rotate with the screw when the matching is done on the other side of center; the angle through which slip-ring is rotated during settings on a number of rings is thus evidently

proportional to the sum of the differences of their diameters from those on corresponding rings on reference plate. Hence in view of Eq. (10) a single reading (of this angle) summarizes the measurement of the whole exposure. Nine or ten rings, alternately dark and light, and near the center, were usually measured.

The device is diagrammed in Fig. 6; there P is a pair of similar right-angled prisms cemented together on their diagonal faces (one of which is half-silvered) and mounted on a carriage which can be moved by the micrometer screw on ways perpendicular to the section represented. The heavy lines s_1 and s_2 represent thin metal strips covering half the right and bottom faces of the prism combination; the lower edge of s_1 and left edge of s_2 are ground accurately straight and the strips are cemented to the prisms in such a way that the image of the former edge in the diagonal mirror exactly coincides with the latter. After traversing a water-cell a beam of light from right of figure passes through the reference plate R, which is mounted on the carriage and has its emulsion side in contact with screen s_1 along a diameter of the ring system; another beam, by way of mirror M, illuminates a similar part of the photograph on the plate B which is to be measured, and both parts are viewed from above through a lens system magnifying about four times. The latter plate is held by springs against stops which fix position of the emulsion side regardless of thickness of plate and of course at such a distance as to eliminate parallax. The exposures can be compared in turn by sliding the plate to right or left of diagram (toward or away from operator). Since the ring system may not be exactly circular and also in order to expedite placing the plates in position for comparison, a sharp notch was cut in each end of the slit behind which the plate is held during exposure; this leaves a sharp point at each end of the photograph which serves for setting accurately along the same diameter. It is to be noted that the comparator is automatically compensated for temperature (both reference and measured photographs being on same material); this compensation was not particularly important for the present purpose because the scheme of interleaving photographs taken twelve hours apart secured the same result.

So accurately and quickly can the settings be made that the measurement of a photograph can be made after some practice with a probable error of a thousandth of a fringe (i.e., a thousandth of the shift that would be produced by changing path-difference by one wave-length) in about five minutes. The labor of comparing the 48 exposures comprising a day's run is thus not great. It was particularly desirable to be able to make rapid measurements during the numerous preliminary adjustments of apparatus, tests of effects of varying the several experimental conditions, etc.

Two precautions were taken in order to keep the operator from being influenced in making settings on the comparator. The slip-ring, on which could be read the average differences of the diameters at any stage of comparison of a particular exposure, was kept covered until the final setting was made, thus preventing unconscious corrections during the later settings. Also, the plates were marked in such a way that the operator was in com-

plete ignorance of times of day at which they were exposed; not until a full day's readings were finished were they arranged in chronological order for computation.

Data and Results for Daily Effect

It was intended when the experiment was proposed to look chiefly for an effect of a change of velocity due to the orbital rather than the rotational motion of the earth. However with the first apparatus constructed, in which the mirrors were mounted in invar frames, it was found impossible to eliminate a slow, rather irregular variation in the interference pattern which would have masked the effect sought; hence it was decided to concentrate on the possible rotational effect. Three series of data were taken with this apparatus (in April and October, 1929 and January, 1930); after an interruption of over a year, during which the apparatus was rebuilt in its final form, three more series were taken in May, July and August 1931. The same form of light source was used in all six series. A large amount of data previously obtained with the water-cooled arc and under less carefully controlled conditions are ignored in the summary because of necessity of applying doubtful corrections to it. No corrections have been applied to the data here presented. Where results of the several series are combined, they are weighted in accordance with the usual theory of errors in terms of probable errors computed from the mean deviations.

Each of the series extended over a period of only a few days; during such a time we may regard $\sin(\theta_1-\omega_1)$ in Eq. (5) as virtually constant. From this equation and Eq. (6), $\delta n=\delta\rho+$a constant. Since θ_1 is proportional to θ_2 we have from Eq. (5)

$$\delta\rho = a \sin(\theta_2 - \omega_2) + b\theta_2 + k'$$

where a, b and k' are constants, the last two including any slow uniform variation such as might result from stresses in the apparatus. Letting computed values $\delta\rho_i$ correspond to angles θ_i, we have according to the principle of least squares the condition that the most probable values of a and ω_2 are those for which

$$\Sigma(\delta\rho - \delta\rho_i)^2 \equiv \sum[a \sin(\theta_i - \omega_2) + b\theta_i - \delta\rho_i]^2$$

is a minimum. When account is taken of the fact that the data are distributed uniformly over the day, we infer from this condition that

$$a = (2/m)\sum_1^m \delta\rho_i \sin(\theta_i - \omega_2) + 2b\cos\omega_2$$

$$\tan\omega_2 = -\Sigma\delta\rho_i\cos\theta_i/(\Sigma\delta\rho_i\sin\theta_i + mb).$$

The constant b can be computed by comparing mean values of $\delta\rho$ on successive days; m is a number of exposures per day, usually 48.

Incidentally, the last two equations show the importance of the procedure of interleaving the exposures so that adjacent ones on any plate are made twelve hours apart. For it is known that the photographic emulsion

is subject to shrinkage which varies from plate to plate, the plates may be slightly curved, and there are probably variable stresses in the apparatus due to different weights of plates; there is also a slight effect on measured diameters due to varying densities of photograph such as would result from different treatment and sensitiveness of plates. All of these errors are evidently automatically eliminated in the process of computing, however, since each is multiplied into a sine or cosine term in θ_i and then added to a similar product into a term of opposite sign. Compensation is made also for the greater shrinkage of emulsion near ends of plates, because the plates were started alternately one and two slit-widths from the end.

TABLE I.

				A	B	C	D
(1)	2.0	(25)	2.2	−2.1	−0.26	1.7	1.70
	2.4		1.6	0.1	0.03	1.5	1.49
	2.0		2.2	0.7	0.27	−1.1	−1.06
(4)	0.7	(28)	1.1	0.9	0.45	−1.7	−1.67
	0.2		1.1	−1.8	−1.10	0.0	0.00
	2.1		2.1	−1.3	−0.92	1.3	1.03
	3.2		1.4	0.8	0.63	2.8	1.98
(8)	0.9	(32)	0.6	0.0	0.00	0.6	0.37
	3.4		2.2	1.8	1.56	0.6	0.30
	2.0		0.0	1.6	1.48	2.4	0.92
	1.0		0.9	1.9	1.83	−1.7	−0.44
(12)	1.4	(36)	1.0	−0.4	−0.40	1.2	0.16
	1.3		2.1				
	2.0		0.2	$\Sigma u_i \sin \theta_i = 3.57$		$\Sigma u_i \cos \theta_i = 4.78$	
	1.7		2.1				
(16)	1.0	(40)	0.4	$\tan \omega_2 = -4.78/3.57$, $\omega_2 = 207°$			
	0.8		1.1				
	0.3		1.3	$\sin \omega_2 = -80$, $\cos \omega_2 = +0.60$			
	1.2		2.5				
(20)	−0.2	(44)	0.7	$a = (2/48)\ (0.60 \times 3.57 + 0.80 \times 4.78) = 0.26$			
	1.6		0.3				
	1.5		0.6				
	1.7		2.4				
(24)	0.8	(48)	2.7				

A sample of data for a period of three days and the computations for the resultant amplitude and phase of the sine curve to which it most closely conforms is given in Table I. The numbers in the two columns at the left are means of the three values of $\delta\rho$ at the same hour of each day, arranged in chronological order. Column A contains sums and differences of the four terms in the previous columns for which the sines of the corresponding phase angles are equal or opposite.[4] Column B contains products of the terms of

[4] The summation in the formula above for the amplitude can evidently be expanded as follows:

$$\sum_1^m \delta\rho_i \sin(\theta_i - \omega_2) = \cos\omega_2 \sum_1^{48} \delta\rho_i \sin\theta_i - \sin\omega_2 \sum_1^{48} \delta\rho_i \cos\theta_i$$

$$= \cos\omega_2 \sum_1^{12} (\delta\rho_i + \delta\rho_{25-i} - \delta\rho_{24+i} - \delta\rho_{49-i}) \sin\theta_i$$

column A into the sines of the corresponding phase angles. Columns C and D contain the corresponding quantities to A and B, using the cosine instead of the sine.

The results for the daily effect are summarized in Table II. The column headed ω contains the phase angles corresponding to the sidereal time of the maximum value of δn. The amplitudes are expressed in thousandths of a fringe.

TABLE II.

Time of year	Weighted amplitude	ω
January	0.16	89°
April	0.27	273
May	0.18	18
July	0.14	43
August	0.30	128
October	0.22	183

Since the total velocity of the earth could vary during the year by no more than twice the orbital velocity it is probably as well to average these results without reference to the first term in Eq. (5) that is, by simply adding them vectorially. When that is done, the amplitude of the resulting sine curve is 0.06 ± 0.05. Substituting in (5) this is found to correspond to a velocity $V_\beta = 24 \pm 19$ kilometers per second.[5]

SEARCH FOR LONG PERIOD EFFECT

Because the apparatus in its final form appeared to be permanently in adjustment and the average values of the ring diameters proved to be nearly constant, it became feasible to test whether an effect exists due to orbital motion, i.e., to determine the coefficient V_α in first term bracketed in Eq. (5). The direct way of doing this would evidently be like that for daily effects which has just been discussed, i.e., to determine δn for a large part of a year and fit the data to a curve of the required form. Instead, a modification of this procedure was adopted in order to make it unnecessary to keep all the experimental conditions the same for long times. It is based on the assump-

$$- \sin \omega_2 \sum_1^{12} (\delta\rho_i - \delta\rho_{25-i} - \delta\rho_{24+i} + \delta\rho_{49-i}) \cos \theta_i.$$

The terms in parentheses in the last two summations are the quantities in the columns A an C, respectively.

[5] There is a superficial appearance that this result conflicts with the assumption introduced in Eq. (5), i.e., that v_1 and v_2 are negligible in comparison with v_α and v_β, since the value just determined for v_β is even less than the orbital velocity v_1. The contradiction is merely apparent however; it arises from the adoption of a corresponding velocity as a means of expressing the accuracy of the result, as has been customary in discussions of the Michelson-Morley experiment. From that experiment it is not inferred that the velocity of the earth is but a few kilometers per second, but rather that the dimensions of the apparatus vary very nearly as required by relativity. From the present experiment we similarly infer that the frequency of light varies conformably to the theory.

tion that the most probable rate of variation of δn (computed from measured values of $\delta\rho$ over short times) is equal to the derivative of the most probable first term in Eq. (5). Each of three series of data, taken for periods varying from eight days to a month, and at intervals of three months, was used to compute the daily rate of change of $\rho\delta$ at those times of year. This rate was found by averaging arithmetically the readings of each day of a given series and determining by the method of least squares the slope of the most probable straight line represented by them. Similarly the most probable sine curve corresponding to these three derivatives is computed. Some 300 exposures comprised the three series.

The three computed rates of change were 0.050 ± 0.020, 0.007 ± 0.013 and -0.015 ± 0.021, all expressed in thousandths of a fringe per day. The computed sine curve has an amplitude of 2.96 thousandths and this corresponds to a velocity $V_\alpha = 15 \pm 4$ km per sec. Since the relatively small probable error is based only on the internal consistency of the data and is therefore not to be taken very seriously, this result can scarcely be regarded as indicating a real velocity. Furthermore the direction of the computed velocity is 123° away from that computed above.

As we have used only 300 exposures in the application of this method, it is evident that the accuracy could be increased by a large factor if data were taken steadily for a few months. The proverbial brevity of life, however, argues against laboring the point.

If the last result and that for the rotational effect are given the same weight and combined vectorially (ignoring difference of direction of V_α and V_β[6] their resultant is 10 ± 10 km per sec. In view of relative velocities amounting to thousands of kilometers per second known to exist among the nebulae, this can scarcely be regarded as other than a clear null result; it is of the same order of precision as that of the Michelson-Morley experiment. It is perhaps best expressed as at present in terms of a velocity, although of course the conclusion to be drawn is that the frequency of a spectral line varies in the way required by relativity.[7] This appears to be the only investigation in which a quantum phenomenon is shown to conform to Einstein's theory.

Insofar as the radiating atom may be regarded as a typical clock, the result of this experiment can be combined with assumption (b) to derive the Lorentz-Einstein transformations. Throughout the foregoing discussion we have dealt with time regarded as measured only at a fixed place in the moving system S; in order to specify unambiguously the time at another point of S it is necessary to specify the operations which define it. Perhaps the most natural meaning to attach to the concept is that the time at any point is the indication of a clock which has been moved with infinitesimal velocity to the

[6] The two results can be combined only by making some approximation.

[7] It is of course altogether possible that there is a real (inherently observable) velocity which is so nearly perpendicular to the orbital and equatorial planes as to have components in them small enough to have escaped observation, but the probability seems small in view of the nebular velocities mentioned above.

point, and from the same location as an identical clock with which it was originally in agreement; it turns out that this definition is equivalent to that of synchronizing by means of light signals.

We have shown that the frequency ν' of an atom moving with velocity v bears the relation $\nu' = (1-v^1/c^2)^{1/2}\nu$ to that of a fixed atom. Let us assume that the indications of clocks under similar conditions bear the same ratio. Suppose that at time $t=t'=0$, the origins of parallel coordinates in S and S' (previously defined) coincide, and that the S-clock passes through the origin with a small velocity with respect to S. Because of this motion, the velocity of the clock with respect to S' will have components, say, $v+u_x$, u_y, u_z; hence the times t' and t indicated by a clock in S' and the clock in S will thereafter stand in the relation

$$t = t'\left[1 - \frac{(v+u_x)^2 + u_y{}^2 + u_z{}^2}{c^2}\right]^{1/2} = \left[t'^2\left(-\frac{v^2}{c^2}\right) - \frac{2t'^2u_xv}{c^2} - t'^2u^2\right]^{1/2}.$$

Now u_xt' is equal to S'-measure of distance x traversed in S by the clock; hence $u_xt' = (1-v^2/c^2)^{1/2}x$. If this is substituted in the second term of the right side of the above equation and u is made to approach zero,

$$t = \left[t'^2\left(1-\frac{v^2}{c^2}\right) - \frac{2vxt'}{c^2}\left(1-\frac{v^2}{c^2}\right)^{1/2}\right]^{1/2}$$

and so

$$t' = \frac{1}{(1-v^2/c^2)^{1/2}}\left[\frac{vx}{c^2} + t\left(1+\frac{v^2}{c^4}\frac{x^2}{t^2}\right)^{1/2}\right].$$

Here x/t is the velocity of clock with respect to S, and it approaches zero with u; hence the coefficient of t in the last expression is unity, and

$$t' = [1/(1-v^2/c^2)^{1/2}][t + (v/c^2)x]. \tag{11}$$

The statement that the systems are in uniform relative velocity, together with fact that t' is independent of y and z implies

$$x' = x'(x+vt)\ ;\ \text{hence}\ \partial x'/\partial x = (1/v)(\partial x'/\partial t). \tag{12}$$

The measurement in S' of the lenth of an interval δs in S is obtained by observing the distance $\delta s'$ between points in S' with which the ends of the interval coincide at same S'-time. For measurement along x' axes we have, because of Lorentz-Fitzgerald contraction

$$\delta x' \equiv \frac{\partial x'}{\partial x}\delta x + \frac{\partial x'}{\partial t}\delta t = \left(1-\frac{v^2}{c^2}\right)^{1/2}\delta x$$

when

$$\delta t' \equiv \frac{1}{(1-v^2/c^2)^{1/2}}\left(\delta t + \frac{v}{c^2}\delta x\right) = 0, \text{ i.e.,}$$

when $\delta t = -(v/c^2)\delta x$. Hence

$$\frac{\partial x'}{\partial x}\delta x - \frac{v}{c^2}\frac{\partial x}{\partial t}\delta x = \left(1 - \frac{v^2}{c^2}\right)^{1/2}\delta x.$$

From this and (12)

$$\frac{\partial x'}{\partial x} = \frac{1}{(1 - v^2/c^2)^{1/2}} \quad \text{and} \quad \frac{\partial x'}{\partial t} = \frac{v}{(1 - v^2/c^2)^{1/2}}.$$

Hence

$$x' = (1 - v^2/c^2)^{-1/2}(x + vt).$$

This equation and (11) together with $y' = y$, $z' = z$, are the Lorentz-Einstein transformations; because they are known to possess the group property, the system S' which has been used as a tentative standard of reference evidently loses all trace of uniqueness.

The research set forth in this paper has been carried on over a period of several years, during which many obligations have been incurred. Preliminary work on it served as basis for the senior author's doctoral thesis at Johns Hopkins University. The main work was done at the California Institute of Technology with the aid of fellowships granted by the National Research Council, the Guggenheim Memorial Foundation and the Institute; it was completed during leave of absence granted by the University of Washington. Particularly acknowledgment is made to Professors E. T. Bell, R. C. Tolman and R. A. Millikan, whose interest and encouragement have made the work possible, and to Mr. Julius Pearson to whom several essential refinements of the apparatus are due.

Propagation of Large Barkhausen Discontinuities. II

By K. J. Sixtus and L. Tonks
General Electric Company, Schenectady, New York

(Received September 9, 1932)

A new formula for the penetration time of large Barkhausen discontinuities is given which is based on definite assumptions regarding the condition for magnetic reversal. In order to bring this formula into agreement with experimental results, it must be modified by the introduction of a length of 0.035 cm of unknown origin. The modified formula agrees well with the results observed for wires of various diameters, a strip, for various impressed fields, tensions and torsions, and for variations of jump magnitude and electrical resistivity. The behavior of the discontinuity in a 15 percent NiFe wire relative to heat treatment was investigated. Changes in critical (minimum propagating) and coercive fields were indicative of the internal state of strain in the wire. The presence of cold-work strains appears to be necessary for the occurrence of the jump but the addition of strains arising from cooling through the γ-α transformation reduces the tendency to form the large discontinuity. Propagation was observed at temperatures up to 350°C. With increasing temperature the slope A of the v-H curves increased. At the same time the range between the critical field and the field at which propagation starts spontaneously at some point in the wire decreased. Etching the surface of a wire also increased A and decreased propagation range. Cracks appearing in the wire surface indicated that the release of surface strains may well have been responsible. It was established that neither the removal of material nor the absorption of hydrogen were the cause.

I. Introduction

THE earlier work which has already been reported upon under the same title and in two additional notices[2,3] has been continued and extended. Some phases of the new material will be discussed in the present paper and additional results will be published shortly.

As a considerable number of symbols denoting various magnetic fields are required we list them here: H, longitudinal main field impressed on the wire; H_0, critical field, minimum longitudinal field for propagation; $\Delta H = H - H_0$, excess field; H_s, starting field, minimum value of H which initiates propagation in the wire; H_e, eddy current field; H_p, field arising from the magnetic pole distribution; H_m, total field at a point; and H_c, coercive force, used in place of H_0 when the large discontinuity is absent.

II. Revised Formula for the Penetration Time

1. Old formula

In I we have shown that one has to distinguish between the propagation in two different directions: A propagation into the wire, which depends on

[1] K. J. Sixtus and L. Tonks, Phys. Rev. **37**, 930 (1931). This paper will be referred to as I in the text. On page 932 a was erroneously defined as the wire diameter. Throughout I and here also a is the radius of the wire.

[2] K. J. Sixtus and L. Tonks, Phys. Rev. **39**, 357 (1932).

[3] I. Langmuir and K. J. Sixtus, Phys. Rev. **38**, 2072 (1931).

eddy currents arising in the material, and a propagation in the longitudinal direction, depending, we believed, on conditions in the surface of the wire. The propagation into the wire requires a time interval δt which we have called the penetration time. The approximate calculation made in I gave values one-fourth of those found experimentally in a 0.038 cm diameter wire. We shall here give the derivation of Eq. (8A)[2] previously stated without proof. In the interim an independent derivation[4] has appeared which is, however, less satisfactory for our purpose.

2. Basic assumptions

Any exact calculation of this time must take the actual manner of penetration into consideration. The hypothesis adopted is that stated in I, p. 947, with the additional assumption, already implicit in I, Eq. (7), that magnetization reverses when the total field H_m at a point in the discontinuity exceeds the critical field H_0, and that it reverses so rapidly that the eddy currents generated reduce H_m to H_0 at every instant. This, in turn, implies that the discontinuity is of infinitesimal thickness, but the results of the calculation will be valid to the extent that this thickness is small compared to the diameter of the wire.

For clarity, we shall call the portion of the wire already traversed by the discontinuity, and which has therefore changed magnetization, the *saturated phase*, the unchanged portion, the *antisaturated phase*. Thus the moving discontinuity can be looked upon as a propagating phase boundary.

3. Calculation of eddy current field

Denoting distance along the wire and in the direction of propagation by x, and representing the shape of the phase boundary by the unknown function, $R=R(x)$, our first problem is to set up this function.

The change in flux in a cross section of the wire during the time dt is $2\pi RdR\cdot 4\pi\Delta I$, where $4\pi\Delta I$ is the change in induction between the two phases. The line integral of e.m.f., E, around the wire at a radial distance $r>R$ is thus

$$2\pi rE = (8\pi^2 R\Delta I/c)dR/dt \tag{1}$$

(of course, for $r<R$, $E=0$). By introducing the longitudinal velocity of propagation $v(=dx/dt)$ and using R' for dR/dx this becomes

$$E = 4\pi vRR'\Delta I/rc. \tag{2}$$

Since the current density I is E/ρ, the total circular current per cm length of wire is

$$\int_R^a Edr/\rho = (4\pi vRR'\Delta I/\rho c)\ln(a/R) \tag{3}$$

where a is the radius of the wire.

[4] W. Wolman and H. Kaden, Zeits. f. techn. Physik **13**, 330 (1932).

This eddy current, in turn, gives rise to a magnetic field H_e at R which is given by

$$H_e = -(16\pi^2 v\Delta I/\rho c^2)RR'\ln(a/R) \tag{4}$$

the negative sign indicating that H_e is in opposition to H, the impressed field.

4. Field relations and shape of phase boundary

It is readily seen that H, H_e, and the field H_p arising from the magnetic poles created in the reversal all contribute to H_m, so that

$$H_m = H + H_e + H_p. \tag{5}$$

It will be shown later that in the propagating wave it is justifiable to neglect H_p because the poles are distributed over such a great length of the wire. The application in Eq. (5) of the fundamental assumption that $H_m = H_0$ leads to the appearance of the quantity $H - H_0$ in the equation, a quantity which will be called the "excess field" and will be denoted by ΔH. Then eliminating H_e with Eq. (4) gives

$$RR'\ln(a/R) = (\Delta H\rho c^2)/(16\pi^2 v\Delta I) \tag{6}$$

as the differential equation of the boundary. Integration gives

$$R^2[\ln(a^2/R^2) + 1] = (\Delta H\rho c^2 x)/(4\pi^2 v\Delta I) \tag{7}$$

the integration constant being chosen so that the discontinuity intersects the axis at $x = 0$. The length, λ, of the discontinuity is then the value of x when $R = a$.

5. Penetration time

Noting that

$$\lambda/v = \delta t \tag{8}$$

Eq. (7) gives

$$\begin{aligned} \delta t &= 4\pi^2 a^2 \Delta I/\rho c^2 \Delta H \\ &= 3.94 \times 10^{-8} a^2 \Delta I/\rho \Delta H \end{aligned} \tag{9}$$

in practical units. Thus the exact definition of the discontinuity under our assumptions doubles the numerical factor in **I**, Eq. (8), thereby reducing the discrepancy between $\delta t_{\text{exp.}}$ and $\delta t_{\text{calc.}}$ which is noted in **I**, Table I, column 7, from the factor 4 to the factor 2. In the case of a strip the corresponding formula is

$$\delta t_{\text{strip}} = 7.88 \times 10^{-8} b^2 \Delta I/\rho \Delta H \tag{10}$$

where b is the half-thickness.

The derivation of these equations was based on the assumption that the surface of magnetic discontinuity makes only a small angle with the axis, but a plot of Eq. (7), as given in Fig. 1, shows that the discontinuity is perpendicular to the axis both at the axis and at the surface of the wire. Other considerations must apply in these two regions. At most, however, the ex-

ceptional districts include less than one percent of the discontinuity, so that Eqs. (9) and (10) may reasonably be expected to be valid.

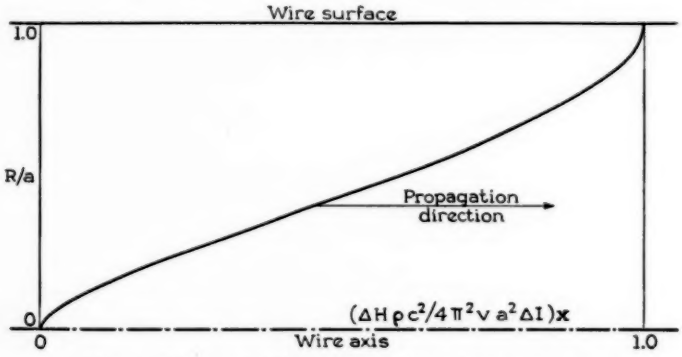

Fig. 1. Theoretical shape of the boundary in a wire.

6. Test of formula and empirical modification

For the further testing of these formulas a new series of oscillograms were taken covering variations in a, ΔI, and ρ. The procedure is described in I, page 944. It immediately appeared that δt was proportional to a rather than a^2, the missing power of a being replaced by an empirical constant which in an earlier note[2] was given as 0.031 cm. A more complete and critical examination of the data leads, however, to the present slightly higher value, 0.035 cm. Accordingly, Eq. (9) was changed to

$$\delta t_{\text{wire}} = 3.94 \times 10^{-8} \times 0.035\ a\Delta I/\rho\Delta H. \tag{11}$$

The results of applying this modified equation to a series of 15 percent NiFe wires under both tension and torsion are shown in Table I. No systematic variation of $\delta t_{\text{calc.}}/\delta t_{\text{exp.}}$ is evident. Only the torsion case, subdivision 3, shows a marked general deviation from unity. It is remarkable and doubtless significant that the empirical length of 0.035 cm determined by tension experiments should apply even this well to a case where the strains are so different. The fact that the jump is only 50 percent of the double saturation value appears, in the light of later results,[4,5] to arise from a transverse component in the reversal as well as from a probable absence of reversal near the axis where the shearing strain approaches zero. The former case is covered by the theoretical formula, but in the latter the necessary correction would reduce the calculated time, thus making the discrepancy worse. This case certainly demonstrates, however, that three- to four-fold changes in ΔI are accompanied by only a 20 percent difference between formula and experiment.

The theoretical formula for a strip was modified in exactly the same way as the wire formula, that is, to

$$\delta t_{\text{strip}} = 7.88 \times 10^{-8} \times 0.035\ b\Delta I/\rho\Delta H. \tag{12}$$

[4,5] See also R. M. Bozorth and J. F. Dillinger, Phys. Rev. **41**, 345 (1932).

Subdivision 6 shows that this semi-empirical formula applies. In addition it should be noted that this is an extreme case in that b is less by half than the smallest wire radius.

TABLE I. *Experimental and calculated times of penetration in 15 percent NiFe wire and ribbon under tension or torsion.* Wire No. 37; resistivity, $\rho = 31 \times 10^{-6}$ ω cm.

Osc. No.	ΔH oersted	ΔI e.m.u.	v cm/sec.	δt, millisec. exp.	calc.	$\frac{\delta t_{calc.}}{\delta t_{exp.}}$	λ cm
	1. Diameter, $2a = 0.0533$ cm; tension, 71 kg mm^{-2}; $H_0 = 1.40$ oersted						
124	0.21	2960	2500	18.5	16.7	0.90	47
123	0.44	3040	6000	8.0	8.2	1.02	48
122	0.67	3060	10000	5.0	5.5	1.10	50
	2. Diameter, $2a = 0.038$ cm; tension, 77 kg mm^{-2}; $H_0 = 2.07$ oersted						
109	0.11	2320	2100	11.4	18.0	1.57	24
118	0.47	3170	8800	6.2	5.7	0.92	59
111	0.69	3210	13800	3.8	3.9	1.02	52
107	1.04	3260	21600	2.3	2.6	1.14	50
	3. Diameter, $2a = 0.038$ cm; torsion, 4 turns/80 cm; $H_0 = 2.49$ oersted						
120	0.16	830	3000	5.6	4.4	0.78	17
119	0.39	1030	8000	2.9	2.3	0.79	23
	4. Diameter, $2a = 0.026$ cm; tension, 85 kg mm^{-2}; $H_0 = 3.49$ oersted						
104	0.31	3170	6500	6.2	6.0	0.96	41
105	0.66	3280	15000	2.8	2.9	1.03	42
	5. Diameter, $2a = 0.013$ cm; tension, 158 kg mm^{-2}; $H_0 = 5.93$ oersted						
133	0.39	1600	7400	1.6	1.20	0.75	12
134	0.63	3150	11600	2.1	1.45	0.69	24
132	0.87	3320	15800	1.2	1.10	0.92	19
135	0.97	3320	17800	0.9	0.97	1.08	16
131	1.21	3320	22000	0.75	0.78	1.04	17
	6. Strip, 0.0071×0.0685; tension, 85 kg mm^{-2}; $H_0 = 3.80$ oersted						
127[b]	0.35	2450	4600	3.0	2.20	0.73	14
127[a]	0.47	2920	5800	2.4	1.95	0.81	14
126	0.81	3130	9800	1.5	1.24	0.83	15
125	1.39	3130	19600	(1.2)*	0.70	(0.58)	(24)

* Uncertain because of the shortness of the time interval.

7. Further tests of formula

Table I, as remarked, covers experiments in which ΔI shows some variation from one test to the next. A greater range was embraced by using wires of different compositions. These wires showed, in addition, marked differences in resistivity, the 39 percent Ni-Fe having 71×10^{-6} ω cm and the 90 percent Ni-Fe having 13.5×10^{-6} ω cm. The 39 percent alloy lies in a range where it is difficult to obtain large discontinuities. After quite a number of trials it was found that combined torsion and tension were required to give large enough jumps to work with. The 90 percent alloy lies in a range where tension reduces the size of discontinuities. Accordingly torsion alone was used in this case.

The results are exhibited in Tables II and III. Although there are deviations from unity in column 7 of each table, these show no correlation with

TABLE II. *Experimental and calculated times of penetration in 39 percent NiFe wire under combined tension and torsion.* Wire No. 26; resistivity, $\rho = 71 \times 10^{-6}$ ω cm; diameter, $2a = 0.0388$ cm; torsion, 15 turns; tension 30.5 kg/mm²; $H_0 = 8.36$ oersted.

Osc. No.	ΔH oersted	ΔI e.m.u.	v cm/sec.	δt, millisec. exp.	calc.	$\frac{\delta t_{calc.}}{\delta t_{exp.}}$	λ cm
255	0.24	690	4300	1.40	1.08	0.77	6.0
254	0.36	728	6400	0.80	0.76	0.95	5.1
253	0.48	765	8700	0.75	0.60	0.80	6.5
252	0.61	803	11400	0.60	0.50	0.83	6.8
256	0.74	820	14000	0.50	0.42	0.84	7.0

A vibrator with natural frequency 5000 cycles/sec. was used for these oscillograms.

TABLE III. *Experimental and calculated times of penetration in a 90 percent NiFe wire under torsion.* Wire No. 6a; resistivity $\rho = 13.5 \times 10^{-6}$ ω cm; diameter, $2a = 0.0386$ cm; torsion, 5 turns; $H_0 = 4.02$ oersted.

Osc. No.	ΔH oersted	ΔI e.m.u.	v cm/sec.	δt, millisec. exp.	calc.	$\frac{\delta t_{calc.}}{\delta t_{exp.}}$	λ cm
209	0.46	460	1000	1.82	1.97	1.08	1.8
206 213 214	0.58	500	1300	1.96	1.70	0.87	2.5
202 205 208 211	0.80	520	1900	1.60	1.28	0.80	3.0
215	1.04	550	2800	1.21	1.04	0.86	3.4
204 210	1.15	550	3400	1.28	0.94	0.74	4.4

variations in any of the listed quantities. In this connection it must also be borne in mind that there is some indefiniteness in interpreting the oscillograms of the discontinuity which yield the values of δt, particularly in the lower velocity cases. The general shape of the trace is that of an isosceles triangle with the sides curving into the zero line. The time occupied by the curved portion in relation to the velocity of propagation represents roughly the distance along the wire that one should expect the effects of an advancing (and receding) magnetic change to reach ahead (and persist behind) when the actual size of the search coil is taken into account. Thus the search coil had an outer radius of 1 cm and an axial thickness of 0.6 cm and the distances found from the oscillograms were about 1 cm.

8. Significance of empirical constant

It is interesting to observe that the special constant, 0.035 cm, appearing in Eqs. (10) and (11), lies in the neighborhood of the radius above which propagation does not occur. For example, as mentioned in I in connection with Fig. 9, the 0.071 cm diameter wire showed propagation but only with

decreasing jump magnitude, and other tests on larger wires have also failed to show propagation without decrement. What significance, if any, is to be attached to this coincidence is not known.

III. Annealed Wires

1. Introduction

It was thought that the effect on the magnetic properties of the material of annealing at different temperatures might give more information regarding the influence of various factors, such as inhomogeneous strains and crystal orientation. Such tests have already been reported by Preisach.[5] Practically all of the measurements in this and the following section were made on 15 percent NiFe (Ingot No. 37) so that unless otherwise stated all results and conclusions apply to this alone. The exact percentage composition of this wire by weight as determined by chemical analysis was: Ni, 14.75; Mn, 0.11; C, 0.02; P, 0.02; S, 0.016; Si, trace; Fe, remainder.

Although many different heat treatments have been tried, we shall only describe the results obtained on a series of wires heated for 10 hours in hydrogen at 400°, 600°, 800° and 1250°C, since these exhibit the important phenomena very clearly. Using the equilibrium diagram and with the help of x-ray spectrograms and photomicrographs we shall attempt to explain these observations. The transformation points for the alloy of 15 percent Ni-Fe were taken from the extensive report of Peschard[6] which furnished the main basis for the diagram published in the National Metals Handbook (p. 608). In a 15 percent alloy with very pure constituents the transformation from α- to γ-phase occurs between 570° and 670° in heating, whereas in cooling the change from γ to α structure occurs between 300° and 140°C. In a rough test it was found that the α-γ transformation in the present wire began as low as 450°C. The difference between this value and the one found by Peschard can be ascribed to impurities.

The original wire had undergone a severe cold working as it had been drawn cold from 0.080 to 0.038 cm diameter and had, accordingly, a fibrous structure with very fine crystal grains whose boundaries, even with a magnification of 1500, could not be recognized. X-ray spectrograms showed the well-known orienting effect of cold working. In the center portion of the wire one could observe a preferred crystal orientation of the (110) axis parallel to the wire axis; but near the surface to a depth of about $\frac{2}{3}$ of the radius there was random crystal orientation.

2. Properties of annealed wires

The changes in the magnetic properties of the wire after annealing are given in Figs. 2 and 3. Annealing at 400°C, below the transformation range, caused a marked reduction of coercive force and critical field for all tensions, and the large discontinuity appeared at a lower tension than before. The x-ray pattern did not differ from the one obtained with the original wire.

[5] F. Preisach, Ann. d. Physik **3,** 737 (1929).
[6] Peschard, Rev. de Met. **22,** 490 (1925).

Obviously, the only effect of annealing in this case was the release of internal strains, a result well known in connection with the reduction of coercive force of ferromagnetic materials.

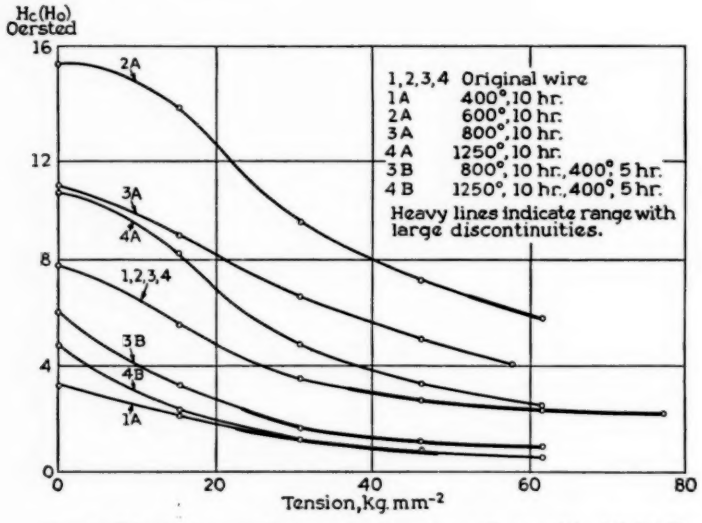

Fig. 2. Effect of annealing on coercive force H_c or critical field H_0.

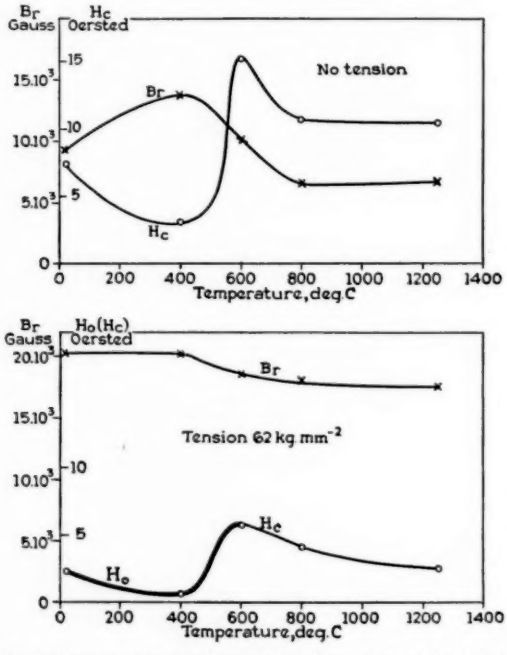

Fig. 3. Remanence and coercive force (or critical field).

After the anneal at 600°C, where the wire had at least partly undergone the α-γ transformation, H_0 and H_c had been increased many fold, and a discontinuity could only be obtained with very high tension. At the same time

the remanence had decreased. Again the x-ray analysis showed no change in crystal orientation, and besides gave no indication of the presence of the γ-phase.

We therefore have to conclude that the increase in H_0 or H_c, as the case may be, is not due to a variation in crystal orientation nor to the presence of the γ-phase. Presumably the wire shows persisting effects of the transformation between γ- and α-phase, even though the sample was cooled slowly with the furnace. These observations are consistent with the view that large inhomogeneous strains are present whose suppression to an extent sufficient to align the preferred directions of the elementary districts requires large applied tension.

The 800° wire showed increased H_c, and photomicrographs revealed a certain grain growth of the crystals, while there was no apparent change in crystal orientation as seen from the x-ray spectrograms. No large discontinuities could be obtained in this wire. In a wire with only 2 hours anneal a 50 percent discontinuity was observed for high tension (72 kg mm^{-2}).

The 1250° wire, having high H_c and no discontinuities, had lost its fibrous structure entirely. It had recrystallized and new crystals of 0.01 to 0.05 cm linear dimensions had formed. In the center portion preferred crystal orientation was still noticeable, although it was less pronounced than before.

Both the 800° and the 1250° wire were tempered for 5 hours at 400°C. This treatment reduced their H_c (see Fig. 2) nearly to the value of the original 400° wire, but only in the 800° wire was the discontinuity restored. The effect on H_c is consistent with the view, expressed above, that intense strains were set up during the γ-α transformation which were relieved by subsequent tempering below the transformation temperature. The recrystallization of the 1250° wire, i.e., the formation of large crystals with new orientations in this case, is accompanied by the complete disappearance of the jump, and the release of strains by tempering cannot bring it back.

In all the wires tested the slope A of the v-H curves was only slightly affected by the heat treatment with no apparent tendency to either increase or decrease. The variations which were found were no larger than those already observed in unannealed wires (**I**, Fig. 9), lying for different wires under various tensions between 19,000 and 32,000 cm sec.$^{-1}$ oersted^{-1}.

3. Theory

It is difficult to formulate any approximately complete explanation of these effects. One conclusion does seem possible, however, and that is that uniform crystal orientation is not necessary for the occurrence of the jump. Too small a fraction of the wire cross section shows partial orientation compared to the complete reversal of the whole wire which is often observed. Secondly, experiments have been made[7] which show that the preferred direction dominating the discontinuity can be in the surface layers where no uniform crystal orientation exists, and this direction coincides with a principal strain axis which can make any angle up to 45° with the wire axis.

The following not quite satisfactory hypothesis for the response of the

NiFe wire to heat treatment is offered in the absence of complete and convincing data: The type of strain distribution introduced by cold working is necessary for the occurrence of the jump. A possible explanation for the relationship between strain and critical field is offered by the ideas of Bloch.[8] On his view it is the presence of local variations in strain which establishes magnetic barriers and thereby leads to Barkhausen discontinuities. Annealing at 400°C reduces the strains, with a consequent decrease in H_c (H_0). Annealing at 800°C does not eliminate them completely even though the α-γ transformation range has been traversed, but on the return from this temperature the γ-α change introduces widely dispersed strains of a different type which tend to obliterate the jump. When this treatment is carried on for 10 hours, the jump is actually eliminated. Subsequent heating at 400° has no additional effect on the cold-work strains, but does decrease the transformation strains so that the jump reappears. Finally, a 10-hour 1250° anneal does eliminate the cold-work strains to such a degree that no jump can be found subsequently.

4. Special experiments

A few special cases remain which should be mentioned. The wire, which apparently had the smallest internal strains as judged by its decreased hardness and the fact that it had the smallest H_c (H_0) observed so far for any

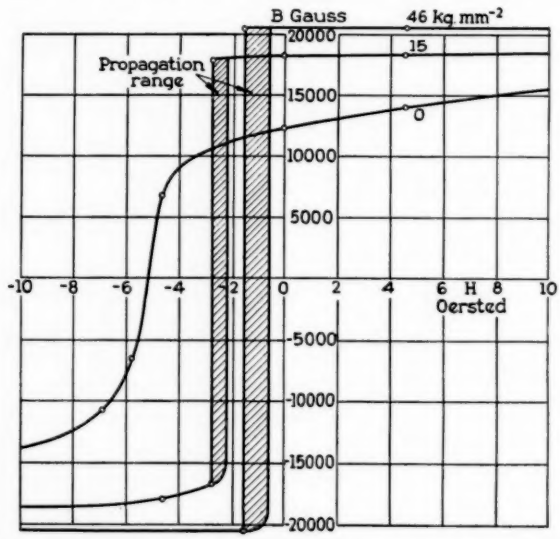

Fig. 4. Hysteresis loops under different tensions for wire annealed at 800° for 1 hr., then at 400° for 6 hrs.

given tension, had been heated for 1 hour at 800°C and subsequently for 6 hours at 400°. Besides it gave a large discontinuity with an extremely low applied tension (approximately 10 kg mm^{-2}). The hysteresis loops for various tensions are given in Fig. 4.

[7] L. Tonks and K. J. Sixtus, Phys. Rev. **41,** 539 (1932).
[8] F. Bloch, Zeits. f. Physik **74,** 332 (1932).

All the wires so far mentioned were annealed without tension. In one experiment a wire was annealed under a tension of 82 kg mm^{-2} for one hour at 300°C. It showed very nearly the same variation of H_0 with tension as a wire given the same heat treatment without tension.

A soft permalloy wire (78.5 percent NiFe, annealed for 1 hour at 900°) gave no jump when tension was applied, but after it had been stretched plastically by about 1 percent of its length, the same tension produced a large discontinuity in its hysteresis loop. Both the soft and the deformed wire had a slight preferred crystal orientation at the center and to about the same degree. The theory formulated above is consistent with this behavior if we assume that the strains introduced by stretching are of the same nature as those caused by drawing or rolling.

A 35 Ni, 20 Fe, 45 Ni perminvar wire showed an anomalous behavior for which no explanation can at present be offered. This wire had been annealed at 1000°C for 1 hour and was extremely soft. It is known[9] that under these conditions a large jump occurs with no applied tension. Its v-H curves were taken over a considerable range of H and their slopes were found to be nearly equal to those of Ni under torsion. When tension or torsion was applied, the discontinuity diminished, and if these stresses were sufficiently large, the phenomenon disappeared completely. An x-ray spectrogram showed the crystal structure to be of the face-centered cubic type.

IV. Propagation at Elevated Temperatures

1. Experimental procedure

In order to extend the propagation measurements to higher temperatures, the set-up comprising the wire, the main coil, the two search coils and the adding coil had to be placed into a furnace. This was accomplished in the following way:

On the middle part of a Nonex capillary tube (120 cm in length, 0.15 cm in inside, and 0.5 cm in outside diameter) two search coils (each 0.6 cm long with 500 turns of 0.0075 cm diameter enameled copper wire) were wound at a distance of 20 cm from each other. Beyond one of them and 15 cm away, 10 turns of enameled copper wire (of 0.05 cm diameter) were wound to serve as an adding coil. The glass tube and coils fitted into an alundum tube (of 1.6 cm outside diameter) on which the coil to give the main field was directly wound. This coil consisted of 1200 turns of 0.05 cm diameter enameled copper wire in a single layer occupying a length of 67 cm, thus having a constant of 22.5 oersteds/amp. All the coils and leads were covered by a cement of waterglass and flint, which protected the copper from too rapid oxidation in the temperature range used.

Both tubes were placed in an electric furnace which had an equal temperature zone about 70 cm long. A copper-copnic thermocouple in the furnace was used to determine this temperature. The wire was inserted in the capillary tube and put under tension by an arrangement similar to the one used before.

[9] H. Kühlewein, Wiss. Veröff. Siemens-konz., **10** (2), 72 (1931).

The leads to the different coils were brought out at both ends of the furnace. During the measurements the heating current was turned off in order to avoid any possible influence of its magnetic field. In that interval the temperature of the furnace fell at most 20°. This comparatively small change did not affect the results.

All supports, etc., were made of brass as it had been noticed that iron parts, even if only slightly magnetized, disturbed the homogeneity of the field sufficiently to result in low starting fields. The velocity measurements were taken in as short a time as possible to avoid large changes in temperature. Since the tension was maintained by a spring, the flow occurring at the higher temperatures reduced this stress and constant readjustment was necessary to keep it constant. These measurements have led to several general observations.

2. Variation in H_0

Figs. 5 and 6 show a typical family of v-H curves for a fresh wire when heated to 300°C and cooled to room temperature again. One feature is that the critical field decreased markedly as the wire was heated for the first time, but with decreasing temperature H_0 remained practically constant at a value

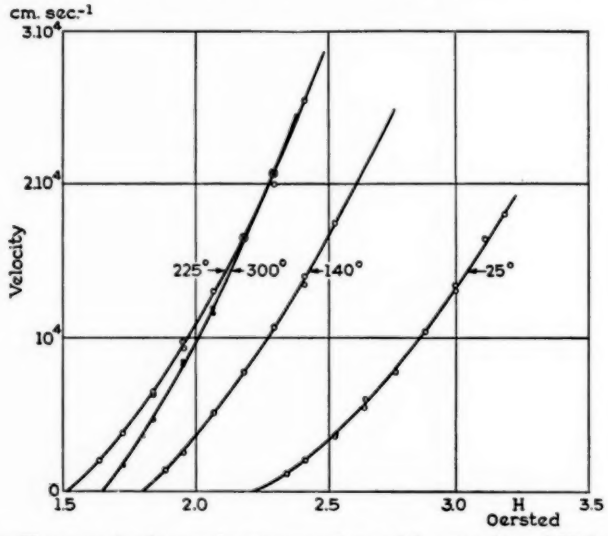

Fig. 5. v-H curves for increasing temperature with a tension of 77 kg mm^{-2}.

somewhat above the minimum reached during the heating. Fig. 7 shows this behavior for a wire at two different tensions. Subsequent heat cycles in which the maximum original temperature was not exceeded only retraced the first cooling curve. The explanation given in the present section III applies here. The permanent, if partial, relief of internal strains leads one to expect that the only effect of subsequent heating and cooling would be of the same character as the usual change in coercive force with temperature. A rough estimate from the curve for annealed Fe[10] puts the expected reduction in the

[10] Handbuch der Physik, **15**, p. 194.

neighborhood of 25 percent for a 300-degree rise in temperature, while actually almost no change with temperature was observed. We were, of course,

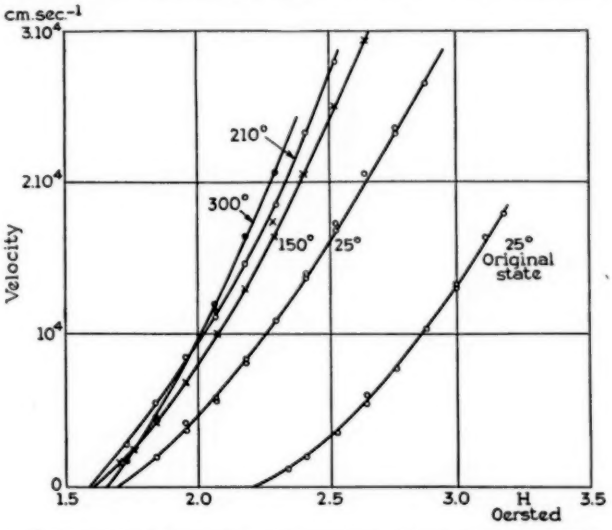

Fig. 6. v-H curves for decreasing temperature with a tension of 77 kg mm^{-2}.

dealing with a wire still having high internal strains and these, together with the uniform applied tension, may easily cause this very different behavior.

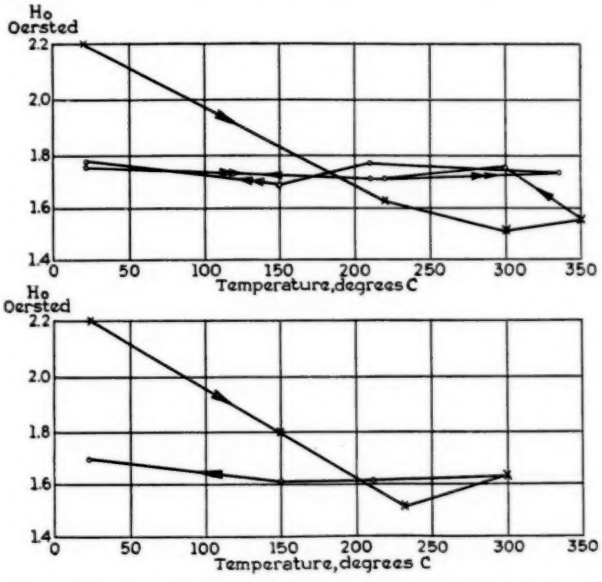

Fig. 7. Effect of temperature on H_0. Tension: 62 kg mm^{-2} for upper curve, 77 kg mm^{-2} for lower curve.

3. Variation in H_s

Comparing Fig. 5 with Fig. 6 we observe that the propagation range, $H_s - H_0$, was greater at any temperature for a wire heated previously to a

higher temperature than for a fresh wire. The same result was found in section III at room temperature for wires annealed at 400°C. This indicates that the strain irregularities which gave rise to the weaker starting nuclei were eliminated by this low temperature heat treatment.

We further observe that $H_s - H_0$ decreased with increasing temperature. This probably arose from the increase in thermal energy which enhances the chance for the spontaneous formation of a nucleus at a particular field strength.

Above 350°C a new effect appeared. The starting field became so erratic that velocity measurements could not be made. The discontinuity frequently broke up into several part jumps in the same way that can occur at room temperature at small excess fields. The latter action is probably caused by local variations in H_0 which, at small values of ΔH, are comparable with or even exceed it, so that H does not exceed H_0 for every point in the wire. Thus portions of the wire are left unreversed until a larger main field is applied. In the present case, however, it is not possible to assign a reasonable cause for increased variability of H_0. The α-γ transformation does not change the saturation intensity appreciably below 450°C. It might still be supposed that highly localized portions of the alloy had transformed at 350°C, but, if the local forces were such as to cause the change 100° below the general transition, one should expect this γ-phase to persist even below the main γ-α transformation which begins at 300°. Actually, the wire when cooled to 300°C had regained in full its ability to propagate, so that this explanation is not convincing.

4. Variation of A

If Fig. 8 the variation with temperature of the slope A of the v-H curve is plotted. These results are taken from Figs. 5 and 6, from experiments with

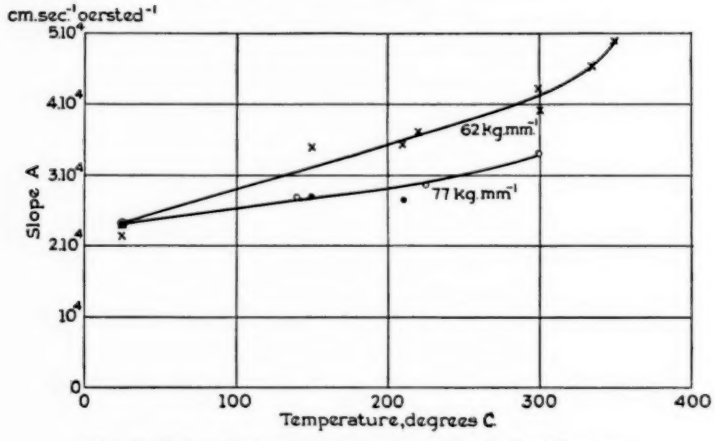

Fig. 8. Effect of temperature on slope A of v-H curves.

a wire under 77 kg/mm² tension, and from tests on a wire of different composition, namely 25 percent Ni, under a tension of 92 kg/mm². In those cases where the v-H curves were not straight lines, a tangent to these curves at

$v = 10^4$ cm sec.$^{-1}$ represented approximately the average slope of the curve and gave the value of A used in the diagram.

The increase in A shown by the figure might easily be caused by the increase in resistivity of the wire which amounts to about 90 percent from room temperature to 320°C for the 25 percent Ni wire. The factors, aside from the excess field, which determine v are not definitely known so that it is possible that resistance changes may affect it. On the other hand, we have noted in I, section II, that measurements at room temperature on wires of different compositions and hence of different resistivities gave values of A which showed no correlation with resistivity.

Another feature of the curves of Figs. 5 and 6 holds more hope for an explanation of the increase in A. It is the accompanying decrease in propagation range. Similar behavior was remarked in earlier experiments[2] where the point to point properties of a cold wire were investigated with the result that greater values of A were found at those places where the reversal could be started by the smaller adding fields. The minimum adding field is the least field which will start a reversal at a particular point. The starting field for the wire is the field which will just reverse the magnetization at that point where the minimum adding field is the least. Accordingly, it is permissible to assume that H_s is a rough measure of the average minimum adding field for the whole wire. The result is that both present and earlier observations record the same relation between slope and propagation range whether the variable factor is temperature or the local state of the wire.

The possibility of developing a theory relating slope to average minimum adding field seems very hopeful and the attempt to do this will be made in a later paper.

V. Etched Wires

1. Effect of etching

In our picture of the discontinuity, the velocity of propagation depends upon conditions at the wave front and hence at the surface of the wire. On this view it was expected that changes in the surface, such as caused by etching of the wires, would affect the propagation.

Wires of 15 percent NiFe (No. 37), 0.038 cm diameter were etched to various smaller diameters in a 15 percent solution of hydrochloric acid. This decreased the critical field for constant tension per unit area, an effect which presumably arises from the release of internal strains accompanying the removal of the outer layers of the wire.

In all cases the etching resulted in a marked increase in the v-H slope A amounting to 50 percent on the average. Even a reduction in diameter of as little as 5×10^{-4} cm had this effect. Fig. 9 shows a typical case. Subsequent polishing of etched wires with emery paper had erratic results, usually decreasing but sometimes increasing A. In the single case in which the etched and polished wire (0.0360 cm dia.) was drawn through a die (0.0355 cm dia.) there was a complete restoration of the original slope. Since the same stress was applied to the etched wires as to the unetched, the tension being ad-

justed to the reduction in cross section, the increase in A is not to be attributed to a change in applied stress. Besides, in unetched wires A is practically constant for wide variation in tension. Neither does the increase in A arise from the reduction in wire size, for it has been found that A is independent of diameter in unetched wires.

Etching has a marked effect on the starting field. A wire having a propagation range of 1.07 oersteds before etching would, after a slight removal of

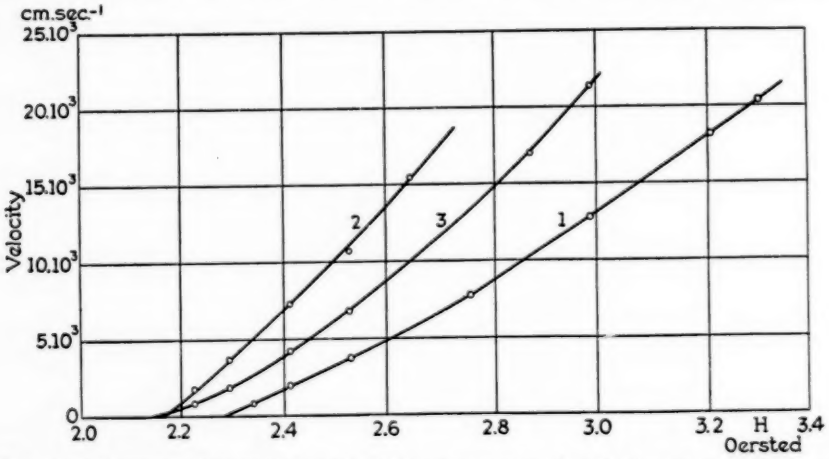

Fig. 9. v-H curves after etching and polishing of a wire. (1) Original wire; 0.0380 cm dia., tension of 77 kg mm^{-2}. (2) Wire after etching; 0.0375 cm, 75 kg mm^{-2}. (3) Etched wire after polishing; 0.0350 cm, 65 kg mm^{-2}.

surface material, show a reduction to 0.55 oersteds. If the wire was then polished, the range again increased with decreasing $v-H$ slope to 0.85 oersteds (see Fig. 9). Here again we have the same relation between propagation range and A which has been noted twice before. When the etching experiments were in progress neither this behavior nor its probable significance had been recognized. Still, the following conclusions reached in a rather exhaustive search in other directions furnish data which are fundamental to any complete explanation.

2. Surface effects and propagation

The etching changes the surface in several respects. They are absorption of hydrogen, roughening of the surface, and formation of cracks. It is well known that in etching iron or steel in HCl or H_2SO_4, large amounts of atomic hydrogen are taken up by the metal. But two experiments showed that this cannot be the explanation. First, heating the wire to 200°C for several hours to remove the hydrogen did not reduce the slope; second, etching in HNO_3 where no hydrogen is produced had the same effect on the slope as etching in HCl or H_2SO_4. On the other hand, there was no change in slope when the wire was used as cathode in the electrolysis of NaOH, where, presumably, large amounts of hydrogen were absorbed but the surface of the wire was not attacked. All these observations provided ample evidence that hydrogen was not responsible for the effects.

Under the microscope the surface of the wire looked smooth before the etching but appeared coarse afterwards. It was thought that roughening of the surface of a fresh wire with coarse emery paper would give the same magnetic effect, but the resulting variation from the normal value of A was within the normal range of variation.

One possibility of explanation remains. According to metallurgical references,[11] acid attacks the different crystal faces with different rapidity, and in some cases it dissolves the intergranular substance more quickly than the grains. This is especially true of materials with internal strains. This latter action may cause the formation of cracks in the material if high stresses across the notches formed by the acid are present.

Such fissures parallel in general to the wire axis were actually observed under the microscope on all the etched wires. Sometimes as many as five were found around the circumference at a given point along the wire. They were of several mm in length and of various widths averaging, as well as could be judged, 10^{-3} cm. It must be admitted that it is hard to understand how a crack of this width can open up as the result of the removal of only 2.5×10^{-4} cm of material. If these fissures had been the cavities which the photomicrographs show in the wire, they should also have been seen after polishing, but this was not the case. If the cracks arise from intense stresses, one should be able to prevent their formation by a preliminary annealing of the wire which is not so complete as to destroy the discontinuity. The attempt was made by heating a wire at 400°C for 10 hours. Its stiffness showed that it still contained internal strains, so that the appearance of etching cracks was not surprising. Even so, some annealing had occurred, for the heat treatment had reduced the coercive force from 7.8 to 3.3 oersteds. It may well be the release of surface strains made evident by the formation of cracks which reduces the starting field and increases A. Subsequent polishing would, on the other hand, reintroduce strains with contrary consequences.

3. Strips

A length of No. 37 wire of 0.024 cm diameter was cold rolled down to a strip 0.0076 cm thick and 0.071 cm wide. A portion cut from this was etched and it, like the wires, showed an increase in slope and a decrease in propagation range. The increase in A was, however, only 30 percent, which is considerably smaller than that found for wires. Under the microscope the etched strip showed no cracks but only a general roughness.

Two other samples cut from the same length of strip were reduced in thickness by polishing with emery paper. Erratic increases in slope up to 100 percent resulted but there was no correlation with propagation range apparent.

The taking and interpretation of the x-ray spectrograms used in studying the effect of heat treatment was done by Dr. W. P. Jesse of this laboratory to whom we express our thanks. Dr. I. Langmuir has, with his continued interest and suggestions, contributed essentially to this paper and also to the other papers on this same subject which are now in preparation.

[11] G. Tammann, *Lehrbuch der Metallographie*, 1920; Z. Jeffries and R. S. Archer, *The Science of Metals*, 1924.

ERRATUM

Supersonic Dispersion and Absorption in CO_2

By W. H. PIELEMEIER
Pennsylvania State College

(Phys. Rev. **41**, 833, 1932)

The third sentence in the footnote on page 837 should read, "The value of τ computed from Grossmann's maximum A is approximately $9(10)^{-7}$."

LETTERS TO THE EDITOR

Prompt publication of brief reports of important discoveries in physics may be secured by addressing them to this department. Closing dates for this department are, for the first issue of the month, the twenty-eighth of the preceding month; for the second issue, the thirteenth of the month. The Board of Editors does not hold itself responsible for the opinions expressed by the correspondents.

Raman Effect in Gases: CO and NO

With the high pressure apparatus described by the author in earlier communications,[1] the Raman spectra of gaseous carbon monoxide at a pressure of about 35 atmospheres and of gaseous nitric oxide at a pressure of about 20 atmospheres have been obtained. Besides unresolved rotational wings in the close proximity of the Rayleigh lines, Raman lines corresponding to vibrational transitions have been recorded in both cases. The frequency shifts are compared, in the table, with the respective vibration frequencies of these molecules in the ground state as deduced from absorption spectra (infrared for CO and ultraviolet for NO).[2] The agreement between the two sets of values is very satisfactory. It may be noted that the values

Gas	Raman frequency	Absorption frequency
CO	2139	2138
NO	1877	1878

2155 and 2142 reported earlier by Rasetti[3] for carbon monoxide differ to some extent from that given in the table. The vibration frequency of nitric oxide from Raman spectra is reported here for the first time.

The two gases used in the above investigation are generated under pressure by permitting the necessary chemicals to react with each other in closed and evacuated steel cylinders. In the case of CO, formic and concentrated sulphuric acids are used and the gas obtained appears to be very pure. Potassium ferrocyanide, potassium nitrite and acetic acid are used for generating NO, and it appears from the Raman spectrum of the resulting gas that it contains, besides nitric oxide, large proportions of nitrogen, nitrous oxide and carbon dioxide.

S. BHAGAVANTAM

210, Bowbazar Street,
Calcutta, India,
September 14, 1932.

[1] Bhagavantum, Ind. Jour. Phys. **6**, 319 (1931).

[2] Int. Crit. Tab. **5**, 412 and 415.

[3] Rasetti, Nature **123**, 205 (1929) and Nuovo Cim. **6**, 356 (1929).

Note on the Electric Field in Paramagnetic Crystals

The work[1] of Kramers, Bethe, and especially of Van Vleck and his collaborators has created the possibility of drawing conclusions from magnetic data about the electric fields in paramagnetic crystals and hence about the spatial arrangement of atoms and molecules in the crystal.

In his recent paper Van Vleck[1] has shown that it is possible to account for the different magnetic behavior of crystals of hydrated Co and Ni compounds by assuming that to a first approximation the electric fields possess cubic symmetry around the magnetic ion, but that in the second approximation a rhombic term must be added. Quantitative calculations amplifying the theory are to be

[1] H. A. Kramers, Comm. Leiden **60**; Proc. Amsterdam Acad. **33**, 959 (1930); H. Bethe, Ann. d. Physik **3**, 133 (1929); Zeits. f. Physik **60**, 218 (1930); J. H. Van Vleck, *The Theory of Electric and Magnetic Susceptibilities*, Oxford University Press; Phys. Rev. **41**, 208 (1932); O. M. Jordahl, W. G. Penney and R. Schlapp, Phys. Rev. **40**, 637 (1932); W. G. Penney and R. Schlapp, Phys. Rev. **41**, 194 (1932); Schlapp and Penney, Phys. Rev. (in press).

published shortly by Schlapp and Penney in this journal.

If the potential energy of an electron in the lattice can be developed as a power series in the displacement from the center of the magnetic ion, the terms which give rise to a decomposition of the energy levels are

$$\Phi = \Sigma_i \{ Ax_i^2 + By_i^2 + cz_i^2 + D(x_i^4 + y_i^4 + z_i^4) \}.$$

Van Vleck concludes that D must be positive to account for the experimental data on hydrated salts of the iron group. The purpose of the present note is to consider what atomic groupings will lead to a positive D.

Since the contribution to D due to the different charges in the neighborhood of the central ion is proportional to R^{-5} (where R is the distance from the central ion), it is evident that only the immediate neighbors will give a noticeable contribution to the value of D.

If the metal ion is surrounded by 6 oxygen ions or water-dipoles[2] in an octahedral arrangement, D will be positive.[3] If on the contrary the ion is surrounded by 8 or 4 negative charges in a cubic or tetrahedral arrangement, D will be negative. This leads to the conclusion that in the hydrated salts of the iron group the metal ion is surrounded by six molecules of crystal water.

Dr. C. A. Beevers of the University of Liverpool kindly expressed to me his opinion that, from the result of x-ray researches, the arrangement indicated above may be regarded as probable, though not proved for the alums and the hepta- and hexa-hydrated sulphates. It seems probable to me that also in solutions the metal ions will be surrounded by six water molecules.

Penney and Schlapp have performed calculations on rare earth salts, and have shown that it is possible to explain the temperature variation of the susceptibilities of the octahydrates of Pr and Nd sulphates, assuming a cubic field again with a positive value of D. Consequently, here also, the octahedral grouping of the oxygen atoms is suggested. This demands six oxygen neighbors for the metal ion, but in the substances so far investigated there are only four water molecules to each such ion. Hence it is necessary to suppose either that oxygen atoms belonging to the SO_4-group figure among the immediate neighbors, or else that a water molecule may be shared by two metal ions. Both assumptions could give rise to deviations from cubic symmetry, which can perhaps account for any magnetic anisotropy which may be disclosed when measurements, on the principal susceptibilities of single crystals of rare earth salts become available.

A quantitative discussion of the arrangements proposed above will be able to decide whether the picture corresponds to reality.

C. J. GORTER
Natuurk. Laborat. v. Teylers Stichting,
Haarlem, Holland,
September 15, 1932.

[2] The dipoles will orient themselves in the field of the positive ion with the negative charge inside. With the octahedral arrangement the negative charges are at the face centers of a cube embracing the positive ion.

[3] Cf., for instance, H. Bethe, Ann. d. Physik **3**, 196 (1929).

Possibility of the Existence of the Chlorine Isotope Cl^{39}

Hardy and Sutherland[1] in a recent paper found no evidence for the existence of a third isotope of chlorine, Cl^{39}, in the absorption spectrum of HCl. They made a careful search for lines due to HCl^{39} in the 1.7μ absorption band, but failed to confirm the maxima reported by Hettner and Böhme,[2] even with much greater path lengths than used by the German investigators. A year ago, the writers[3] studied the ultraviolet absorption spectrum of AgCl vapor[4] at high vapor densities expressly to test the assertions of Becker[5] as to the existence of this isotope. Our results were entirely negative, a contradiction made more striking by the subsequent confirmation of Becker's conclusions by Hettner and Böhme. The latter authors refrained from commenting on our results, pending more complete publi-

[1] J. D. Hardy and G. B. B. M. Sutherland, Phys. Rev. **41**, 471 (1932).

[2] G. Hettner and J. Böhme, Zeits. f. Physik **72**, 95 (1931).

[3] M. Ashley and F. A. Jenkins, Phys. Rev. **37**, 1712 (1931).

[4] B. A. Brice, Phys. Rev. **35**, 960 (1930).

[5] H. Becker, Zeits. f. Physik **59**, 583 and 601 (1930).

cation of these. However, most of the essential data, including an estimate of an upper limit for the abundance of Cl^{39}, were included in our abstract.[3]

The question of the existence of this isotope is of considerable interest for the systematics of nuclei, for if it were actually present it would make Cl the only known element, outside of the radioactive families, of odd atomic number having more than two isotopes. Such a violation of one of the few generalizations we have about the stability of nuclear types should certainly be critically examined. Furthermore, according to the theories of Urey[6] and of Bartlett,[7] Cl^{39} lies in the very interesting region immediately following the completion of the "closed shell" of nuclear protons and neutrons at A^{36}. Hence we wish to give here a somewhat more complete account of the evidence we obtained from the AgCl spectrum.

The accompanying reproduction shows the absorption of AgCl vapor in the region of the 0,1 band at various densities of the vapor, as photographed in the first order of a 21-foot grating. The vapor was contained in a quartz tube without windows, the heated portion being about 80 cm long and 2 cm in diameter. Temperatures along the tube were determined by a thermocouple. The source of the continuous spectrum was a high-current hydrogen discharge.[8] The two observed heads of $AgCl^{35}$ and $AgCl^{37}$ are indicated in the figure, as well as the expected position of the $AgCl^{39}$ head. It is seen that the region where the latter head should appear remains clear of structure from the 0,0 sequence up to a density corresponding to 800°C and that no trace of the head is visible. The microphotometer trace (upper curve), at the left, is from the 800° spectrogram, and also fails to show the head in question. At 850° the background begins to interfere; the lower curve is from a plate taken at this temperature. Here the absorption of even the $AgCl^{37}$ head is complete, but no evidence for an $AgCl^{39}$ head appears. The gradual rise of the curves in the neighborhood of the black edge is probably to be ascribed to the Eberhard effect.

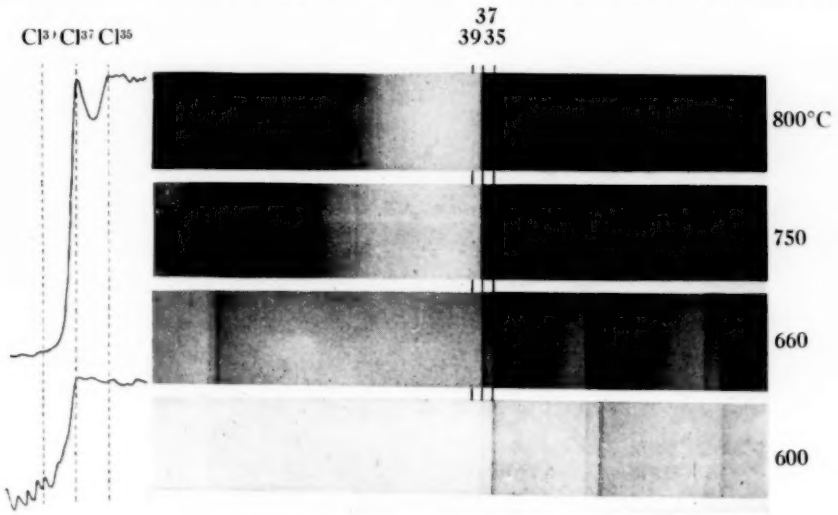

Fig. 1.

Our estimate for the upper limit for the abundance of Cl^{39} was obtained as follows. On a plate taken at 550°C the $AgCl^{37}$ head was just visible, and easily detectable by the microphotometer. From the equation given in I.C.T. Vol. **3**, p. 214 for the vapor pressure of AgCl, with a considerable extrapolation to low pressures, one finds the values 2.6×10^{-4} and 3.6×10^{-1} mm at 550° and 850°, respectively. The vapor densities are then approximately in the ratio 1:1400 at these two temperatures, so that if Cl^{39} were present in this

[6] H. C. Urey, J. Am. Chem. Soc. **53,** 2872 (1931).

[7] J. H. Bartlett, Jr., Nature **130,** 165 (1932).

[8] E. O. Lawrence and N. E. Edlefson, Rev. Sci. Inst. **1,** 45 (1930).

proportion relative to Cl^{37}, it should be detected on the 850° plate. Now Cl^{35} is 3.15 times as abundant as Cl^{37}, so the maximum value possible for the ratio Cl^{39}:Cl^{35} is 1:4400. The limit obtained in the infrared work of Hardy and Sutherland, using a path of seven meters, was 1:1600. It is apparent from the practically complete absorption of the $AgCl^{37}$ head that our sensitivity is somewhat greater than that of the infrared work, where even the strongest HCl^{37} lines gave an appreciable deflection. It is to be regretted that neither Becker nor Hettner and Böhme have given any estimate of the relative abundance of Cl^{39}, but it is obvious from their absorption curves that if the HCl^{39} maxima are real, the abundance must be much greater than either of the above limits.

MURIEL F. ASHLEY
F. A. JENKINS

University of California,
The Physical Institute, Utrecht,
September 20, 1932.

Simple Amplifier for Geiger-Müller Counters

The numerous uses to which Geiger-Müller counters have been put and their general effectiveness seem to warrant the publication of a simple amplifying and recording device which has been used in this laboratory during the last several months.

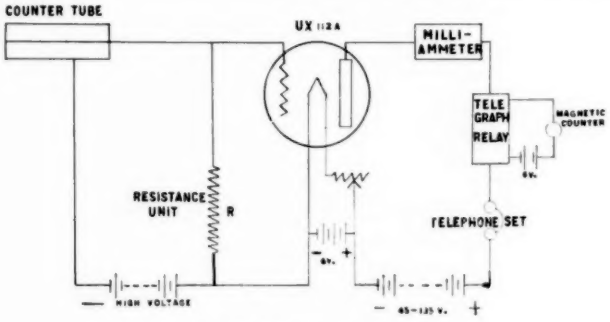

Fig. 1. Circuit diagram.

The circuit follows. The crucial part of the circuit is the resistance R. There is a definite value for this resistance which for each set of characteristics of the counter, the counting rate, and the voltage applied to the counter, gives the greatest amplification. The impulses

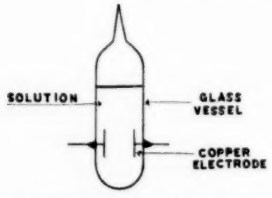

Fig. 2. Resistance unit.

are recorded as momentary diminutions of the normal filament plate current which are sufficient to actuate the ordinary telegraph relay with contact reversed so the magnetic counter circuit will be closed by each current diminution. Counters of surface area from 5 cm² to 100 cm², of lengths from 1 to 10 cm, and made of copper, nickel, zinc, and aluminum with wires of steel, tungsten, or aluminum have been used. Counting rates from 10 per minute to 400 per minute have been observed with the various counters and various exciting sources and the appropriate resistances, R.

The resistances consist of solutions of isopropyl alcohol in pentane of the proper compositions sealed in glass vessels with sealed-in electrodes, as shown in Fig. 2.

The solutions must be nearly pure pentane of compositions ranging up to approximately 7 volume percent of alcohol.

The resistance determines both the time of recovery of the system after each impulse and the size of each "kick" so that the product of the two is approximately constant if other conditions are not changed. As a result, it is possible to obtain "kicks" which completely repress the filament-plate current, (normally about 5 m.a.) if the counting rate is not higher than about 40 per minute, for this type of "kick" can be obtained with a minimum period of about a 0.5 second with a counter of about 75 cm² area and 25 cm length. For a rate as high as 300 or 400 per minute the kicks cannot be much greater than 1/10 of the

TABLE I.

Speed of count (min.$^{-1}$)	Size of kick (percent of filament-plate current)	Approximate volume percent of isopropyl alcohol
200	5–10	6
40	80–100	1

filament plate current. The counter characteristics affect the composition of the best solution very little. The following table contains the compositions and "kick" size for counters approximately the same as that described immediately above.

The amplifying tube can be any radio tube which will give a filament plate current of 3 or more milliamperes. The relay is an ordinary 680 ohms telegraph relay.

Argon gas at about 5 cm of Hg pressure is generally used in the counter, and the applied voltage is generally between 600 and 1500 volts.

W. F. LIBBY

Department of Chemistry,
University of California,
September 28, 1932.

High-Speed Hydrogen Ions

In a paper on the production of high speed light ions without the use of high voltages[1] a method and apparatus were described in detail for producing 1,220,000 volt-protons. The value of such high-speed protons for studies of the atomic nucleus has been shown recently by Cockcroft and Walton.[2] Using the above mentioned apparatus, their results have lately been checked and somewhat extended in this laboratory by disintegration of the lithium nucleus.[3] It is obvious that for further nuclear studies ions of still higher energies will be exceedingly valuable and an apparatus of larger dimensions has now been developed which produces hydrogen ions with energies equivalent to 3,600,000 volt-electrons.

An essential part of the apparatus is an electromagnet which gives uniform fields over considerable areas; indeed, the maximum producible ion energies are proportional to the area of the useful region of the magnet's field.

Although the magnet now being used has an iron coil 45 inches in diameter, for this first step the pole face diameter has been reduced to 27.5 inches, giving fields in excess of 15,000 gauss over a gap of 3.5 inches. Actually only a region of 20 inches diameter in the center of the poles has been used in the present experiments. The chamber between the poles was evacuated by means of a high-speed pumping system which kept the pressure of heavy gases and vapors down to the order of 10^{-6} mm of mercury and a pressure of hydrogen of approximately 10^{-5} mm of mercury was maintained by a suitable capillary leak. The ions were produced in this hydrogen gas by an electron beam from a filament near the center of the chamber which could be moved to the proper position, i.e., such that the ions started from a point away from the geometrical center of the apparatus by a distance equal to the radius of their first circle in the magnetic field. The high-frequency fields were applied across the diametral gap between two large hollow semi-circular electrodes, (one of which was at ground potential) by means of a "tuned plate—tuned grid" oscillator circuit, using a Federal Telegraph 20 kilowatt water-cooled tube. Wave-lengths down to 25.8 meters were used and voltages applied on the electrodes of approximately 15,000 volts or less. At the edge of the 20 inch circle the ions passed through an electrostatic deflecting system which bent them out of the beam (and at the same time measured their energies) into a collector connected to a suitable electrometer. From the electrostatic voltages applied on the deflecting plates the energies were calculated, and were found to check closely in each case with those expected.

Using a 28.5 meter wave-length, and a magnetic field of 14,000 gauss, hydrogen molecule ions were produced with energies of 3,000,000 volt-electrons and with a current of approximately 10^{-9} amperes. Using 25.8 meters and 15,250 gauss, 3,600,000 volt ions were produced. Due to the efficient focussing action of the high-frequency electrodes, the ion currents remain approximately the same throughout the range from 1 to 3.6 million volts. These H_2^+ ions with energies of 3,600,000 volt-electrons are, for nuclear purposes, essentially equivalent to protons of energies

[1] Ernest O. Lawrence and M. Stanley Livingston, Phys. Rev. **40,** 19 (1932).

[2] Cockcroft and Walton, Proc. Roy. Soc. **A137,** 229–242 (1932).

[3] Lawrence, Livingston and White, Phys. Rev. **42,** 150 (1932).

of 1,800,000 volt-electrons. Hydrogen molecule ions rather than protons were accelerated in the present experiments because protons require a much lower wave-length (for the same magnetic field), which is difficult to obtain due to the large capacity in the oscillating circuit.

It appears now entirely practicable to go to much higher energies by using a still larger chamber. However, it seems more desirable to hesitate awhile on the road to higher voltages and use these 1,800,000 volt protons for some nuclear studies. This we intend to do.

I wish to express my deepest gratitude to Prof. Ernest O. Lawrence for his constant help and guidance in this development, and to Commander T. Lucci for his invaluable assistance. These experiments have been made possible through the help of the Federal Telegraph Company, the Research Corporation and The Chemical Foundation.

M. Stanley Livingston

Radiation Laboratory,
Department of Physics,
University of California,
Berkeley, California,
October 3, 1932.

The Heisenberg Theory of Ferromagnetism

The theory of the existence of ferromagnetism, due to Heisenberg,[1] disagrees in some of its consequences with experiment. It is here shown to be not quite as unphysical as has been supposed. Heisenberg's principal result is contained in the well-known simultaneous equations:

$$\text{I.}\quad y=\tanh x$$
$$\text{II.}\quad x=\tfrac{1}{2}(\beta-\beta^2/z)y+\beta^2y^3/4z \qquad (1)$$

$\beta=zJ/kT=$(number of nearest neighbors of atom in crystal)$\times$(e.s. exchange integral)$/kT$. $y=I_w/I_0$. I_w is the magnetization in a field only strong enough to orient the large crystal spin (if extant) and to overcome the small magnetic interactions[2] of the electrons (here neglected). I_0 is the intensity of absolute saturation. The atomic spin is that of one electron.

The prevalent interpretation of these equations has been based on a graphical solution similar to that of the Weiss theory, neglecting the fact that II does not give a straight line the graphical manner of solving (1), but must bear in mind that the equations do not hold for zero external field, when the magnetization may change in direction. The part of the magnetization curve treated by (1) when the term $\mu H/kT$ is added to χ is, of course, only that beyond the usual experimental saturation. In that region Kapitza has measured that with 240,000 gausses the magnetization of Fe and Ni at room temperature increases not more than 1 percent. After simplifying (1) by taking II linear (see footnote 3), calculation shows that the increase for Ni should be 1 percent and for Fe less than one-tenth as much. The corresponding increase for Ni at 330°C should be about 10 percent.

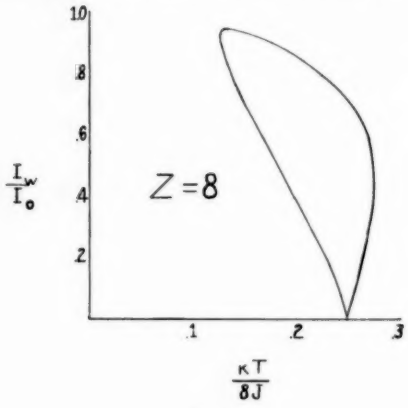

Fig. 1.

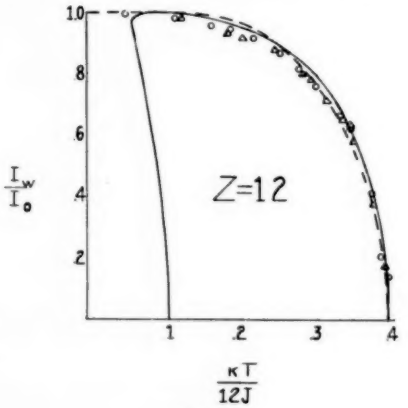

Fig. 2.

[1] W. Heisenberg, Zeits. f. Physik **49**, 619 (1928).

[2] The magnetic interactions are largely responsible for direction effects, remanence, hysteresis, and demagnetizing forces, which may not be expected of the Heisenberg model, unmodified. One might expect hysteresis from

(Heisenberg's Fig. 1), that is, neglecting y^3. One obtains ($z \geqq 8$) only the axis-intercepts of Figs. 1 and 2, two positive critical temperatures (coincident for $z=8$) between which ferromagnetism should exist.

Numerical solution of (1) is simpler in the following form of the equations:

$$\beta = \frac{z}{2-y^2}\left\{1 \pm \left[1 - \frac{2(2-y^2)}{zy} \log \frac{1+y}{1-y}\right]\right\}. \quad (2)$$

Solutions are plotted in Figs. 1 and 2 for $z=8$ (Fe) and $z=12$ (Ni, Co). The first is an extreme case, where the results are very sensitive to small changes in the assumptions, and have very little semblance to physics. In the second, the higher-temperature branch of the curve is theoretically, as well as experimentally, preferred. Its intercept is taken as the Curie temperature. Data from the experiments of O. Bloch,[3] e.g., for Ni (circles) and Co (triangles) lie very close to the curve.

The lower-temperature branch of each curve is a mathematical ghost of which the origin may be explained as follows. The theory in the approximation used seeks only the spin with an extreme value of the probability, presumably a maximum. At a high temperature very low spins of the crystal are most probable. Higher spins have lower energies, and with decreasing temperature become more probable, giving the higher-temperature branch of the curve. In reckoning this effect, the distribution-in-energy of states of each value of spin is approximated with the central part of a Gaussian distribution. The distant parts of this distribution are small and neglected. Unfortunately they extend to infinity, whereas the corresponding physical distribution has definite and fairly narrow limits. At very low temperatures only the very few states of high spin have a high probability, but, due to the Gaussian distribution, the tremendously numerous states of low spin have each a finite (mathematical) probability, so the total probability may be greater for low spins. As the temperature decreases below the Curie point, a probability peak may thus develop at zero spin. Between this and the maximum giving the higher-temperature branch of the curve is a minimum, corresponding to the lower branch. (This identification of the curves has been verified by reckoning second derivatives.) The lower branch is thus nonmagnetic. As the temperature further decreases, the low-spin states overwhelm the others, and the two extrema merge.

Thus we see that the higher branch of the curve alone gives the magnetization resulting from the assumption of a Gaussian distribution. It differs very little, so far as it goes uninterrupted, from the curve obtained by assuming an infinitely sharp distribution[3]—i.e., that states with the same spin have the same energy—if we determine the constant J from the Curie point in each case. (The latter curve is drawn with dots in Fig. 2 to a different scale of absissae than that shown, its axis intercept being $kT/12J' = \frac{1}{2}$.) We conclude that the numerical results of the theory are fairly insensitive to variation of the distribution assumed. Because of this insensitivity, we may be satisfied that the simple assumption of an infinitely sharp distribution gives a fairly good approximation to the result that would be obtained from the actual, incalculable distribution.

This justifies, as an approximation, a simplified form of the theory having quite satisfactory consequences, and lends weight to the usual conclusion that the Heisenberg concept of ferromagnetism is physically correct.

Note added October 17, Zurich. For small z the Gaussian "spread" is relatively broader and there appears no extremum of probability, except that at zero spin. The condition that z be at least 8 for ferromagnetism is thus also a consequence of the mythical, low-spin, low-energy states to which Heisenberg[1] ascribed the second critical temperature.

D. R. INGLIS

Landheim Pulvermühle,
Dusslingen bei Tübingen,
October 4, 1932.

[3] See a paper by Bitter, Phys. Rev. **39**, 340 (1932). A similar comparison made by Tyler, Phil. Mag. **11**, 596 (1931), shows the "theoretical" curve (which also appears in Van Vleck's book) bulging not enough towards its ends. The equations there used, (1) lacking terms in β^2, may be very simply derived by modifying Heisenberg's theory to the extent of endowing all states having a given spin with the same energy.

Note on the Term System of Ir I

The first regularities in the spectrum of Ir I were found by Mr. C. P. Snyder about 1900. He discovered a constant difference wave number array consisting of 12 columns and 54 rows, the array containing 240 lines. Snyder never published his work but sent it to

Professor H. A. Rowland, who turned the array over to Dr. N. E. Dorsey, his assistant, who later turned it over to Dr. W. F. Meggers. The author obtained the loan of the original array through the courtesy of Dr. Meggers.

The underwater spark spectrum of Ir has been photographed by Meggers and Laporte.[1] With the results obtained they were able to determine the ground state and fix the relative energy values for the 12 columns in Snyder's array. They also noted all the lines appearing in the underwater spark which were involved with the interval of the two ground states, 2835.0 cm^{-1}. Meggers and Laporte tentatively called the two ground states $^2D_{2\frac{1}{2}}$ and $^2D_{1\frac{1}{2}}$, but mentioned that they might be $^4F_{4\frac{1}{2}}$ and $^4F_{3\frac{1}{2}}$.

The above results have been extended by the writer, using the wave-length data of Meggers[2] for the region 8426 to 4500A° and of Exner and Haschek[3] for the region 4500 to 2200A°.

The present array consists of 16 low even terms and 77 middle and high terms. It contains 566 lines, including nearly all the strong lines of the spectrum.

The J values of the terms have been deduced from a study of the intensities and combinations, and a knowledge of the theoretical number of times each value of J for the low even terms should occur. The two ground states have the same J value of $4\frac{1}{2}$, and are most probably ^4F terms. The raie ultime is given by a combination of the second lowest odd term with the ground state. This term has a J value of $5\frac{1}{2}$ and is possibly $^4G_{5\frac{1}{2}}°$.

At present, further progress is hindered because of the incompleteness of the data. The region from 4500 to 1900A° is particularly incomplete. This region is to be photographed in a search for new lines and for better wave-length determinations of the old lines. An attempt will also be made to obtain the Zeeman patterns of the strongest lines.

It has been thought worth while to publish a list of the strongest combinations and terms, since they have not been published before.

TABLE I.

λ air	I	comb.	λ air	I	comb.
5894.06	−6	N-7° 7°-M	3334.19	−6	38°-K
5625.56	−8	9°-M	3266.45	−10	16°-D
5449.50	−10		3241.52	−6	12°-C
5364.32	−8		3220.79	−15 (R.U.)	9°-B
4938.09	−6	5°-I	3219.53	−6	
4778.16	−7	9°-J	3168.88	−6	20°-E
4728.86	−6	13°-L	3133.31	−8	22°-E
4616.37	−6	9°-I	3100.42	−15	13°-B 24°-E
4548.50	−6	1-3°	2951.23	−8	9°-A
3800.10	−10	1°-A	2943.17	−10	29°-E
3636.22	−8	25°-H	2936.71	−8	
3628.69	−10	9°-E	2934.63	−8	63°-M 30°-E
3617.23	−8	19°-G	2924.81	−10	10°-A
3609.78	−8	3°-B	2849.74	−8	13°-A
3573.74	−10	4°-B 13°-F	2839.18	−6	71°-K
3559.01	−8	9°-D	2824.44	−6	22°-B
3522.05	−10	5°-C	2797.72	−5	24°-B
3515.96	−10		2694.22	−5	53°-G 28°-B
3513.67	−15(R.U.)	2°-A	2664.77	−5	19°-A
3448.99	−10	7°-C	2661.98	−5	30°-B
3437.05	−10	15°-E			
3368.50	−10	6°-B			

[1] Meggers and Laporte, Phys. Rev. **28,** 660 (1926).

[2] Meggers, Sci. Papers Bur. of Standards, No. 499. Bull. Bur. of Standards **20,** p. 19 (1925).

[3] Exner and Haschek, Spektren der Elemente bei normalem Druck, **II.**

TABLE II.

Term symbol	J	Term value cm^{-1}	Term symbol	J	Term value cm^{-1}
		Even terms			
A ^4F	$4\frac{1}{2}$	0.0 (S)	L	$4\frac{1}{2}$	13939.8 (A)
B ^4F	$4\frac{1}{2}$	2835.0 (S)	M	$2\frac{1}{2}$	16103.4 (S)
C	$1\frac{1}{2}$	4079.1 (A)	N	$3\frac{1}{2}$	17779.3 (A)
D	$2\frac{1}{2}$	5784.9 (S)	O	$1\frac{1}{2}$	18547.0 (A)
E ^4F?	$3\frac{1}{2}$	6323.9 (S)	P	$2\frac{1}{2}$	19060.5 (S)
F ^4F?	$3\frac{1}{2}$	7106.7 (S)	1	$4\frac{1}{2}$	52508.9 (A)
G	$2\frac{1}{2}$	9877.8 (S)	2	$4\frac{1}{2}, 3\frac{1}{2}$	54892.6 (A)
H	$1\frac{1}{2}$	11831.1 (S)	3	$3\frac{1}{2}$	55381.9 (A)
I	$2\frac{1}{2}$	12218.5 (S)	4	$4\frac{1}{2}, 3\frac{1}{2}$	56416.1 (A)
J	$2\frac{1}{2}$	12951.6 (S)	5	$3\frac{1}{2}$	56792.7 (A)
K	$3\frac{1}{2}$	13087.8 (S)	6	$4\frac{1}{2}, 3\frac{1}{2}$	59878.0 (A)
		Odd terms			
1° ^4F°?	$4\frac{1}{2}$	26307.6 (A)	13°	$4\frac{1}{2}$	35080.6 (M)
2° ^4G°?	$5\frac{1}{2}$	28452.3 (A)	15°	$3\frac{1}{2}$	35410.7 (S)
3°	$3\frac{1}{2}$	30529.7 (A)	16°	$1\frac{1}{2}$	36390.1 (A)
5°	$1\frac{1}{2}$	32463.5 (S)	18°	$2\frac{1}{2}$	37446.3 (S)
6°	$4\frac{1}{2}$	32513.4 (A)	19°	$3\frac{1}{2}$	37515.4 (S)
7°	$2\frac{1}{2}$	33064.8 (S)	20°	$4\frac{1}{2}$	37871.7 (M)
9°	$3\frac{1}{2}$	33874.3 (S)	21°	$3\frac{1}{2}$	38158.3 (A)
10°	$5\frac{1}{2}$	34180.4 (M)	22°	$4\frac{1}{2}$	38229.9 (S)
12°	$2\frac{1}{2}$	34919.9 (S)	23°	$2\frac{1}{2}$	38358.0 (A)
24°	$3\frac{1}{2}$	38567.9 (S)	49°	$3\frac{1}{2}$	45896.3 (S)
25°	$2\frac{1}{2}$	39324.4 (S)	50°	$2\frac{1}{2}$	46093.7 (S)
27°	$2\frac{1}{2}, 3\frac{1}{2}$	39806.0 (S)	51°	$4\frac{1}{2}$	46220.7 (M)
28°	$3\frac{1}{2}, 4\frac{1}{2}$	39940.4 (M)	52°	$3\frac{1}{2}$	46979.6 (M)
29°	$3\frac{1}{2}$	40291.3 (S)	53°	$1\frac{1}{2}$	46983.3 (S)
30°	$4\frac{1}{2}$	40389.9 (S)	54°	$2\frac{1}{2}$	47165.1 (S)
31°	$1\frac{1}{2}$	40524.6 (S)	55°	$2\frac{1}{2}$	47537.5 (S)
32°	$3\frac{1}{2}$	40710.7 (S)	56°		47548.7 (S)
33°	$4\frac{1}{2}$	41118.7 (M)	58°	$2\frac{1}{2}$	48206.5 (S)
34°	$2\frac{1}{2}$	41522.5 (S)	71°	$4\frac{1}{2}$	48299.1 (M)
36°	$1\frac{1}{2}$	42268.2 (S)	59°	$3\frac{1}{2}$	48448.8 (S)
38°	$2\frac{1}{2}$	43071.7 (S)	60°	$1\frac{1}{2}$	48802.1 (S)
39°	$3\frac{1}{2}$	43176.2 (S)	61°	$2\frac{1}{2}$	49146.6 (S)
40°	$1\frac{1}{2}$	43200.9 (S)	62°		49621.4 (S)
41°	$3\frac{1}{2}$	43592.2 (S)	64°		51814.6 (S)
42°	$2\frac{1}{2}$	44596.8 (S)	65°		51852.3 (S)
43°	$3\frac{1}{2}$	44642.6 (S)	66°		52051.7 (S)
44°	$4\frac{1}{2}$	44652.6 (M)	67°		52134.2 (S)
45°	$1\frac{1}{2}$	44785.5 (S)	68°		52224.4 (S)
46°	$2\frac{1}{2}$	45111.7 (S)	70°		52806.6 (S)
47°	$2\frac{1}{2}$	45186.0 (S)			

Table I contains a list of all lines of intensity 6 or greater as estimated by Exner and Haschek on an intensity scale of 15 for the strongest lines and 1 for the weakest. Column one gives the wave lengths in I.A.; column two, the estimated intensity; column three, the combination giving the line.

Table II contains a list of the most certain terms. Column one gives the term symbol; column two, the J value; column three, the term value expressed in cm^{-1}. A term value followed by (*S*) indicates the term as in Snyder's array; (*M*) indicates the term was first noted by Meggers and Laporte; (*A*) indicates the term was noted by the author.

WALTER ALBERTSON

Massachusetts Institute of Technology,
Cambridge, Massachusetts,
October 6, 1932.

The Isotope of Hydrogen in the Atomic Spectrum

Urey, Brickwedde and Murphy[1] have shown the existence of H^2 by photographing the lines due to H^2 in the atomic spectrum with a 21-ft. grating. Professor Urey has informed the author that Professor Shenstone at Princeton has succeeded in getting some indication of the H^2 lines but his photographs were complicated by very bad ghosts from his grating (see also[2]).

Using a long discharge tube of the type described by Wood[3] the $H^2\gamma$ line was photographed with a glass prism spectrograph. The tube used was 220 cm long and 8 mm diameter and was observed end on through about 40 cm of the central portion of the tube. The tube was supplied with moist electrolytically prepared hydrogen which was admitted by means of a long fine capillary. This tube operated in a very black stage and the spectra was excited by a transformer which could deliver a maximum current of about 310 m.a.

The spectrograph was a six prism glass instrument used as a littrow which makes it effectively twelve prisms and gave a dispersion in the $H\gamma$ region of about 1.09 angstroms per mm. The author expects to publish a full description of this instrument as well as a photograph showing the $H^2\gamma$ line in J.O.S.A. in the near future.

On passing a current of 190 m.a. through the tube a 2.5 hour exposure did not record the presence of the $H^2\gamma$ line although a 1 sec. exposure recorded $H^1\gamma$ with about five times the intensity necessary to make it visible on the plate. Upon increasing the current to 310 m.a. the $H^2\gamma$ line appeared with a 35 minute exposure. This type of behavior has been observed and explained by (U., B. and M.[4]). Since the transformer used could only deliver 310 m.a. a further enhancement of $H^2\gamma$ with respect to $H^1\gamma$ could not be produced. From these results it might be concluded that the ratio of H^2 to H^1 is not more than 1 part in 80,000 in ordinary H_2 if the reciprocity law held for the photographic plate. Due to failure of this law for low intensities Bleakney's[2] value of 1 part in 30,000 is probably much more reliable. Measurements of the plates gave for the wave-length of $H^2\gamma$ 4339.256A or $d\lambda = 1.211$ in substantial agreement with U., B. and M.'s value of 1.206 for ordinary hydrogen.

DAVID H. RANK

Physics Laboratory,
Pennsylvania State College,
State College, Pennsylvania,
October 10, 1932.

[1] Urey, Brickwedde and Murphy, Phys. Rev. **39**, 164 (1932); **40**, 1 (1932).

[2] Walker Bleakney, Phys. Rev. **41**, 32 (1932).

[3] R. W. Wood, Proc. Roy. Soc. **97**, 455 (1920).

[4] Urey, Brickwedde and Murphy, Phys. Rev. **40**, 464 (1932).

Intensity of Cosmic-Ray Ionization in Western North America

This letter is a preliminary report of one of the ten cosmic-ray expeditions organized and supplied with apparatus by Professor A. H. Compton and supported in part by the Carnegie Institution of Washington. Measurements of ionization intensities due to penetrating radiation were made by this expedition in Alaska, California and Colorado.

The apparatus was a duplicate of that already described in this journal,[1,2] and the method of making measurements was also essentially the same. It might be mentioned that the effect of high humidity made it necessary to discard some of the earlier observations. This difficulty was overcome by maintaining a fairly constant high temperature in the observation tent by means of a stove.

Table I gives the time, place, elevation, mean barometer, and duration of observations at each place where measurements were made. One observation (column 7) involved a radium comparison test, a ground radiation test and a cosmic-ray test, and required about 3 hours. Thus a six-hour shift consisted of (1) four electrometer drifts in each direction with the radium at 1 meter; (2) four cosmic-ray drifts in each direction with the radium distant; (3) three cosmic-ray drifts in each direction with the radium distant and the outer of the three shields removed; (4) a repetition of

[1] A. H. Compton, Phys. Rev. **41**, 111 (1932).

[2] A. H. Compton, Phys. Rev. **41**, 681 (1932).

TABLE I. *Relative cosmic-ray intensities.*

Place	Dates	Lat. N	Long. W	Elev. meters	Mean bar cm	No. of obs.	Mean C_{123}	Mean dev. % δ	$\delta/n^{1/2}$%
Ft. Yukon	6/24–7/2	67°	145°	129	75.1	61	0.170	2.8	0.4
Kennecott	7/9–7/19	62°	143°	1840	61.2	75	0.254	2.8	0.3
Berkeley	7/30–8/2	38°	122°	116	75.1	18	0.166	5.2	1.2
Tioga Pass	8/4–8/15	38°	119°	3040	53.0	80	0.363	3.9	0.4
Pasadena	8/17–8/21	34°	118°	259	73.6	30	0.174	3.8	0.7
Denver	8/26–8/29	40°	105°	1616	62.3	23	0.240	4.4	0.9
Summit Lake	8/30–9/9	40°	105°	3900	48.3	80	0.492	3.7	0.4

(1); (5) a repetition of (2). The single set of measurements (3) served to make the small ground radiation correction for both cosmic-ray measurements. The electrometer sensitivity was adjusted at each elevation to such a value that a single cosmic-ray drift required about ten minutes. Observations at each place were made continuously, the shortest series being 54 hours and the longest 240 hours.

The value C_{123} is a net ratio of cosmic-ray ionization current to gamma-ray ionization

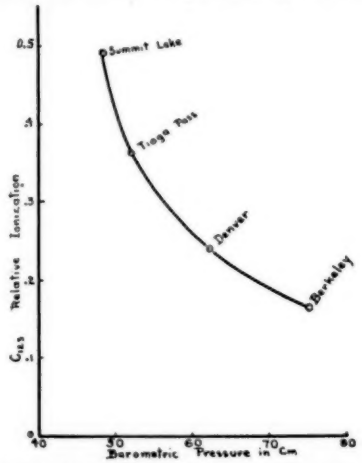

Fig. 1. Variation of ionization with barometric pressure at lat. 40°N.

current, corrected for ground radiation. Therefore these values are only relative.

Because of possible systematic errors we feel that the values of $\delta/n^{1/2}$ give an unduly optimistic indication of the probable error of these measurements. It may be as large as one or two percent even in the longer series of observations.

The values obtained at Berkeley, Tioga Pass, Denver and Summit Lake represent intensities at nearly the same latitude. These four sets of observations give the curve of ionization against barometric pressure shown in Fig. 1.

This curve agrees fairly well with those obtained by Millikan and Cameron[3] and Compton.[1] Using this curve to reduce the values at Pasadena, Berkeley and Ft. Yukon to sea level, we get the lower curve of variation with latitude for this region, shown in Fig. 2. The

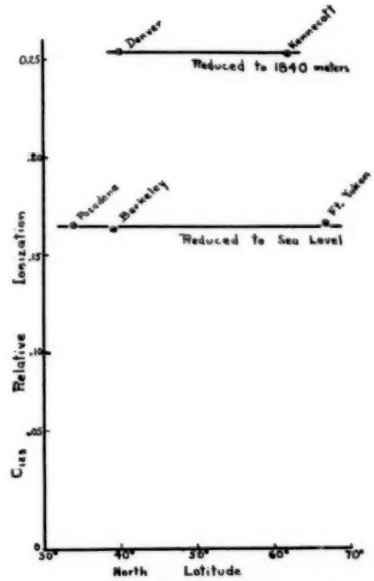

Fig. 2. Variation of ionization with latitude.

upper curve of this figure shows the relative values at Denver and Kennecott both reduced in the same manner to 1840 meters.

These results indicate no significant variation of intensity of ionization due to penetrating radiation (when measured by this method) in the region covered.

R. D. BENNETT, Mass. Institute of Tech.
J. L. DUNHAM, Harvard University
E. H. BRAMHALL, Mass. Institute of Tech.
P. K. ALLEN, Yale University
October 14, 1932.

[3] Millikan and Cameron, Phys. Rev. **37**, 242 (1931).

The Dielectric Constant and Electric Polarization of Mixtures in the Neighborhood of the Critical Point

There exist many mixtures of liquids, chiefly organic liquids, which disclose critical phenomena in the system liquid-liquid. As a result of a long series of experiments, I am able to state that the most suitable medium for dielectric tests is the pair of liquids: hexane-nitrobenzene, the critical temperature of dissolution of which is 16.9°, and the critical concentration 51.4%. The object of the present work was to test the behavior of the dielectric constant ϵ, the density d, the gram polarization of the mixture P_{gr}, and the molecular polarization P of the dissolved nitrobenzene, when approaching the critical point where, as is well known, considerable fluctuations of density take place, manifesting themselves by the critical opalescence.

The measurements of the dielectric constant were conducted as in the recently published research A. Piekara, Nature **130**, 93 (1932). The measurements of the density were carried out in the dilatometer. The condenser and the dilatometer were placed in a specially constructed thermostat enabling the maintenance of any constant temperature between $-4°$ and $+60°$C.

The results obtained for the mixture having the critical concentration are shown in Fig. 1. With the fall from higher temperatures to the critical temperature, the dielectric constant increases, but at a decreasing rate; the corresponding curve is bent downwards, which does not occur at other concentrations. The molecular polarization of nitrobenzene at first increases, but from 22° it decreases more and more rapidly. It is obvious that the density fluctuations are responsible for such a considerable decrease of the polarization of nitrobenzene. The critical opalescence begins at 18.7°. It is interesting that even above 18.7°, where no opalescence can be detected, the fluctuations of density, although very feeble, cause the decrease of polarization.

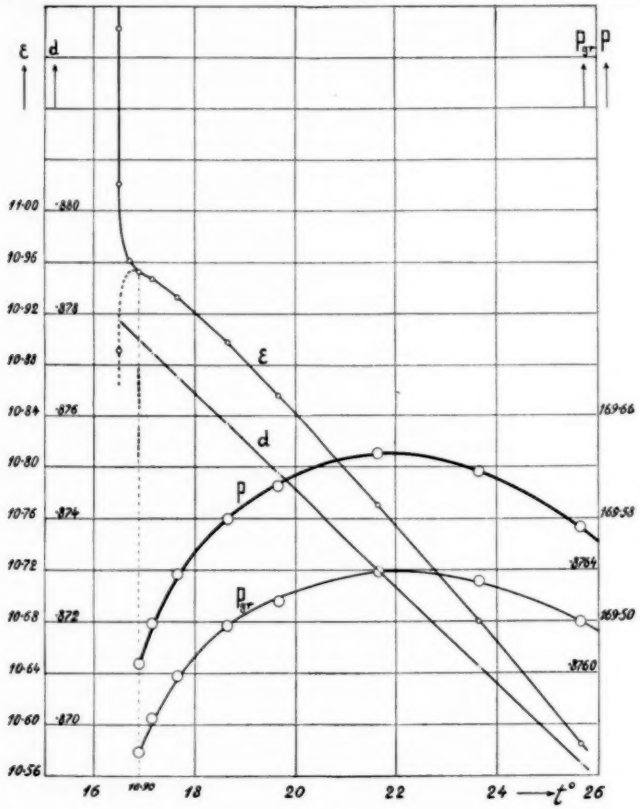

Fig. 1.

At the temperature of 16.9° the separation

of phases occurs. The dielectric constant increases rapidly, in connection with the production of the emulsion hexane-nitrobenzene.

Mixtures were also tested having concentrations lower, and higher, than the critical concentration, especially in the neighborhood of the point at which the separation of phases takes place. The dielectric constant undergoes a rapid fall if the emulsion nitrobenzene-hexane is formed, or a rapid increase if the emulsion hexane-nitrobenzene is produced.

The detailed results of these investigations will be published later in the Bull. Acad. Polonaise (Cracovie).

A. PIEKARA

Physical Laboratory,
Sulkowski Gymnasium,
Rydzyna, Poland,
September 12, 1932.

The Electric Moment of the Molecule of Nitrobenzene

Recently there have been published a number of investigations establishing the fact that in the neighborhood of 9.6° nitrobenzene undergoes some, as yet not clearly understood, modification (M. Wolfke and J. Mazur, Zeits. f. Physik **74,** 110, 1932; G. W. Stewart, Phys. Rev. **39,** 176, 1932; H. Trotter, Phys. Rev. **40,** 1052, 1932). At the same time, however, there appeared publications denying the existence of these allotropic forms of liquid nitrobenzene (M. Wolfke and S. Ziemecki, Acta Phys. Polonica **1,** 271, 1932; Massy, Warren and Wolfenden, Nature **129,** 441, 1932; J. N. Friend, Nature **129,** 471, 1932; A. Piekara, Nature **130,** 93, 1932). Studying the problem of the critical point of dissolution—chiefly on the mixtures of nitrobenzene and hexane—I resolved to derive profit from the occasion and to examine if the electric moment μ and the polarizing ability γ of the molecule of nitrobenzene undergo any change when passing the temperature point of 9.6°. Already the first measurements have been shown that such change does not occur. Now I am able to give more accurate data concerning this matter.

I experimented with dilute solutions of nitrobenzene in hexane. Both substances have been carefully purified and dried. Fig. 1 shows the

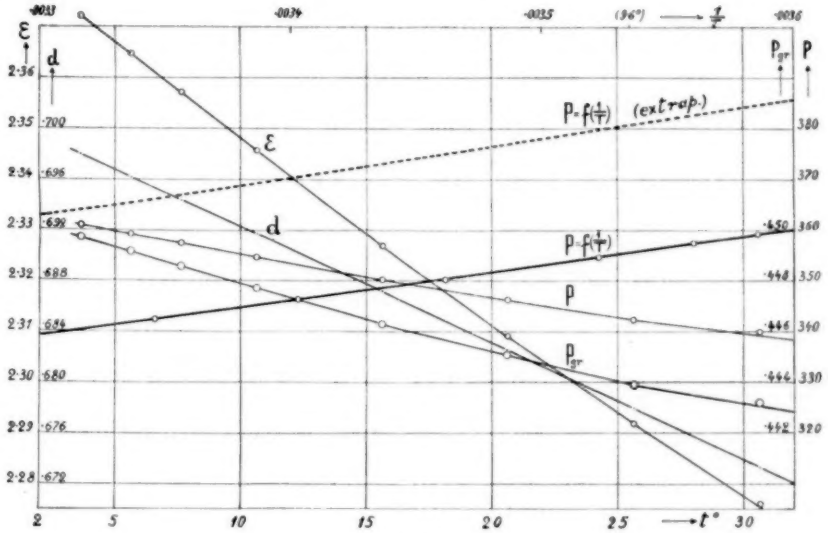

Fig. 1.

graphs of the dielectric constant ϵ, density d, gram polarization

$$P_{gr} = \frac{\epsilon - 1}{\epsilon + 2} \cdot \frac{1}{d},$$

and the molecular polarization of nitrobenzene P, for one of the solutions tested, having a concentration (by weight) $c = 0.04034$. P is to be computed from the formula

$$P = \frac{M}{c}[P_{gr} - (1 - c)P_{gr}']$$

where P_{gr}' is the gram polarization of the pure solvent, and M is the molecular weight of

nitrobenzene. According to the theory of Debye, P is composed of two parts, a "dielectric" one P_d, and a "paraelectric" one P_p, and, if the association does not exist, can be expressed:

$$P = P_d + P_p = \frac{4\pi}{3}N\gamma + \frac{4\pi N\mu^2}{9KT}.$$

The relation between P and $1/T$ is visible from the straight line in Fig. 1. The dotted line refers to the polarization value, extrapolated for the concentration $c=0$. The value of angular coefficient of this line gives us: $\mu=3.5_4\times10^{-18}$. The accuracy of this value is too small to attribute to it any greater importance, since the association of the molecules of nitrobenzene makes an accurate extrapolation impossible.

For calculating the μ value, another frequently employed method may be used, according to which it is supposed that $P_d=R_\infty$ (molecular refractivity, extrapolated for infinitely long waves). According to J. W. Williams (Phys. Zeits. **29**, 174, 1928) we have: $P_d=32.0$ cc. Since (for 25°) $P=366.7$ cc, we find $P_p=334.7$ cc, and $\mu=4.0_2\times10^{-18}$. A third method may also be used which is based on the supposition that P_d is equal to the molecular polarization of solid nitrobenzene. My measurements (l. c.) give the following results (0°): $\epsilon=3.44$, $d=1.342$, hence $P_d=41.1$ cc. Consequently $P_p=325.6$ cc (at 25°), and $\mu=3.97\times10^{-18}$.

As a result of the application of the two last methods, we may assume:

$$\mu=4.0_0\times10^{-18}:$$

the error involved in this value is less than ±1 percent. This μ value is a little greater than the one ($3.9_0\times10^{-18}$) found by J. W. Williams (l. c.).

Since the polarization, reciprocal of temperature ($1/T$) graph on Fig. 1 is a straight line, it is obvious that neither the electric moment μ nor the polarizability γ of the molecule of nitrobenzene undergo any change (cf.: L. Meyer, Zeits. f. Physik **75**, 421, 1932). Consequently the structure of the molecule of nitrobenzene does not undergo any change.

The full report of these investigations will appear in the Bull. Acad. Polonaise (Cracovie).

A. Piekara

Physical Laboratory,
Sulkowski Gymnasium,
Rydzyna, Poland,
September 12, 1932.

BOOK REVIEWS

Tables of Cubic Crystal Structure of Elements and Compounds. I. E. KNAGGS AND B. KARLIK. With a section on alloys by C. F. Elam. Pp. 90. Adam Hilger, Ltd., London, 1932. Price 11/6d.

This little book will be of great aid to the crystal-structure worker when dealing with cubic substances. Table I lists all investigated inorganic substances in alphabetical order with chemical formulas and complete references. Table Ia contains the relatively few cubic organic compounds. Table II enumerates the 513 cubic substances in the order of increasing length of the edge of the unit cell.

Tables III and IV are corresponding tabulations of alloys. Bibliographies of about 1000 references complete this excellent up-to-date catalogue. The printing and binding are of high quality.

J. W. GRUNER
University of Minnesota

Electrons and Waves. H. STANLEY ALLEN. Pp. 316+vii, Figs. 60. MacMillan and Co., Ltd., London. 1931. Price $2.50.

This account of modern physics follows a middle course. The discourse is of an essentially popular nature suited to the intelligent layman; yet there is preserved some degree of rigor in the exposition of the newer physical theories and therefore the book should be of interest to some physicists, particularly those that have only a slight familiarity with modern developments. The historical sketches given are especially noteworthy both from the point of view of the expert and the layman. But this account of recent progress will be appreciated more by the reader who has not specialized in physics. The book is well written and contains many good figures that illustrate modern physical phenomena, such as electron and x-ray diffraction pictures and Wilson cloud-chamber photographs.

E. O. LAWRENCE
University of California

Gmelins Handbuch der anorganischen Chemie, 8 Auflage. Heransgegeben von der Deutschen Chemischen Gesellschaft; Verlag Chemie, Berlin, 1932. System Nummer 59 Eisen, Teil B. Lieferung 5; page 294+xviii+xxxviii*, Figs. 62; 53.50 R.M. System Nummer 58 Kobalt; Teil A. Lieferung 2, page 282+xviii+xvi, Figs. 33; 48 R.M.

With the fourth continuation on iron and the first on cobalt, both volumes have reached completion. An extensive table of contents accompanies each issue, thus facilitating looking up special subjects in these exhaustive monographs on iron and cobalt. In previous announcements of sections of Gmelins 8th edition, the work has been warmly praised and the present additions uphold the high scientific standing of the preceding volumes. According to the reviewer's knowledge, Gmelins Handbuch offers the most complete, exhaustive and modern compilation of the physical and chemical properties of the elements and their compounds.

I. M. KOLTHOFF
University of Minnesota

CURRENT LITERATURE OF PHYSICS

Extracts from the Tables of Contents of Some of our Contemporaries

NATURE

VOL. 130, No. 3283 — OCTOBER 1, 1932

Magnetism and Quantum Mechanics. By **E. C. S.** 490
Measurements of Solar Radiation. By **S. Chapman** 497

Letters to the Editor:

Selective Transmission of γ-Radiation by Lead. By **F. L. Hopwood, T. E. Banks and T. A. Chalmers** 506
Magnetic Moment and the Chemical Bond in Alloys. By **J. Dorfman** 506
Expanding Universe. By **D. D. Kosambi and E. A. Milne** 507
Electron Oscillations. By **Antonio Rostagni** 509

NATURE

VOL. 130, No. 3284 — OCTOBER 8, 1932

Letters to the Editor:

Has Physics Discarded Mechanism? By **J. E. Turner** 544
Change of Paramagnetic Susceptibility due to Absorption of Light. By **D. M. Bose and P. K. Raha** 544
Causes of Ionization in the Upper Atmosphere. By **Ivo Ranzi** 545

ZEITSCHRIFT FÜR PHYSIK

VOL. 78, NOS. 3 AND 4 — SEPTEMBER 21, 1932

Double Band of Solid Hydrogen Chloride. By **G. Hettner** 141
Structure of Atomic Nuclei. By **W. Heisenberg** 156
Liberation of Neutrons from Beryllium. By **F. Rasetti** 165
Absorption Measurements on Balmer Lines in a Neon-Hydrogen Mixture with Condensed Discharges. By **T. Takamine, L. S. Ornstein and J. M. W. Milatz** 169
Flexible Electron Beams. By **E. Brüche** 177
New Investigations on the Electrolytic Rectifying Action. By **A. Güntherschulze and Hans Betz** 196
Wood's Method for Separating the *D*-Lines. By **E. Gaviola and Peter Pringsheim** 211
Relation between Infrared Characteristic Frequencies and Dielectric Losses. By **M. Czerny and W. Schottky** 220
Magneto-Elastic Phenomena in Vibrating Wires and Rods in a Magnetic Field. By **O. v. Auwers** 230
Influence of the Superposition of High Frequencies on the Corona Current. By **A. Gemant** 240
Accurate and Absolute Measurement of Small Capacities. By **J. Clay** 250
Most Dense High-Order Packing of Spheres. By **E. K. Broch** 257
Variation with Pressure of the Ionization by Cosmic Rays. By **Bernhard Gross** 271
Wave Mechanical-Classical Picture of the Neutron. By **Hans K. Kudar** 279

DIE NATURWISSENSCHAFTEN

VOL. 20, No. 40 — SEPTEMBER 30, 1932

Oxide Cathodes. By **A. Gehrts** 732

Short Original Communications:

Method of Multiplying Canal-Ray Energies and its Application to Atomic Disintegration. By **Chr. Gerthsen** 743

PHYSIKALISCHE ZEITSCHRIFT

VOL. 33, No. 18 — SEPTEMBER 15, 1932

Limit of Possibility in Physical Observations. By **F. Ehrenhaft** 673
Radiation in the Gravitational Field. By **A. Maior** 683
Electric Moments of Acetone, Acetaldehyde, Acetylchloride, Chloracetone and Chloracetylchloride. By **C. T. Zahn** 686
Scattering of X-Rays and Cathode Rays by Free Molecules. By **L. Bewilogua** 688
Excitation of Hertzian Waves by Diodes. By **J. Sahánek** 693

PHYSIKALISCHE ZEITSCHRIFT

VOL. 33, No. 19 — OCTOBER 1, 1932

Absorption of the Debye-Falkenhagen Relaxation Force in a Neutral Partially Ionized Gas (Plasma, Kennelly-Heaviside-Layer). By **K. F. Miessen** 705
Dipole Moments of Unsaturated Compounds I. By **I. M. A. Bruyne, R. M. Davis and P. M. Gross** 719
Influence of a Magnetic Field on the Viscosity of Oxygen. By **H. Engelhardt and H. Sack** 724
Influence of Humidity and Temperature of Air on the Characteristics of the Discharge in an Electrofilter. By **S. P. Zebrowski** 727
Electric Moments of Some Fatty Acid Esters. By **C. T. Zahn** 730
Variation with Solvent of Measured Dipole Moments. By **H. Müller** 731
Simple Resonance Detector for Short Sound Waves. By **H. Kröncke** 733
Two Hydrodynamic Demonstration Experiments for the Elementary Theory of the Top. By **J. Jaumann** 734

PHYSICA

VOL. 12, No. 7 — AUGUST, 1932

Dr. H. J. Oosting 225
Experiments with a Simple Physical Pendulum and a Problem Connected Therewith. By **H. J. Oosting** 229
Measurements of Dielectric Losses in Castor Oil. By **J. L. Snoek** 234
Visibility of Stars. By **J. Th. Groosmuller** 239

COMPTES RENDUS

VOL. 195, No. 11 — SEPTEMBER 12, 1932

(No articles of interest to physicists.)

COMPTES RENDUS

VOL. 195, No. 12 — SEPTEMBER 19, 1932

On an Analogy between the Dirac Electron and the Electromagnetic Wave. By **Louis de Broglie** 536

HELVETICA PHYSICA ACTA

VOL. 5, No. 4

Higher Order Scattering Processes. By **P. Güttinger** 237
Problems of Electrical Images in Dielectrics. I. By **J. J. Weigle** 262
New Method of Constructing a Galvanometer with Moving Astatic Magnets. By **Léon Meylan** 276
Station for Cosmic-Ray Investigation on the Hafelekar (2300 m) Near Innsbruck. (Abstract) By **Victor F. Hess** 296
One Year's Observations (Automatically Recorded) of Cosmic Radiation on the High Sonnblick (3106 m). (Abstract) By **Josef A. Priebsch and Rudolf Steinmaurer** 298
Interaction of Gamma-Radiation and Atomic Nuclei. (Abstract) By **E. Stahel and H. Ketelaar** 299

Proof of the Crystal Structure in Organic and Inorganic Bone Substance. (Abstract) By **R. Straumann** 300
Anomalous Specific Heats of Metals. Lithium. (Title only) By **K. Alexopoulos and P. Scherrer** 302
Magnetic Behavior of Solid Nitrogen. (Title only) By **P. Scherrer and P. Widmer** 302
Raman Effect in Silica-Esters and Silica-Gels. (Abstract) By **J. Weiler** 302
Alternating Current Zero Instrument with Direct Current Sensitivity. By **H. König** 302
Crystal Lattice and Spontaneous Striction. By **A. Perrier** 306
Gamma Radiation from Radium. (Abstract) By **E. Stahel and W. Johner** 310
Goethe's Color Theory with Experiments. (Abstract) By **W. Heim** 311
Further Investigations on the Acoustical Electrical Transformation by Loud Speakers. (Abstract) By **H. Zickendraht and W. Lehmann** 312
Electron Diffraction Experiments with Amorphous Carbon. (Title only) By **Ch. Mongan** 314
Chronograph of High Precision to 1/10 Second. By **H. Rosat** 314

JOURNAL OF THE OPTICAL SOCIETY OF AMERICA

VOL. 22, NO. 11 NOVEMBER, 1932

Corresponding Retinal Points, the Horopter and Size and Shape of Ocular Images. Part II. By **A. Ames, Jr., Kenneth N. Ogle and Gordon H. Gliddon** 575
Relation Between the Composition and the Density and Optical Properties of Glass. I. The Soda-Lime-Silica Glasses. By **G. W. Morey and H. E. Merwin** 632